2016

Long-term Relationships between Carbon Sequestration, Hydrology, and Tephra Disturbance in a Northern Peatland (Kamchatka Peninsula, Russia)

Tilotta, Kristen Marie

LAKEHEAD UNIVERSITY
DEPARTMENT OF GEOGRAPHY AND THE ENVIRONMENT

Long-term relationships between carbon sequestration, hydrology, and tephra disturbance in a northern peatland (Kamchatka Peninsula, Russia)

BY

KRISTEN TILOTTA

Submitted in partial fulfillment of the degree of
MASTERS OF ENVIRONMENTAL STUDIES
NORTHERN ENVIRONMENTS AND CULTURES

COMMITTEE MEMBERS:
DR. FLORIN PENDEA (SUPERVISOR)
DR. MATTHEW BOYD
DR. ROSARIO ADAPON TURVEY

Abstract

Northern peatlands are one of the most important carbon reservoirs, storing one-third to one-half of the world's soil carbon pool and thus changes in their carbon balance have the potential to cause a positive feedback to climate change. While recent studies have made progress in understanding the climatic controls on the global carbon cycle, few have studied the important interaction between landscape disturbance (via volcanic eruptions), carbon accumulation, and peatland hydrology. Kamchatka Peninsula in the Russian Far East provides a unique opportunity to study long-term peatland hydrology and carbon accumulation with respect to the role of disturbance, as the area has been subjected to repeated landscape disturbance by tephra deposition over the last 10,000 years. In this study, I use a 10,000-year-old peatland record from Krutoberegovo, Kamchatka Peninsula (Russian Far East) to examine the interaction between carbon accumulation, peat surface wetness, and landscape disturbance in the form of peat surface burial by volcanic ash (tephra). I specifically ask whether tephra deposition affected the hydrological regime of the peatland, its nutrient status, and its ability to store carbon. To answer this question, I use a suite of palaeoecological and geochemical analyses as follows. First, I use 16 AMS ^{14}C age measurements to create an absolute timescale for peatland development. Second, I use the peatland chronostratigraphy and measurements of peat carbon content to reconstruct the long-term carbon accumulation rates (LORCA). Third, I employ testate amoeba (TA) as a hydrological proxy to reconstruct peat surface wetness over time. Fourth, I reconstruct the nutrient status of the peatland by comparing the carbon to nitrogen ratios (C/N), where higher nitrogen values and lower carbon values are indicative of more nutrient-rich environments and vice versa. My results show that the Krutoberegovo peatland experienced thirty-four different tephra deposition events during the last 10,000 years, of which nine were considered major regional markers, based on their thickness, unique geochemical signatures, and area of dispersal. The carbon sequestration potential of the Krutoberegovo peatland measured as long-term apparent rates of carbon accumulation (LORCA) shows a wide variability over the course of the Holocene ranging from 74.5 g C m^{-2} yr^{-1} to 7.91 g C m^{-2} yr^{-1}, with a substantial decrease in accumulation rates during periods of high tephra loading. Although the mechanisms responsible for this process remain unclear, I hypothesize that changes in carbon sequestration following tephra loading of peat surface could be mediated by changes in microbial activity and wetland vegetation cover. High-resolution analysis of testate amoebae (TA) communities over the course of the Holocene shows a high degree of variability with frequent shifts in taxa dominance. The statistical analysis of testate amoeba taxa in relation to tephra-related environmental variables (total ash content and major eruptions) shows that tephra deposition explains to a large degree the shifts in TA communities. Total ash content explains 77.3% of the taxa variability, while major volcanic eruptions as discrete events explain 6.3%. However, when TA communities are grouped according to their hydrological affinities, tephra deposition does not seem to affect any particular hydrological group suggesting that tephra disturbance does not play a role in peatland hydrology. Analysis of carbon and nitrogen chemistry of the Krutoberegovo peat profile suggest that tephra loading of the peat surface induced a net loss of both carbon and nitrogen. The C/N ratios – a measure of nutrient availability in

peatland ecosystems – show a variable but overall increasing trend, which may be related to an autogenic replacement of nutrient rich with nutrient poor wetland plant communities. However, periods with lower or decreasing C/N ratios seem to be associated with high tephra loading, suggesting that tephra deposition may have also played a role.

Keywords: Northern peatlands, carbon sequestration, hydrology, disturbance, tephra, testate amoebae, Holocene, Kamchatka Peninsula

Acknowledgements

First, I would like to start by thanking Dr. Florin Pendea, my thesis supervisor, for the guidance and assistance that he afforded me throughout my Masters journey. Dr. Pendea constantly kept me motivated and focused throughout the entire experience, and encouraged me when undertaking each step of the process. I am very grateful for the opportunity that you have provided me with to work on this project, and for providing me with the rare opportunity to work on samples from such a remote and foreign location. My sincerest and heartfelt thank you Dr. Pendea for providing your wisdom, understanding, motivation, and encouragement.

Secondly, a very special thank you to my internal committee advisors, Dr. Matthew Boyd and Dr. Rosario Adapon Turvey, as well as my external reviewer Dr. Francine McCarthy. Your expertise, guidance, and constructive criticisms added great value to the overall final product of this thesis. Thank you for taking the time to read this thesis, provide your insights, and help strengthen the final product. Your ongoing support and words of encouragement meant a great deal to me throughout this process.

This project relied indirectly on the funding and support from a number of sources. I would like to thank the National Science Foundation, Grant Award# 0915131, Ezra B. Zubrow P.I., for funding the ICCAP project (a larger project from which these samples were taken). I would also like to thank Vera Ponomareva for providing the tephrochronological data referenced throughout this paper. This research would not have been possible without her expertise.

I would also like to extend my gratitude to the wonderful faculty and staff at both the Lakehead Orillia and Thunder Bay Campuses. A special thank you to Dr. Victoria

TeBrugge, for her guidance and infinite wisdom on all things laboratory related. To my fellow graduate peers- Lindsey, Steven, Crystal, Debbie, Steven, and Kayla – thank you for all the coffee breaks, discussions, assistance, wisdom, and overall good times. I will miss seeing you all around the graduate student's office. I owe all of you a lot for the continual motivation that you afforded me, for listening to my ideas, and allowing me to think aloud while working through ideas.

A very special thank you to my mom Lynn, who has been a constant source of encouragement through my entire academic career. She encouraged me to take this opportunity and has been more supportive than I could have ever dreamed. I hope one day I can repay the kindness, support, and love I have been shown. It is my hope that I have made you proud; as proud as I am to have you as my mother.

Lastly, I would like to thank my amazing husband Anthony, and our two wonderful children, Hayley and Emmett. Undergoing a Master's degree is no easy feat, but doing it while being a wife and mother is even more of a challenge. If it was not for the three of you- my reasons for starting and completing this degree, I would not have been able to complete this journey. Thank you to my husband for bearing the extra parenting load, when I had longer days at the school, or late nights working on my thesis. Thank you for allowing me to follow one of my dreams and for being their every step of the way as I reach for my goals. Hayley and Emmett, I love you more than words could ever express. I hope this whole experience will teach you one day that if you work hard enough, dream big enough, and remind yourself to never quit, no matter what, that you can accomplish whatever you set your mind to.

Table of Contents

List of Tables and Figures

Figures

Tables

Chapter 1

1) Introduction

Northern peatlands are one of the most important global carbon reservoirs, storing approximately 400-500Gt of carbon (Roulet, 2000) or one-third to one-half of the world's soil carbon pool (Holden, 2005), thus changes in their carbon balance have the potential to cause a positive feedback to climate change (e.g., Yu et al., 2011). Peatland hydrology measured as peatland surface wetness is an important factor in the carbon flux (i.e., peatland carbon sequestration potential), thus changes to the hydrological regime of a peatland (i.e., changes in water table depth) can also affect how much carbon a peatland can sequester. Extensive research in the last two decades has led to significant progress in understanding the carbon balance in peatlands and peatland hydrology (Charman et al., 2012). However, there is still uncertainty over how peat surface disturbance such as peat burial or peat removal by natural or anthropogenic processes impacts peatland communities and carbon stocks. Furthermore, very few studies have taken into account the possible synergies between disturbance, hydrology, and carbon sequestration as part of a causal continuum.

This research uses a 10,000-year-old peatland record from Krutoberegovo, Kamchatka Peninsula (Russian Far East), to examine the interactions between carbon accumulation, hydrology, and landscape disturbance, specifically partial and total peatland surface burial via volcanic eruptions. Kamchatka Peninsula provides a unique and rare opportunity to study long-term peatland hydrology and carbon accumulation with respect to the role of disturbance, as the area has been subjected to repeated

landscape disturbance events through the deposition of large quantities of volcanic ash (tephra) upon the peat surface over the last 10,000 years. These deposits can influence local environments by obliterating ecosystems, or conversely by supplying nutrients to the soils and altering ecosystems functions.

1.1 Research Questions

This study looks at the role of volcanic ash deposition in peatland development. More specifically, I ask if:

1) carbon storage is affected by volcanic ash deposition?
2) the peatland hydrological regime is affected by volcanic ash deposition?
3) nutrient availability is affected by volcanic ash deposition?

1.2 Aim and Objectives

The primary aim of this research is to decipher if a relationship exists between peat surface burial by volcanic ash and changes in carbon accumulation rates, hydrology, and nutrients. To decipher if relationships exist, this research has two main objectives:
1) to reconstruct long-term (millennial-scale) relative humidity variation in a peatland affected by repeated tephra loading of peat surface;
2) to reconstruct long-term carbon accumulation rates and carbon to nitrogen chemistry, the latter as a measure of nutrient status.

The following chapters provide an overview (chapter 2) of the available literature on carbon sequestration, hydrology, and disturbance around the world, and within Kamchatka and surrounding regions. Chapter 3 provides a characterization of the

research area. The applied methods and data analyses are described in chapter 4. The results are presented in chapter 5 and discussed in chapter 6. Chapter 7 provides the conclusion of the research, limitations, and suggestions for future studies.

Chapter 2

2) Background and literature review

2.1. Peatland habitats

2.1.1. Wetlands, peatlands, and mires

Wetlands, peatlands, and mires are the main terms used in the current literature and are defined somewhat differently, although there is considerable overlap amongst them. The broadest concept is wetlands. A *wetland* is characterized by a water table that is near the ground surface and consequently the substrate is poorly aerated. Inundation lasts for long periods of the year in these ecosystems, and as a result, the dominant plants and other organisms are those that can exist in wet and reducing conditions. The RAMSAR Convention (also known as The Convention of Wetlands; named after the city of Ramsar, Iran, where the intergovernmental treaty was signed in 1971), provides a very broad definition for wetlands. Wetlands are referred to as areas of swamp, marsh, fen, peatland, or water; whether natural or artificial, permanent or temporary, with water that is static or flowing, fresh, brackish or saline. It also includes areas of marine water with a depth at low tide that does not exceed six meters. A swamp for example, is a wetland that is dominated by woody plants (shrubs and trees), and is often found near rivers or streams which sometimes floods, and the water from the flood carries nutrients to the swamp area. A marsh, which is another type of wetland, is dominated by herbaceous (grasses, reeds etc.), rather than woody plant species, and can often be found at the edges of lakes and streams and transition between aquatic and terrestrial ecosystems. For the most part,

a marsh is found in area of low-lying land that is flooded in wet seasons and high tides, and typically, remains waterlogged at all times (Davis & Anderson, 2001).

Peat is defined as the remains of plant and other organic constituents, accumulating under more or less water-saturated conditions owing to incomplete decomposition. Peat is also defined as organic material that has formed *in situ* (i.e., as sedentary material) in contrast to aquatic sedimentary deposits (Rydin & Jeglum, 2006). Thus, '*peatland'* is the term used to encompass these peat-covered terrains. Usually a minimum depth of peat is required for a wetland to be classified as a peatland; in most countries, this depth is 30cm (Joosten & Clarke, 2002). A *mire* is a term given to wet terrain dominated by living peat-forming plants. Both peatland and mire are narrower concepts than wetland, because not all wetlands have conditions that enable peat accumulation (Rydin & Jeglum, 2006).

2.1.2. Peatland classification

Northern peatlands have been forming during the last few thousand years, following the end of the last glaciation. Peatlands are classified based on several criteria such as vegetation characteristics, geomorphology, hydrology, geochemistry, stratigraphy, and peat characteristics, or a combination of these (Blodau, 2002). According to Davis and Anderson (2001), peatlands can be classified into two major types: bogs and fens. Fens cover a vast array of minerotrophic peatlands and as a result, are more difficult to define (Charman, 2002). According to Davis & Anderson (2001), fens are minerotrophic ecosystems where plants growing on their surface receive some of their mineral nutrients from surface or ground water that is in contact with the underlying or surrounding mineral substrates. Fens are influenced by more alkaline, nutrient-rich groundwater and support a wide variety of plants such as sedges, grasses, forbs, and brown mosses

(Bryidae). However, fens can be oligotrophic (nutrient poor), eutrophic (nutrient rich), or intermediate, depending on hydrology, local mineralogy, and geology (Davis & Anderson, 2001). In contrast to fens, bogs are ombrotrophic, meaning that mineral nutrients received by the plants comes entirely from the atmosphere in wet (precipitation) and dry fallout. Bogs are oligotrophic, as the supply of vital nutrients from the atmosphere is severely limited. *Sphagnum* mosses represent the dominant vegetation in bogs; these mosses are uniquely suited to get their nutrients in this way. In North America, there are four basic types of peatlands, ombrotrophic bogs, minerotrophic fens, intermediate or "poor" fens, and calcareous fens (Mullen et al., 2000). These types of peatlands differ with respect to pH, base cation concentrations, dominant vegetation, and hydrologic regime (Mullen et al., 2000). For example, ombrotrophic bogs are peatlands that generally have a convex shape, where the centre is raised above the edges, not allowing for water influenced by mineral soil to reach the centre.

2.1.3. Peatland structure

Peatlands are structured both horizontally and vertically. An important concept of peatland function and development is that they are diplotelmic (i.e., have two layers). Vertical peat profiles consist of a saturated zone known as the "catotelm". This zone is constantly anoxic and it is considered the 'inactive layer' as there is a slow exchange of water with the underlying substrate and the surrounding area, no access to atmospheric oxygen, anaerobic microorganisms, and reduced decomposition activity (Rydin & Jeglum, 2006). Above the catotelm there is a second layer known as the "acrotelm". This 'active layer', which is found above the lowest level of the water table, is characterized by an intensive exchange of water with the atmosphere and the surrounding areas,

fluctuations in the level of the water table and moisture content, and a large population of microorganisms promoting more or less rapid decomposition (Rydin & Jeglum, 2006). The geochemical interactions between the acrotelm and catotelm dictate the rate of peat accumulation. While most of the hydrological and geochemical processes within a peatland occur in the acrotelm and near the surface, it is actually within the catotelm where peat accumulates. Essentially, the acrotelm 'selects' the more slowly decaying plant and other organic parts and 'passes' them below to the catotelm (Clymo et al., 1998).

2.1.4. Peat productivity versus decomposition

According to Mitsch & Gosselink (1986), wetlands are the amongst the most productive ecosystems in the world, as they support a wide variety of species of microbes, plants, insects, amphibians, reptiles, birds, fish, and other wildlife. The biomass of a peatland is defined as the total mass of living material within a certain area, and productivity can be defined as the rate of formation of new biomass (Rydin & Jeglum, 2006). Primary productivity can be referred to as the biomass produced by plants through photosynthesis, but since plants use up some of the carbon during the process of photosynthesis, net primary production can be defined as the difference between the rate of photosynthesis and respiration. Productivity is controlled by factors such as water level, water flow rate (which can affect oxygen content and thus growth, form, and species composition), as well as nutrient levels. In terms of productivity, peatland ecosystems differ widely. The productivity in marshes is greater than in swamps, which in turn are more productive than fens. The least productive are the bogs, but reversals to this order can occur (Rydin & Jeglum, 2006).

Peat accumulates due to an imbalance in the production and decay of the dead organic (plant) matter (Tuittila et al., 2012). As such, peatlands build themselves both laterally and vertically over long time scales (Clymo, 1984). Most peatlands, however, are not characterized by a high net primary productivity because their positive balance is attributed to slow rates of decay, which is a result of waterlogged, anoxic, and acidic conditions causing limited microbial activity as well as peat resistance to decomposition (Blodau, 2002). The most important reason for peat accumulation, however, is retarded decay due to the abundance of water (Clymo, 1984).

Impaired decomposition from waterlogged conditions is the main factor in the net gain of carbon in peatlands. Decomposition is the breakdown of organic matter into inorganic substances such as carbon dioxide (CO_2), methane (CH_4), and ammonia (NH_3), primarily by protists, bacteria, and fungi, but also by soil invertebrates (Rydin & Jeglum, 2006). Generally, the rate at which peat decomposes is determined by the aeration status of the peat, the quality of the substrate, and by abiotic factors such as pH and temperature. The main abiotic factor influencing the rate of decomposition in peatlands is the position of the water table and its effect on the type of microbial respiration. Substrate quality refers to the ability or ease with which microorganisms can decompose organic material. These organic compounds can be ranked in order of increasing resistance to decomposition: 1) sugars, starches, and amino acids, 2) carbohydrate polymers, amorphous cellulose, and hemicellulose, which make up the main part of a plant biomass; 3) crystalline cellulose, aromatic polymers such as lignin and tannin; and 4) lipids (Rydin & Jeglum, 2006). The type and proportion of these organic compounds are determined by the biotic make-up of the peat, such as *Sphagnum* peat, sedge peat, woody peat, and their

corresponding subtypes. In general, sedge peat decomposes more rapidly than *Sphagnum* peat. *Sphagnum* peat is more resistant to decay because of its biogeochemistry; its litter is of low nutritional quality and soil invertebrates generally avoid it (Rydin & Jeglum, 2006). Woody peat has a higher content of cellulose, lignin, and tannin, and is resistant to decomposition; this is why larger pieces of wood can be preserved in peat for thousands of years. Furthermore, the physical structure of plant litter (i.e. waxy cuticles on needles or shrub leaves) may also inhibit decay. When litter is deposited within the acrotelm, microorganisms begin to breakdown the components. The simplest organic compounds such as sugars decompose first, while more resistant ones such as lipids decompose last (Rydin & Jeglum, 2006). As a specific layer passes through the acrotelm by the new litter being laid down at the surface and the water table rising upward, the proportion of easily decomposed compounds decreases while the more resistant compounds increase. Therefore, production and decomposition processes are most active within the upper oxic (acrotelm) layer of the peatland (Rydin & Jeglum, 2006).

2.1.5. Peatlands around the world

Most of the peatlands that exist today have begun forming at the end of the Late-Glacial and in the first part of the Holocene (Halsey et al., 1998; Gorham et al., 2007). Since peat formation is primarily a function of climate (temperature and precipitation), most peatlands are concentrated in specific climatic regions. Climate ultimately determines the amount of water that is available to an ecosystem (via the amount of net precipitation), and temperature affects both the production and decay of organic material. Accumulation of peat is only possible when production of biomass exceeds the loss through decay. Peatlands are therefore abundant in cold (i.e., boreal and

subarctic) and wet (i.e., oceanic and humid tropical) regions. When the precipitation/evaporation balance is less favourable for peat accumulation, peatlands are highly fragmentary and only found in ecosystems that have the ability to collect water (Parish et al., 2008).

Providing accurate peatland estimates worldwide is a challenge because of varying land and soil survey information found throughout the world. Furthermore, not every country uses the same scheme to define and classify soil and land types. Therefore, providing and interpreting these terms into standard peatland categories is difficult. However, global peatland estimates have been increasing over the last century as more accurate and better inventories and methodologies have become available. This is especially true for tropical areas. One of the best available datasets on global peatland inventories is the Global Peatland Database of the International Mire Conservation Group (IMCG). Due to the difficulties described above, when assembling data, the IMCG refers to peatlands as those areas with at least 30 cm peat thickness. As a result, many arctic and alpine mire areas, which contain shallower peat layers, are excluded. Given this approach taken by the IMCG, total peatland cover is estimated to be $4.16 \text{ X } 10^6 \text{km}^2$, which is roughly 3% of the globe's total land area (Joosten, 2004). Peatland areas for 44 countries with at least 2000 km^2 have been inventoried by the IMCG. Based on these estimates, Canada and Russia each contain roughly a third of the global peatlands, and together with the USA and Indonesia they contain 85% of all global peatlands. Overall, 44 countries share >99% of all global peatlands. It is important to note that at least 80% of all peatlands are found in areas with northern temperate or colder climates, 15-20% are found in places that are tropical or subtropical, and only a few are found in southern

temperate or cold climates. Countries or territories with the highest percent cover of peat are Falkland Islands, Finland, Estonia, Ireland, Sweden, Indonesia, and Canada (Joosten, 2004).

2.1.6. Peatlands as historical records of change

Climate is one of the most important factors, not only in the global distribution of peatlands, but also in determining peatland typology. There is an abundant body of evidence that documents continuous shifts in the Earth's climate, and peatlands have changed concomitantly with these climatic changes. Peatlands are unique in that they provide a record of their own development. Although climate change is one of the most important factors in peatland development, peatlands also respond to other influences such as ecological succession, human activity, and natural disturbance events. This means that through palaeoecological studies, such as the one presented here, it is possible to trace the changes of a peatland through time. When decomposition rates are slower than production rates, layers of peat are formed from the dead plant remains that once grew on the surface. These layers also incorporate a range of microscopic organisms and geochemical signals of past environmental conditions (Charman, 2002). In fact, almost everything that was living in or around the peatland at the time has the potential to be preserved within the accumulating peat (there is, however, a bias towards material that is more decay-resistant) (Charman, 2002). To reconstruct past environmental conditions, researchers use a variety of biological, physical, and geochemical techniques and apply them to the samples collected from peat profiles. The application of these techniques provides a robust basis for the understanding how peatlands ecosystems have responded to past environmental factors (Parish et al., 2008).

2.2. Carbon storage in northern peatlands and its role in the climate system

Northern peatlands play a fundamental role in global carbon cycle. Over the past 15,000 years, peatland ecosystems have withdrawn enormous amounts of carbon dioxide from the atmosphere and have stored it in the form of peat deposits. This process, known as carbon sequestration, makes northern peatlands one of the most effective carbon (C) stocks of all terrestrial ecosystems. Even though they only cover ~3% of the world's land area (Maltby & Immirzi, 1993), northern peatlands contain approximately 550 Gt of carbon in their peat, which represents about 30% of the global soil C (Gorham, 1991). Within ecosystems, plants convert atmospheric CO_2 into plant biomass, which normally would begin to decay under the influence of oxygen. However, in peatlands the dead plant material is subjected to aerobic decay only for a limited amount time because the biomass quickly arrives in the permanently waterlogged, oxygen-poor anaerobic layer (the catotelm), where carbon is ultimately stored in the form of dead plant matter for long periods of time (millennial scales) (Parish et al., 2008).

During the past few decades, researchers have calculated the rate at which carbon has been sequestered within peat over the millennia. For example, Dean & Gorham (1998) estimate that northern peatlands presently accumulate 100 Tg (teragram) of C annually and that peatlands currently store a total of ~547,000 Tg C (Yu et al., 2010). The rate at which carbon is sequestered in peatland ecosystems has been estimated at an average of 0.02-0.03 kg CO_2-C m^{-2} y^{-1} over the past 5,000 to 10,000 years (Gorham, 1991). Globally, however, peat carbon storage rates and long-term rates of accumulation show strong local and regional variation. Storage rates are dependent upon the variations in a region's climatic, hydrological, and chemical conditions. In general, peat

accumulation rates increase when moving from a nutrient rich to nutrient poor ecosystems, from equatorial to polar regions, and from oceanic to continental conditions (Turunen et al., 2002). The peatlands of Canada (>40cm of peat) for example, are estimated to contain 147 Gt of carbon (Tarnocai, 1998). For the peatlands of Russia (>30cm of peat), Vompersky et al. (1996) estimate a total carbon store of 101 Gt with an additional 13 Gt for peatlands that are 30cm-thick or less. Efremov et al. (1998) have provided higher carbon estimates, with total carbon store of the peat deposits in Russia being more than 118 Gt. For the West Siberian Lowlands, Sheng et al. (2004) provided an estimate of total peat carbon pool of 70 Gt and comparatively, an earlier estimate of 40-55 Gt for peatlands with >50 cm. Botch et al. (1995) estimated a carbon stock of 215 Gt in the peatlands of the Former Soviet Union (including Russia and its now Independent States), while for the boreal and subarctic zones, Gorham (1991) arrived at a peat C-store estimate of 461 Gt. The estimate of 461 Gt by Gorham is much higher than the one provided by Turunen et al. (2001) for the same zones, which estimate the C-store range to be between 270-370 Gt. For the West Siberian Lowlands, Turunen et al. (2001) calculated the apparent long-term rate of carbon accumulation (LORCA) of 17.2 g m^{-2} yr^{-1} and a peat accumulation rate of 0.35 mm yr^{-1}, with the average carbon content of the peat being 52.7%. These results differ from an earlier study by Botch et al. (1995) within the same geographical area, who estimated a LORCA of 31.4 g m^{-2} yr^{-1}, a peat height accumulation (mm yr^{-1}) of 0.70mm yr^{-1} and a carbon content of 57%. Estimates of peat and carbon storage in the Russian Far East have been provided through a joint Russian-American research project, sponsored by the V.N. Sukachev Institute of Forest, Siberian Branch of the Russian Academy of Science, and the USDA Forest Service's Global

Change Research Program (Alexeyev & Birdsey, 1998). In the report, the carbon content was calculated differently because peatlands in the Lower Amur Lowlands, Sakhalin, and Kamchatka areas in the Russian Far East are high in ash content (30 to 50%). Furthermore, the report took into consideration the wide distribution of shallow peatlands and the poorly studied physical-chemical properties of the peat and the organic-matter composition. Considering these factors, the mass and carbon content assumed for the Russian Far East was estimated to be 0.350 g/cm^3 and 25% for the lowland peatlands, 0.120 g/cm^3 and 49.8% for transitional peatlands, and 0.094 g/cm^3 and 46.7% for upland peatlands.

Aside from spatial differences in global C-storage, peatlands are also sensitive to temporal changes. High-resolution peat records have revealed that changes in peat carbon accumulations have occurred throughout the Holocene, not only on millennial time scales but also at centennial scales. Using peatland *Sphagnum* spore data, Yu (2012) argues that changes in peatland carbon stocks show different patterns throughout the Holocene. For the past 7,000 years, the carbon flux showed a higher NECB (net ecosystem carbon balance) of 32± 7.8 g C m^{-2} y^{-1} than for the previous 7,000 years (~11 g C m^{-2} yr^{-1}). Yu et al. (2010) argued that peatland carbon sequestration rates are highly sensitive to minor climatic fluctuations, and Roulet et al. (2007) suggests that sequestration rates can also show considerable year-to-year variability. Due to temporal differences, Holden et al. (2005) concluded that many peatlands might be close to the tipping point between carbon sources and carbon sinks. Although the long-term natural carbon balance for peatlands worldwide is positive, on seasonal and inter-annual time scales, peatlands show a high

degree of variability in rates of carbon accumulation, including short-term negative rates (Alm et al., 1999).

Overall, the discrepancies shown in the estimates of net C accumulation rates and carbon storage, demonstrates the need for more accurate estimations of carbon accumulation rates and a deeper understanding of the processes governing them. While there are differences in exact amounts of C storage between researchers, the role that peatlands play in the global carbon system is undisputed. Since the balance between production and decomposition within peatlands is so delicate, any change to the system can cause peatlands to become carbon emission sources following intervention or disturbance. Some disturbance processes stimulate the decomposition rate, which in turn would cause an increase in carbon loss through emissions of carbon dioxide and methane. One way to stimulate the decomposition rate is by lowering the water table.

2.3. Peatland hydrology and nutrient status

Understanding the palaeohydrology and geochemistry of a peatland is fundamental to understanding how these ecosystems have functioned over time. Peatland hydrology can arguably be considered the single most important condition influencing peatland ecology, development, functioning, and processes. The water quality of a peatland refers to the physical presence (or absence) of water and its associated fluctuating depths and flow patterns (Rydin & Jeglum, 2006). In its simplest form, the water balance of a peatland is determined by its influx (recharge), efflux (discharge), and storage, where all three components must have a balance of zero (Charman, 2002). Once water enters the peatland system, it either moves through it, becomes stored, or a combination of both. Peatland hydrology at all scales (diurnal, annual, or millennial) controls peatland function

and processes, as the hydrology controls the flow of nutrients through the system. It also affects the distribution of peatland species and links the peatland to its surrounding landscape. Hydrology can even control the accumulation of peat mass, although accumulating peat mass itself has an effect on the flow patterns of water as well (Bunting et al., 1998).

The hydrological status of a peatland surface is expressed by changes in the water table and is measured through a variety of modern techniques. Fluctuations in water table occur over different timescales and respond to variety of factors, such as seasonal variations, or water table drawdown caused by human activities. The sources of water in a peatland exercises a strong control not only on the peatland water budget but also on peat chemistry and therefore on the entire peatland ecosystem. For example, ombrotrophic peatlands that rely solely on precipitation for their source of water are typically nutrient poor and acidic, whereas minerotrophic peatlands that rely on groundwater (or a combination of both precipitation and groundwater) typically have a higher nutrient status (Charman, 2002).

The nutrient status of a peatland can be assessed in several ways. In long-term peatland reconstruction studies (palaeoecological studies); one of the best ways to reconstruct the nutrient status is to measure the change of carbon to nitrogen ratio (C/N) of peat sediments over time. Higher ratios of carbon to nitrogen (C/N) indicate a nutrient poor ecosystem, where the nitrogen content of peat sediments is very low. Lower C/N indicates higher nitrogen content for the same carbon content of peat sediments, which is a geochemical make-up characteristic to nutrient-rich peatlands. A peatland with higher nitrogen to carbon ratio would be an indicator of a more minerotrophic/nutrient rich

ecosystem. Nutrient rich peatlands are defined by higher availability of nitrogen, which would stimulate biomass productivity (Bridgham, Updegraff & Pastor, 1998). However, enhanced nutrient availability would also lead to higher decay rates of the organic matter stored as peat as microbial activity is high, which in turn leads to an enhanced release of carbon to the atmosphere in the form of carbon dioxide and methane.

2.3.1 Hydrarch Succession

According to Elliott et al. (2012), a transition or succession from one type of ecosystem to another can occur when one set of ecological or environmental processes in a peatland are replaced by another. In peatlands, the transition, also known as hydroseral succession, can happen gradually or abruptly as thresholds are reached. As peat continues to accumulate it isolates the plant communities from groundwater resulting in a shift from nutrient-rich conditions to nutrient-poor conditions. The 'Fen-Bog transition' (FBT) is an important successional phase and it is characterized by the replacement of nutrient-rich minerotrophic fen communities by ombrotrophic bog communities associated with acidic conditions (Elliott et al., 2012). As a peatland transitions, the rates of carbon sequestration in soils can change significantly. For example, Tolonen & Turunen (1996) looked at carbon accumulation rates in a Finnish bog and a fen and reported 25.5 ± 0.5 g C m^{-2} yr^{-1} and 17.2 ± 0.3 g C m^{-2} yr^{-1}, respectively.

Throughout the Holocene a range of both internal and external processes have been acting on peatland ecosystems, which function through a complex and interrelated system of biotic, chemical, and hydrological processes, and can be affected by environmental changes. These processes can be classified as either allogenic or autogenic. *Autogenic succession* refers to changes occurring in an ecosystem due to internal forces or

mechanisms, such as biotic interactions and biotic modifications of the environment, e.g. soil modification by plants (Glenn-Lewin, Peet, & Veblen, 1992). These internal processes can be considered the primary driving forces behind hydroseral development. *Allogenic succession* refers to changes occurring in an ecosystem due to external forces or mechanisms (Glenn-Lewin, Peet, & Veblen, 1992). These processes act upon the system from outside. Globally, the principal allogenic factor in peatland development is climate, having a connected effect on both vegetation and hydrology. Climate can either increase or decrease the water supply in a system. For example, increases can occur via precipitation, causing a change in seasonal distribution (e.g. wetter summers) (Bunting et al., 1998). In reality, however, the distinction between allogenic and autogenic mechanism can be viewed as 'artificial' as the characterization in long-term successional studies, both allogenic and autogenic forces likely play a combined role in wetland succession. In essence, succession in its entirety cannot be labeled as solely auto- or allogenic, but rather a combination of both (Sharik et al., 1989).

The notion of primary succession was first introduced in the early 1900s by researchers such as Cowles (1901), Ganong (1903), and Transeau (1903). Classical successional studies suggested that succession begins with the infilling of a shallow lake or pond by organic sediments which produces a unidirectional sequence of vegetation communities. The first step is a marsh community characterized by a diversity of aquatic plants such as sedges and reeds. A fen and then a bog stage follows the marsh stage, where plant communities in a fen stage are composed by sedges, and ericaceous shrubs, and in a bog stage composed mainly of *Sphagnum* mosses. The wetland system eventually culminates in mature upland or 'climax' forest. Founding successional

theorists however struggled to describe long-term peatland change because the transition from one type of community to another did not necessarily follow the traditional model of succession. In 1970, Walker provided the first analysis of long-term hydroseral succession using field stratigraphy and fossil palynological evidence to demonstrate that a hydrosere could follow a number of different pathways to succession and that reversals could occur (Walker, 1970). Similarly, research by Hughes & Dumayne-Peaty (2002) reveals that systems may alternate multiple times between a fen and bog throughout the Holocene. Furthermore, in the case of Crymlyn Bog (Hughes & Dumayne-Peaty, 2002), allogenic and autogenic controls were both important in determining the type and timing of succession. A study by Payette (1988) showed shifting patterns of successional change on islands found within a large subarctic lake in northern Quebec (Clearwater Lake). In Clearwater Lake, the repeated alteration and regeneration cycles of *Sphagnum* and black spruce supported the notion that long-term community succession is multidirectional due to external control and can vary amongst different environments. In the absence of external disturbance such as fire, Payette (1988) suggested that cyclic-autogenic succession and climate were the dominating factors operating upon the ombrotrophic peatland of northern Québec, causing the multidirectional successional patterns observed.

2.4. Peatland Disturbance

Disturbance regimes, whether allogenic or autogenic, natural or anthropogenic, have the potential to compromise the ability of a peatland to sequester carbon, its hydrology, geochemistry, and ecological succession. Pickett & White (1985) describe disturbance as a discrete event in time that disrupts ecosystem, community or population structure and changes the resources, substrate availability, and/or the physical

environment. While climate is the greatest global allogenic influence that can affect a peatland, fire, permafrost, or geological processes (e.g., isostatic uplift) may also be important factors in certain regions of the world (Bellen et al., 2011). On the other hand, autogenic (from within/biotic) factors affecting carbon sequestration can include surface microtopography dynamics, and hydrology-induced limits to vertical peat growth (Bellen et al., 2011).

Ecological studies have been developed to assess the role that anthropogenic disturbance has on peatland ecosystems. For instance, Gorham et al. (1984) looked at the ecological effects of anthropogenic acid deposition on peatlands and found that many peatland plants are likely to be susceptible to acidification by atmospheric pollution. Even several distinctly acidophilous species of *Sphagnum* have almost entirely disappeared from the large blanket bogs of the southern Pennines in Britain, subject for many decades to extreme acidification. The virtual extinction of *Sphagnum* from these areas is almost certainly a result of atmospheric pollution in Britain for the last 150 years. Loss of these species has made the bogs more susceptible to erosion and effects on water quality downstream would be expected. Proctor & Maltby (1998) who looked at the effects of acid rain on sixteen ombrotrophic bogs from across Britain obtained similar results. Their research shows that acid rainwater results in a regional depression of surface pH on ombrotrophic bogs of up to 0.7-0.8 pH units.

Mitchell (2004) assessed the response of testate amoebae (TA) to experimental fertilization with nitrogen (N) and phosphorus (P) in an Arctic wet sedge meadow. This study showed that after twelve years of N and P addition, the total density of TA was 77% lower and the biomass carbon was 84% lower in the fertilized plots. In control plots,

thirty-four taxa (e.g., *Amphitrema flavum, Assulina muscorum, Placocista spinosa,* and *Hylosphenia papillio)* accounted for over half (51%) of the population but only for 11.1% of the population in fertilized plots. Two species (*Centropyxis aerophila* and *Phryganella acropodia)* accounted for nearly half (47%) of the population in fertilized plots but only 18% of the population in the control plots. Furthermore, N and P additions affected the vegetation and ecosystem functioning after a six-year period, with a three-fold increase in vascular plants and a significant reduction in total microfossil density and biomass C. Ireland & Booth (2012) revealed similar findings in a kettle peatland in Erie County, Pennsylvania (USA). Their research showed that upland deforestation triggered an ecosystem state-shift in the peatland and that deforestation resulted in a replacement of *Sphagnum* mosses by vascular plants. This was coincident with the inferred timing of European settlement and maximum deposition of mineral matter on the peat surface. Abrupt changes were observed in Erie County for the microfossil communities, where TA communities underwent marked structural changes coincident with mineral matter deposition, nutrient enrichment, and plant community shifts. The data of the study suggested that coincident with the change in plant communities, TA communities shifted towards those species, which were more tolerant of high-magnitude variability in micrometeorological conditions, such as *Difflugia pulex* and *Hyalosphenia subflava.* Ireland & Booth (2012), also suggest that shifts from densely growing *Sphagnum* mosses to less dense vascular plants, would have caused enhanced micrometeorological variability at the peatland surface, in turn affecting the upper few centimeters where TA live. They also suggest that TA food sources may have changed, due to shifts in the

composition of microbial communities, and this could have resulted in changes to TA community composition.

While there has been a large amount of work on the impact of anthropogenic pollutants on peatlands (e.g., Gorham et al., 1984; Proctor & Maltby, 1998), there has been little investigation of the impact of natural pollutants. Extensive regions of peatlands exist throughout the Pacific Rim. These regions span from northern Japan to eastern Russia (e.g. Hokkaido, Kamchatka, and eastern Siberia) and to the Pacific seaboard of North America (Hughes et al., 2013). These carbon-rich peatlands lie in close proximity to chains of active volcanoes that periodically deposit widespread and heavy ash falls. For example, Mt. Mazama (7627 ± 150 years BP) was one of the largest Holocene volcanic eruptions in North America. It distributed volcanic ash (>4cm compacted depth) across much of the North American continent, with ash found as far as 1100 km from the eruption center (Hoblitt et al., 1987). Hughes et al. (2013) argue that the deposition of tephra on peatlands has the ability to alter peatland functioning, nutrient status, and the vegetation communities of the peatland. Deposition of tephra causes enhanced nutrient delivery, smothers vegetation, and introduces plant communities to toxins. Ultimately, the impact of landscape disturbance has the potential to affect the carbon balance of affected peatlands as the partial or total burial of peat alters the primary production and litter decomposition rates of the peatland. Moreover, the addition of nutrients, such as nitrogen, phosphorus, and potassium, to peatlands can cause a shift in plant communities from species that are more resistant to decay, such as *Sphagnum,* to plant communities that are more prone to decay, such as vascular plants, thus reducing the capacity of peatland carbon accumulation (e.g., Malmer & Wallen, 2004).

The role of natural landscape disturbance, such as partial or total peatland burial by tephra has been noted by several researchers who have used visible and microscopic tephra layers found preserved in peatlands throughout the world (e.g., Hotes, Poschlod, & Takahashi, 2006; Yeloff et al., 2007; Payne & Blackford, 2008; Payne, Gauci, & Charman, 2009). One of the first studies of volcanic impacts on peatlands was provided by Griggs (1919), who made observations on plant dynamics of an upland bog in the southwest Alaska region following tephra deposition from the 1912 Katmai eruption. Griggs (1919) observations were divided into "zones of damage" based on the extent of injury to vegetation by the Katmai eruption. In the outermost zone, the plants suffered from acid rains, but ash fall did not do any damage of consequence. The second zone, covering pars of Kodiak and Afognak Islands in Alaska, featured ash fall so heavy, which greatly damaged smaller plants, but trees and bushes were unaffected. The third zone showed slight injury to plants of the mainland and in the fourth zone all trees and bushes were killed but grasses had established themselves without injury. The fifth zone saw very heavy ash fall which killed trees and herbage, and in the sixth zone, every vestige of life was consumed by fire, which left the country sterile. Studies that are more modern have observed the effects of volcanic eruptions on peatlands, such as Hotes et al. (2004), who provided an experimental approach to tephra impact on peatlands by applying varying quantities of tephra and ground glass, which simulated tephra deposition, to mire plots in Hokkaido, Japan. Results from the study showed substantial changes in pore chemistry, increase in pH balance, changes to electrical conductivity, and the addition of nutrients such as sodium. Furthermore, the study revealed changes in species composition, with some species being lost and then re-established later. Similarly, Hotes

et al. (2006) used the same study site in Hokkaido, Japan, to test the hypothesis that tephra deposition causes plant communities to undergo ecological succession leading to a profound change in plant communities. The study yielded inconclusive results as macrofossil composition showed no clear response to disturbance. Although the study by Hotes et al. (2006) showed that there were some changes in plant composition following tephra deposition, these changes were minor and suggest that mire vegetation is resilient to disturbance by moderate tephra deposition.

Yeloff et al. (2007) document that tephra deposition had a major influence on long-term vegetation succession in and around a study site on Marion Island (Sub-Antarctic Indian Ocean). However, the ecosystems of the sub-Antarctic are simple and sensitive to disturbance. They also assert that in this region, episodic environmental events slow or reverse successional development so that the "successional clock" is continually being reset by disturbance. The results of their study outline the sensitivity of ecosystems on Marion Island to disturbance from tephra deposition and associated effects including burial of plants, chemical "scorching" of leaves, and alteration of trophic status through acidification and nutrient enrichment.

Payne & Blackford (2005) documented a complex response to tephra deposition on peatlands in northern Britain. The authors used simulations of different tephra and acidity loading, designed to replicate the prehistoric Hekla-4 ash fall, and monitored these over two years. Impacts on the peatland ecosystem were assessed by qualitative observations of plant health and abundance, semi-quantitative observations of flowering, measurements of peat pH, humification, and testate amoebae community composition. Plots with higher acid loading showed immediate and lasting impacts on plants, although

other treated plots were less affected. Changes in testate amoebae assemblages and peat humification were inconsistent both within and between plots. The experiment demonstrates the potentially severe effects of high acid loading on peatland plants, although some responses remain unclear. A later study by Payne, Gauci, & Charman (2010) looked at the impact of simulated sulfate deposition – a surrogate for tephra deposition - on peatland testate amoebae communities in Morayshire, Scotland. They found higher abundances of *Euglypha strigosa, Placocista spinosa*, *and Hyalosphenia papillio* and lower abundances of *Euglypha rotunda* and *Trinema lineaere* in treated plots.

Due to the inherent difficulties in direct ecological investigations of real volcanic impacts on peatlands and the uncertainty in experimental scenarios, an alternative approach is to use palaeoecological records (Payne & Blackford, 2008). Due to the acidic and anoxic environment below the surface layers of peat i.e., catotelm, organic material does not fully decay and long sedimentary sequences are accumulated. Palaeoecological studies exploit these archives by analyzing the macrofossil plant remains, preserved organisms within the peat, or deposited particles such as pollen. Tephra layers are preserved within the peat and analysis of changes in the palaeoecological record across these layers provides an opportunity to investigate volcanic impacts (Payne & Blackford, 2008). Existing palaeoecological studies of tephra impact on peatlands are, however, very few.

For instance, Payne & Blackford (2008) investigated the impacts of several late-Holocene volcanic eruptions on five peatlands in southern Alaska. Testate amoebae analysis, peat humification analysis, and a basic analysis of plant macrofossil components

were applied across eleven tephra layers. The study shows that changes in macrofossil and testate amoebae assemblages occur across several of the tephra layers but not all. The finding that some tephra is associated with impacts whereas others are not, may relate to the season of the eruption or meteorological conditions at the time of ash fall. These results suggest that peatlands and peatland microbial communities are sensitive to distal volcanic products and imply that changes in key palaeoclimatic proxies may be caused by a mechanism independent of climate change.

Another study, by Hughes et al. (2013), uses a 3000-year peatland record from northern Japan to examine the interactions between carbon accumulation, vegetation community succession, and volcanic ash deposition. Plant macrofossil and testate amoebae records are presented alongside records of total organic carbon, nitrogen, and phosphorous. Their results show that moderate to high tephra loading can shift peatland plant communities from *Sphagnum* to monocotyledon domination. This vegetation change is associated with increased peat humification and reduced carbon accumulation.

Finally, a study by Blackford et al. (2014) investigated the impact of the mid-Holocene eruption of Aniakchak volcano (Aniakchak II) in southwestern Alaska, one of the largest eruptions in the last 10,000 years. The researchers found that once the peatland vegetation returned after the eruption, the flora changed from a Cyperaceae-dominated assemblage to a Poaceae-dominated vegetation cover, suggesting a drier and/or more nutrient-rich ecosystem. The study also found that the eruption may have led to a widespread reduction in peatland carbon sequestration and that the impacts on ecosystem functioning were profound and long lasting.

Chapter 3

3) Site Description

3.1 Research Area

Kamchatka Peninsula, Russia, is one of the most remote and least studied areas within the Northern Hemisphere, and is one of the most volcanically active regions in the world with a dramatic geological history, which is driven by large-scale tectonic processes (Ponomareva et al., 2007). As a result, Kamchatka Peninsula offers a rare opportunity to study the impact of peat surface burial by volcanic ash on water table regimes as well as on carbon accumulation rates. Furthermore, Kamchatka Peninsula contains extensive areas of wilderness, which have had little impact by human populations, which makes Kamchatka an interesting and unique place for study of palaeoenvironmental changes under natural variability (Dirksen et al., 2013). Not only would research in Kamchatka increase the palaeoecological knowledge within a regional setting, but it would also cover the gap in the existing literature on the impact of peat surface burial by volcanic ash on water table regimes as well as carbon accumulation rates.

Kamchatka Peninsula (Fig. 3.1) is situated in the Russian Far East and is a boreal-subarctic landmass of almost 500,000 km^2. It is bordered by the Pacific Ocean to the east and south, Bering Sea to the northeast, and the Sea of Okhotsk to the west. In the north, a narrow strip of land links the peninsula to the Koryak Highlands of southwestern Beringia. Kamchatka Peninsula lies along a very active subduction zone, where late Pleistocene-Holocene volcanism resulted from the Pacific Plate subducting underneath

the peninsula. These complex tectonic processes produced three volcanic belts, the most productive being Central Kamchatka Depression belt, Eastern volcanic front, and Sredinny Ridge belt, which are arranged from southeast to northwest (Ponomareva et al., 2007). These belts create a diverse tectonic landscape and represent one of the most active areas of volcanism on Earth, with thirty-seven volcanic centers and hundreds of monogenetic vents that have been active throughout the Holocene (Ponomareva et al., 2007). Many of these eruptions were highly explosive and formed extensive tephra fall-layers, which partially or totally blanketed much of the peninsula (Braitseva et al., 1997). Typically, tephra layers have unique geochemical signatures, and extensive tephrochronological work undertaken by Braitseva et al. (1997), Kyle et al., (2011), Plunkett et al., (2015), and Ponomareva et al., (2013, 2015), amongst others, provides a good basis for both local and regional stratigraphic correlations.

The research site (56.25°N, 162.71°E, 19 m a.s.l.) is a small peatland nested in a former kettle basin approximately 250 m in diameter (Fig. 3.1). It is situated in the outskirts of Krutoberegovo village, 4 km from a sheltered coastal lagoon. The kettle basin is exclusively rain fed and has no apparent surface drainage. The average annual temperature in the fieldwork area (Ust-Kamchatsk weather station, 56.2°N, 162.7°E, 4 m a.s.l.) is -0.33°C and average precipitation is 718 mm/year (AD 1951 to 2010 average). July and January average temperatures are 11.2°C and -11.8 °C, respectively (Pendea et al., 2016).

The vegetation of the study region is characterized by a strong altitudinal gradient (Krestov et al., 2008). In the fieldwork area (Pendea et al., 2016), from sea level to 500 m a.s.l. the landscape is varied and associates three main ecosystems: the stone birch

(*Betula ermanii)* woodlands, tall grasslands dominated by Poaceae and tall forbs, and fen peatlands characterized by sedges and Bryidae mosses (brown mosses). Above 500 m a.s.l., the stone birch woodlands give way to an oro-arctic shrub tundra dominated by shrub alder (*Alnus fructicosa).* At higher elevations, the alder tundra disappears and is replaced by oro-arctic sedge tundra, unvegetated mineral soils, and perennial snow. A *Myrica tomentosa*-Cyperaceae peatland community dominates the study site with a bryophyte understory characterized by Bryidae mosses and *Sphagnum teres.* The peatland margin associates species-rich communities dominated by *Alnus fructicosa* and tall forbs such as *Senecio canabifolius* and *Filipendula camtschatica.* The upland vegetation surrounding the peatland is composed of *Betula ermanii* stands with a tall herbaceous layer composed mainly of *Aconitum maximum*, *Heracleum lanatum*, *Saussurea pseudotilesii*, *Geranium erianthum*, and *Equisetum hyemale* (Pendea et al., 2016)

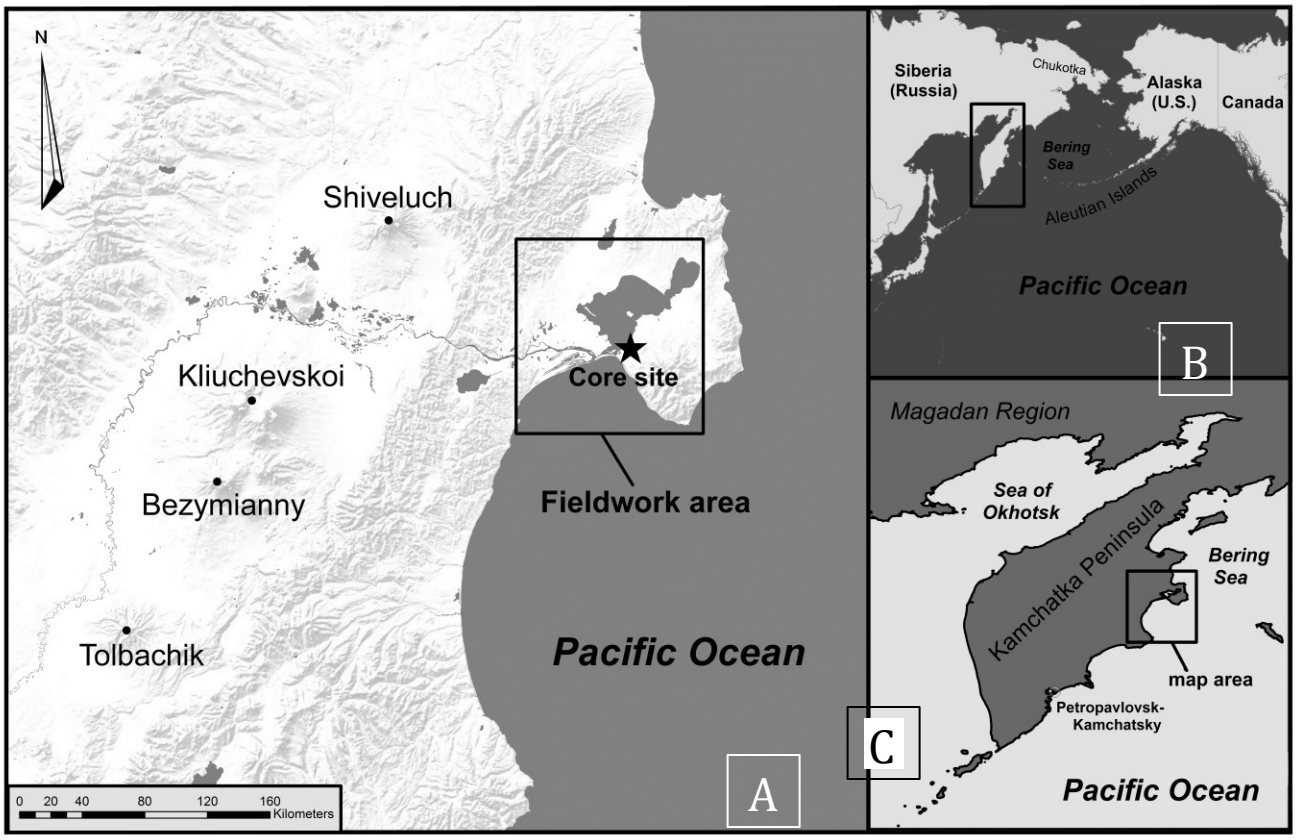

Figure 3.1 Location maps of study area for Krutoberegovo, Kamchatka Peninsula, Russia. A) study area; B) the study region in a global context; C) Kamchatka Peninsula and the surrounding areas.

Chapter 4

4) Methodology

In order to achieve the goal and objectives outlined in this thesis (see section 1.1), a suite of palaeoecological and geochemical methods were employed.

Firstly, a description of fieldwork and core sampling techniques are provided. In order to provide a chronological record for the entire peat profile, AMS (Accelerated Mass Spectrometry) ^{14}C ages were measured on terrestrial plant macrofossil and pollen aliquots. Using AMS dating, a reliable age-depth model was derived. To reconstruct long-term carbon accumulation rates and carbon/nitrogen chemistry, the latter as a measure of nutrient status, carbon and nitrogen content of peat sediments was measured through loss on ignition (LOI) for carbon and through an automated micro-sampler for carbon and nitrogen. Long-term apparent rate of carbon accumulation (LORCA) was calculated using the accumulation of dry mass, rate of peat accumulation, and dry peat bulk density. Repeated tephra loading of peat surface was assessed through tephra analysis. Microprobe analysis of all tephra layers has been performed at GEOMAR Helmholtz Center for Ocean Research (Kiel, Germany) and the detailed results are presented in Ponomareva et al. (2015). Finally, in order to reconstruct long-term (millennial-scale) relative water table variability, microfossil testate amoeba (TA) were used as a hydrological proxy. Testate amoebae are single-celled microorganisms that respond quickly to hydrological environmental change. Their decay-resistant and taxonomically distinctive tests were isolated from the peat, counted, and identified. Species were then qualitatively assigned to one of three groups indicating different

preferences of water table depth and zoned into local TA assemblage zones using constrained cluster analysis by sum-of-squares (CONISS). Detailed descriptions of these methodological approaches are presented below.

4.1 Fieldwork and Core Sampling Techniques

In 2010, four test cores were taken along a transect through the middle of the peatland with an Eijkelkamp® auger equipped with a 1-m long bayonet head, 2.5-cm-diameter. Near the longest test core, palaeoecological and tephra samples were taken as monoliths that were excavated to a depth of 4 m from the excavation walls. From the base of that excavation, coring continued downward with the Russian peat corer, recovering material to a depth of 708 cm, from which the lowest part of the section was sampled. Palaeoecological samples were subsampled from monoliths and cores every 10 cm as well as above and below visible tephra layers.

4.2 AMS Radiocarbon Dating

Sixteen AMS (Accelerated Mass Spectrometry) ^{14}C ages were measured by Beta Analytic Inc., fourteen on terrestrial plant macrofossils and two on pollen aliquots separated from a clay-gyttja matrix. Quoted errors for ^{14}C measurements represent one relative standard deviation statistics (68% probability) and counting errors are based on the combined measurements of the sample, background, and modern reference standards. Radiocarbon ages were corrected for isotopic fractionation and were calibrated using the IntCal13 curve (Reimer et al., 2013) and the calculations were performed using the cubic spline fit (Talma & Vogel, 1993). Calibrated ranges are reported as two standard deviations. The age depth model was derived using the Bacon software (Blaauw & Christen, 2011), which divides a dated sequence into many short sections for which

accumulation rates (in yr cm^{-1}) are modeled. The accumulation rate of any individual section "*i*" depends both on prior information measured and, to a certain degree, on the accumulation rate of previous section (*i*-1). In this way, a "memory" of accumulation rate throughout time is obtained, aimed to reflect environmental conditions that might change gradually over time.

4.3 Peat bulk density quantification and loss-on-ignition (LOI)

The bulk density of the peat profile was measured on a known volume (cm^3) of peat slices taken in contiguous 10 cm depth increments throughout the peat core. Sample volumes were measured by displacement in demineralized water. The samples were transferred to clean, dry, pre-weighed crucibles, weighed and dried overnight at 100°C to evaporate water from the samples. After drying, the samples were reweighed and then transferred to fresh pre-weighed crucibles and burnt in a muffle furnace at 550°C for 4 hours. Samples were then removed from the furnace, cooled to room temperature, and weighed. All volumes and weights were entered into the LOI sheet.

Calculations of bulk density and estimates of organic matter content in the peat samples followed Chambers et al. (2010) procedures. Water content (%) is expressed as the wet weight minus the dry weight, divided by wet weight x 100. Bulk density (g cm^{-3}) is expressed as the dry weight (g) divided by sample volume (cm^3). Organic matter content (%) is expressed as the dry weight minus weight after ashing, divided by dry weight. Ash-free bulk density (OM density; g cm^{-3}) was calculated by multiplying the bulk density by the organic matter content (%). In the absence of direct C measurements in all samples, the measurement of OM in a large number of samples can improve C estimations by using a grand average C content of bulk peat dry mass. As such, the

amount of organic C was calculated assuming a grand mean of 0.52gC/g OM. Clymo et al. (1998) and Gorham (1991) provided the grand average C content of bulk peat dry mass (52%).

4.4 Calculation of carbon accumulation

The long-term apparent rate of carbon accumulation (LORCA) was calculated using the dry bulk density and the organic carbon measurements taken on the peat samples. Long-term apparent rate of peat accumulation was calculated using the equation provided by Hughes et al. (2013): A= r x p x 1000, where A= accumulation of dry mass (g m^{-2} yr^{-1}), r= rate of peat accumulation (mm yr^{-1}), and p= dry peat bulk density (g cm^{-3}). The rate of peat accumulation (r) was calculated by the difference in years. However, this calculation contains two inherent uncertainties derived from possible radiocarbon dating errors and the likely variability of peat accumulation between dated points. The high dating density throughout the peat profile aims to increase the precision of the estimated rates of peat accumulation; however, these will remain best estimates.

4.5 Tephra description and analysis

Tephra samples used for geochemical analyses (Ponomareva et. al, 2015) were extracted from monoliths and core material after shipment to Lakehead University, Canada. Microprobe analysis of all tephra layers has been performed at GEOMAR Helmholtz Center for Ocean Research (Kiel, Germany) and the detailed results are presented in Ponomareva et al. (2015). For the purpose of this thesis, I focus on several marker tephra (see below) and include the observed and sampled tephra in the lithologic log (Table 5.2).

4.6 Microfossil analysis: Testate amoebae

Long-term relative water table variability, through microfossil testate amoeba (TA) analysis, was used to reconstruct the palaeohydrological regime of the study site. Testate amoebae are single-celled microorganisms that respond quickly to environmental change. They produce decay-resistant and taxonomically distinctive tests and they are generally well preserved in Holocene peatland deposits (Lamentowicz & Mitchell, 2005). Counts of TA species abundances were made at 10 cm intervals throughout the core, with greater resolution surrounding major identified volcanic deposition events. Extraction procedures followed the standard protocol from Booth, Lamentowicz, & Charman (2011). Bulk 1-cm^3 peat samples were boiled in distilled water for 10 minutes. One tablet of *Lycopodium* spore was added as an exotic marker to allow for the calculation of test concentrations. Material was sieved at 300µm mesh size to remove the coarse fraction and then back-filtered at 15µm to remove fine, highly degraded organic particles. The resulting material was centrifuged at 2600 rpm for 6 minutes to concentrate the tests and slides were prepared by mixing a sample of the material with glycerol. A total of 150 tests per sample were counted in most samples and identifications were made at 40x, 60x, and 100x magnification using references to Booth & Sullivan (2007), Charman et al. (2000), and Meisterfeld (2001a, b). Assemblages were plotted using Psimpoll 4.27 (Bennett, 2007). A systematic taxonomy of all identified taxa is presented in Appendix 4.

4.6.1. Species grouping

Normally, peat surface wetness is derived quantitatively using transfer functions (e.g. Warner & Charman, 1994; Booth, 2008; Bellen et al., 2014) based on modern testate

amoebae training sets sampled from surface peat with corresponding measurements of environmental variables, such as water table depth and pH. To date, there are no available modern TA training sets for Kamchatka. Although most testate amoebae species are cosmopolitan (i.e. not restricted to a specific region), there are regional variations in community composition and some taxa are limited to certain regions (e.g. Turner at al., 2013). It follows therefore, that I was unable to derive quantitative data for peat surface conditions at our location. Instead, qualitative inferences of water table affinities of various testate amoebae species published in the literature was used (Table 4.6.1).

Based on published literature the identified TA taxa were divided into three groups, "high water table indicators" (HWT), "variable/intermediate water table indicators" (IWT), and "low water table indicator" (LWT) species. A comprehensive description for each water table grouping is provided below based on water table depth tolerance, including minimum, maximum, and water table optimum preferences. Table 4.6.1 provides a breakdown for each species, the study location, researcher(s)/source, and how the information in these studies was used to assess TA peat surface wetness affinities.

High water table indicator (HWT) taxa include taxa with a water-table tolerance range between 0-15cm depth-to-water-table (DWT), but with a preferred a hydrological optimum between 6-10cm. These water-table tolerances and optimums were derived from the following identified HWT species, which include *Amphitrema flavum, Amphitrema wrightianum, Arcella catinus, Arcella discoides, Arcella gibbosa, Arcella hemispherica, Arcella rotunda, Hyalosphenia papilio, Quadrulella symmetrica, Tracheuglypha dentata, Difflugia rubescens, Difflugia bacillifera, Difflugia oblonga, Difflugia lucida, Difflugia globulosa, Phryganella acropodia,* and *Centropyxis aculeata.* Within the existing

literature, both *A. flavum* and *A. wrightianum* are well-established wet indicator species. Magyari et al. (2001), observed in North-east Hungary, that *A. flavum* was a dominate species when peat water content was >95%. Booth & Sullivan (2007) indicated for North American peatlands, that *A. flavum* inhabited areas with wet to moderately wet optimums; sometimes standing water but also in areas with hummock tops in maritime regions, with a depth-to-water table (DWT) range of 0-15cm, but an optimum of 8-9cm. Lamentowicz & Mitchell (2005), observed similar findings in Poland, with *A. flavum* exhibiting an optimum range between 5-8cm. *A. wrightianum* exhibits similar characteristics as *A. flavum*, according to Bellen et al. (2014). *A. wrightianum* is frequently observed in low lawns and according to Booth & Sullivan (2007), occurs in bog pools and wet hollows with an optimum of 4-5 cm DWT, but with a range between -5 and 9 cm DWT. *Arcella catinus* is commonly found in wet *Sphagnum* bogs but occurs in a range of wet to moderately-wet conditions (Booth & Sullivan, 2007). In Northeastern Canada, Lamarre et al. (2013), found this species to inhabit areas with a DTW optimum of 17cm and a ±10cm maximum and minimum range. *Arcella discoides* and *Arcella hemispherica* are also two very strong indicators of HWT, according to Booth & Sullivan (2007), inhabiting very wet-to-wet environments, and occurring in areas of standing water with optimums of 2cm (-3 to 9cm) and 0cm (-5 to 5cm range) DWT, respectively. A study by Woodland et al. (1998) in Cumbria, Britain found *A. discoides* to be the most important species for indicating wet hydrological conditions, inhabiting a very small DWT range of 3-4cm below surface. *Hyalosphenia papilio* was found by Woodland et al. (1998) to exhibit HWT characteristics, with an optimum of 4cm DWT and ranging from 1 to 6cm below surface. Booth & Sullivan (2007) describe

H. papilio as HWT taxa that is found in moderately wet environments such as wet *Sphagnum* peatlands including wetter hummocks but not in pools or hollows, with an optimum of 8 cm below surface. *Quadrulella symmetrica,* another taxa assessed as a HWT taxa, was found by Booth (2001) in Michigan, USA, to occupy hydrological conditions with a range between 3 and 15cm below surface and an optimum of 10cm DWT. Typically, *Q. symmetrica* is found in wet mosses (*Sphagnum* or other), water streams, forest litter, and soil, and has a hydrological optimum in China, according to Qin et al. (2013) of 8cm below ground. *Difflugia rubescens, Difflugia bacillifera, Difflugia oblonga, Difflugia lucida,* and *Difflugia globulosa,* were all assessed as being HWT indicators. Booth & Sullivan (2007) indicate that all of these taxa inhabit areas with very-wet to wet conditions, occurring in bog pools, wet *Sphagnum* bogs or poor fens, and other aquatic areas. Booth & Sullivan describe the DWT optimum for *D. oblonga* to be -1cm above ground, with a range between -5 to 5 cm below ground, the DWT optimum for *D. lucida* as 0 cm (range -4 to 5cm), and the DWT optimum for *D. globulosa* as 0 cm (range -6 to 6cm below ground). In Michigan, USA, *D. bacillifera* exhibited a hydrological DWT optimum of 10 cm (range 0-19cm) (Booth, 2001), and in Britain a DWT optimum of 6 cm (range 4-7cm) (Woodland et al., 1998). Woodland et al. (1998) also assessed *D. rubescens* as having a hydrological DWT optimum of 6cm (range 5-7cm). *Phryganella acropodia* is described by Booth & Sullivan (2007) as a taxon which tolerates a wet environment, with a hydrological DWT optimum of 4cm and of range of -2 to 11cm. Lamarre et al. (2012), found *P. acropodia* to occupy a similar DWT optimum (8.8cm ±4) in Quebec, Canada. Booth & Sullivan (2007) describe *Centropyxis aculeata* as a taxon with a moderately dry optimum in some studies and aquatic in others, therefore likely to

occur across a wide range of hydrological conditions. In North America, Booth & Sullivan (2007) assessed *C. aculeata* to have an optimum of 19cm (range 10-30cm). However, Booth (2001) found *C. aculeata* to have a DWT optimum of 5cm (range -5 to 15cm), Woodland et al. (1998) found a DWT optimum of 5cm (range 2-8cm), and Lamarre et al., (2012) showed an optimum DWT to be 8cm (range 4-12cm). Based on the majority of these studies *C. aculeata* was grouped with the HWT indicators.

Intermediate/variable water table indicator (IWT) taxa include taxa with wide water-table tolerance range, usually between 15-30cm depth-to-water-table (DWT), but with a preferred a hydrological optimum around 15-20cm. These water-table tolerances and optimums were derived from the following IWT species, which include *Euglypha rotunda, Euglypha strigosa, Heleopera petricola, Heleopera sphagni, Difflugia pulex, Cyclopyxis arcelloides, Centropyxis sylvatica, Centropyxis aerophila,* and *Nebela collaris-N. bohemica.* Booth & Sullivan (2007), describe *Euglypha rotunda* as a species which has a dry optimum but occurs in a range of hydrological conditions, with a DWT optimum in North America of 30 cm (range 10-40cm). Woodland et al. (1998) place *E. rotunda* in a wetter DWT optimum (6±4cm), while Qin et al. (2013) provided a more variable assessment for DWT optimum at 20cm (range 10-25cm). Booth & Sullivan describe *Heleopera petricola* as a species that exists in a moderately wet optimum (15cm), but is found in very wet to dry environments. Booth (2001) and Woodland et al. (1998) found varying hydrological DWT optimums for *H. petricola* (20cm and 8cm, respectively). Bellen et al. (2014) described *Difflugia pulex* as a moderately wet species but with a wide water-table tolerance, exhibiting an optimum of 21cm (range ±22cm) for Chile and Argentina, while Lamarre et al. (2012) observed a DWT optimum of 15cm

(range 5-25cm) for *D. pulex.* Booth & Sullivan (2007) describe *E. strigosa* as having a moderately wet optimum (14cm) but occurring in a range of hydrological conditions; normally found in bog hummocks and wet *Sphagnum.* Similar finds are presented by Booth (2001), for Michigan, USA, where *E. strigosa* had a DWT optimum of 15cm. In the same region, *Centropyxis aerophila* had a DWT optimum of 15cm (range 0-25cm) (Booth, 2001). Lamarre et al. (2013) showed intermediate DWT conditions for *Cyclopyxis arcelloides* (optimum 26cm ±11) in Northeastern Canada. Booth & Sullivan (2007) describe *C. arcelloides* as a species with a dry optimum (32cm) but occurring in a range of hydrological conditions (22-50cm). Finally, *Nebela collaris-N. bohemica* is described by Booth & Sullivan (2007) as a species with intermediate water-table depth tolerance, generally found in moderately dry environments with a DWT optimum of 10 cm and a range of 5 to 20 cm.

Low water table indicator (LWT) taxa include taxa with a water-table tolerance range between 25-50 cm depth-to-water-table (DWT), but with a preferred a hydrological optimum around 30 cm. These water-table tolerances and optimums were derived from the following LWT species, which include *Trinema/Corythion type, Trinema lineare, Nebela tincta, Hyalosphenia subflava, Assulina muscorum, Euglypha tuberculata, Heleopera rosea,* and *Trigonopyxis arcula.* Booth & Sullivan (2007) characterize *Assulina muscorum* as a widespread and cosmopolitan species, which prefers a dry DWT optimum (32cm ±12cm). Booth & Sullivan (2007) classification of *A. muscorum* as a dry indicator species is in agreement with Bellen et al. (2014) and Mitchell & Gilbert (2005), who found this species to have an optimum of over 50cm. *Trinema/Corythion* type taxa are classified as dry indicators, with DWT optimums around 51cm in Chile & Argentina

(Bellen et al., 2014), 28cm in Northeastern Canada (Lamarre et al., 2013) and 31cm in North America (Booth & Sullivan, 2007). Booth & Sullivan note that while *Trinema/Corythion* type taxa prefer dry environments, they are found in a wide range of hydrological conditions. One of the most widely recognized dry indicator species is *Trigonopyxis arcula*, preferring dry DWT optimums ranging from 22-60cm (Song et al., 2014; Lamarre et al., 2013; Booth & Sullivan, 2007; and Booth, 2001). *Euglypha tuberculata* is described by Bellen et al. (2014) as a dry indicator taxon, with an optimum of 29cm, which is in agreement with Lamarre et al. (2013), who identified *E. tuberculata*'s DWT optimum as 26cm (range 14-38cm). Booth & Sullivan (2007) describe *Nebela tincta* as a species that thrives in a moderately dry environment (DWT optimum of 20 cm). This optimum is in agreement with Booth (2001), who provided a DWT optimum for Michigan, USA, at 22cm (range 12-35cm). Mitchell & Gilbert (2005) however, estimated the optimum for *N. tincta* to be over 50 cm for the Swiss Jura Mountains. Lastly, Booth & Sullivan (2007) describe *Hyalosphenia subflava* as a species found in dry environments; typically found in soils and drained peatlands, with an optimum of 30±15cm. In a similar study, Booth (2001) provided a similar optimum for *N. tincta* (31cm) for Michigan, USA (range 20-40cm).

Table 4.6.1. Synthesis of testate amoebae found throughout the world. Various studies, by several scholarly articles, were used to classify testate amoebae into three groups: HWT (high water-table indicators), IWT (intermediate/variable water-table indicators), and LWT (low water-table indicator) species.

Species Type	Wetness Assessment in observed studies	Assessment Information/Water Table Depth (cm) optimum and ranges	Study Location	Source	Indicator type for this study
Amphitrema flavum	Wet conditions	>95% peat water content	North-east Hungary	Magyari et al. (2001)	HWT
	Wet conditions	Optimum 5-8cm	Poland	Lamentowicz & Mitchell (2005)	
	Wet to moderately wet	Optimum 8-9cm; range 0-15 cm	North America	Booth & Sullivan (2007)	
Amphitrema wrightianum	Wet conditions	Optimum 8cm; frequently observed in low lawns towards pool transitions	Chile & Argentina	Bellen et al. (2014)	HWT
	Wet conditions	Optimum 4-5cm; range -5 to 9cm	North America	Booth & Sullivan (2007)	
Arcella catinus	Wet- Intermediate/ Variable	Optimum 17cm; range ±10cm	NE Canada	Lamarre et al. (2013)	HWT
	Wet to moderately wet	Optimum 15cm; range ±15cm	North America	Booth & Sullivan (2007)	
Arcella discoides	Wet conditions	Optimum 2cm; range -3 to 9cm	North America	Booth & Sullivan (2007)	HWT
	Very wet conditions	Optimum -3 to -4cm below ground	Britain	Woodland et al. (1998)	
Arcella hemispherica	Very wet environments	Optimum 0cm; range -5 to 5cm	North America	Booth & Sullivan (2007)	HWT
	Very wet conditions	Optimum 5cm; range -5-10cm	Michigan, USA	Booth (2001)	
Hyalosphenia papilio	Wet conditions	Optimum 4cm; range 1-6cm.	Michigan, USA	Woodland et al. (1998)	HWT
	Moderately wet conditions	Optimum 8cm; range 0-19cm	North America	Booth & Sullivan (2007)	
Difflugia globulosa	Hydrophilous- Wet conditions	Optimum 5cm (positioned at the extreme end of the wet WTD range).	Chile & Argentina	Bellen et al. (2014)	HWT
	Very wet conditions (aquatic)	Optimum 0cm; range -6 to 6cm	North America	Booth & Sullivan (2007)	

Difflugia lucida	Very wet conditions	Optimum 0cm; range -4 to 5cm	North America	Booth & Sullivan (2007)	HWT
Difflugia oblonga	Very wet conditions	Optimum -1cm above ground; range -5 to 5 cm below ground	North America	Booth & Sullivan (2007)	HWT
	Wet conditions	Optimum less than 10cm	China	Qin et al. (2013)	
Difflugia rubescens	Wet conditions	Optimum 6cm; range 5-7cm	Britain	Woodland et al. (1998)	HWT
Quadrulella symmetrica	Wet conditions	Optimum 10cm; range 3-15cm below ground	Michigan, USA	Booth (2001)	HWT
	Wet conditions	Optimum 8cm; range 0-19cm	China	Qin et al. (2013)	
Phryganella acropodia	Wet conditions	Optimum 4cm; range -2 to 11cm	North America	Booth & Sullivan (2007)	HWT
	Wet conditions	Optimum 8.8; range ±4.4	Quebec, Canada	Lamarre et al. (2012)	
Centropyxis aculeata	Moderately dry to aquatic conditions	Optimum 19cm; range 10-30cm	North America	Booth & Sullivan (2007)	HWT
	Wet conditions	Optimum 5cm; range -5-15cm	Michigan, USA	Booth (2001)	
	Wet conditions	Optimum 5cm; range 2-8cm	Britain	Woodland et al. (1998)	
	Wet conditions	Optimum 8 cm; range 4-12cm	Quebec, Canada	Lamarre et al., (2012)	
Difflugia bacillifera	Wet conditions	Optimum 10cm; range 0-19cm	Michigan, USA	Booth (2001)	HWT
	Wet conditions	Optimum 6cm; range 4-7cm.	Britain	Woodland et al. (1998)	
Centropyxis platystoma	Variable or intermediate	Optimum 38cm; range ±13cm	Chile & Argentina	Bellen et al. (2014)	HWT
Difflugia pulex	Moderately wet- but wide tolerance	Optimum 21cm; range ±22cm	Chile & Argentina	Bellen et al. (2014)	IWT
	Moderately dry conditions	Optimum 15cm; range 5-25cm	Quebec, Canada	Lamarre et al. (2012)	
Euglypha rotunda	Wet conditions	Optimum 6cm; range 4-10cm	Britain	Woodland et al., (1998)	IWT
	Dry but occurs in a range of conditions	Optimum 30cm; range 10-40cm	North America	Booth & Sullivan (2007)	
	Drier conditions	Optimum 20cm; range 10-25	China	Qin et al. (2013)	
Heleopera petricola	Variable	Optimum 20cm; range 9-25cm	Michigan, USA	Booth (2001)	IWT

	Moderately wet	Optimum 8cm; range 7-9cm	Britain	Woodland et al. (1998)	
	Moderately wet/wet to dry environments	Optimum 15cm; range 0-20cm	North America	Booth & Sullivan (2007)	
Euglypha strigosa	Moderately wet	Optimum 10cm; range 0-15cm	Michigan, USA	Booth (2001)	IWT
	Wet but occurs in range of conditions	Optimum 8cm; range -5-20cm	North America	Booth & Sullivan (2007)	
Centropyxis aerophila	Variable	Optimum 15cm; range 0-25cm	Michigan, USA	Booth (2001)	IWT
Cyclopyxis arcelloides type	Intermediate/ variable	Optimum 26cm; range ±11	NE Canada	Lamarre et al. (2013)	IWT
	Dry to variable	Optimum 32cm; range 22-50cm	North America	Booth & Sullivan (2007)	
	Variable	Optimum 18cm; range 0-30cm	Michigan, USA	Booth (2001)	
Nebela collaris-N. bohemica	Intermediate hydrological conditions	Optimum 10cm; range 5-20cm	North America	Booth & Sullivan (2007)	IWT
	Variable	Optimum 10cm; range 7-14cm	Britain	Woodland et al. (1998)	
Heleopera sphagni	Variable or intermediate	Optimum 35cm; range ±15cm	Chile & Argentina	Bellen et al. (2014)	IWT
Assulina muscorum	Dry- High WTD	Optimum 54cm	Chile & Argentina	Bellen et al. (2014)	LWT
	Dry	Optimum over 50cm	Swiss Jura Mountains	Mitchell & Gilbert (2005)	
	Dry	Optimum 32cm; range 18-42cm	North America	Booth & Sullivan (2007)	
Corythion-Trinema type	Dry- High WTD	Optimum 51cm	Chile & Argentina	Bellen et al. (2014)	LWT
	Dry	Optimum 28cm; range ±12cm	NE Canada	Lamarre et al. (2013)	
	Intermediate/Dry	Optimum 31cm; range 17-42cm	North America	Booth & Sullivan (2007)	
Trigonopyxis arcula	Dry	Optimum 10-60cm	NE China	Song et al. (2014)	LWT
	Dry	Optimum 30cm; range ±10cm	NE Canada	Lamarre et al. (2013)	
	Very dry environments	Optimum 35cm; range 25-45cm	North America	Booth & Sullivan (2007)	
	Dry	Optimum 22cm; range 12-35cm	Michigan, USA	Booth (2001)	

Euglypha tuberculata	Dry- High WTD	Optimum 29cm	Chile & Argentina	Bellen et al. (2014)	LWT
	Intermediate/ variable	Optimum 26cm; range ±12cm	NE Canada	Lamarre et al. (2013)	
Nebela tincta	Dry	Optimum over 50cm	Swiss Jura Mountains	Mitchell & Gilbert (2005)	LWT
	Dry	Optimum 22cm; range 12-35cm	Michigan, USA	Booth (2001)	
Hyalosphenia subflava	Dry environments	Optimum 30cm; range 15-45cm	North America	Booth & Sullivan (2007)	LWT
	Intermediate/dry	Optimum 9cm, range 7-13cm	Britain	Woodland et al. (1998)	
	Dry	Optimum 31cm; range 20-40cm	Michigan, USA	Booth (2001)	
Assulina muscorum	Dry	Optimum 31cm; range 18-42cm	North America	Booth & Sullivan (2007)	LWT
	Dry	Optimum 18cm; range 15-25cm	Michigan, USA	Booth (2001)	
Heleopera rosea	Intermediate to dry conditions	Optimum 12cm; range 2-25cm	North America	Booth & Sullivan (2007)	LWT

4.6.2. Zonation

Zonation analysis was performed with the Psimpoll 4.27 program (Bennett, 2007). The testate amoebae diagram was subdivided into local TA assemblage zones using constrained cluster analysis by sum-of-squares (CONISS) as developed by Grimm (1987). Ten zones representing significant clusters according to the broken-stick method were identified (Bennett, 2007).

4.7. Geochemical analysis (carbon/nitrogen ratios)

Analysis of sediment geochemical signatures, namely carbon/nitrogen (C/N) analysis, was performed using a Carlo-Erba NA 1500 analyzer, to determine the total nitrogen and carbon concentration of a sample. Prior to analysis, wet weight was taken and bulk sediment was dried at 75ºC overnight. Using a mortar and pestle, samples were ground into a fine powder and sent to the Stable Isotope Facility (SIF) in the Department

of Forest and Conservation Sciences at the University of British Columbia. Here samples were collected onto glass fiber filters and HCI-fumed in a desiccator for forty-eight hours to remove all inorganic carbon. Acid fume filters are dried in an oven overnight at 50ºC before being pressed into small pellets wrapped in tin foil. An autosampler is used to introduce 15-20mg samples into a Carlo Erba Na-1500 CNS Elemental Analyzer and these were combusted at 1000ºC along with a stream of oxygen to form a mixture of CO_2, NO_x, and H_2O. A standard with a known amount of both C and N were analyzed to produce a standard curve, which allows conversion of the instrument to μg of organic C and N. Carbon–nitrogen ratios (C/N) are based on micrograms of organic C and N normalized to 100% and adjusted for the molar weight difference between C and N (PerkinElmer, Inc., 2010). Results were plotted using the Psimpoll 4.27 program (Bennett, 2007).

4.7. Statistical analysis and visualization of the results

Redundancy analysis (RDA) was performed with CANOCO ver. 4.5 (ter Braak & Smilauer, 2002) using testate amoeba percentages, to explore the dynamics of testate amoeba communities in relation to volcanic eruptions, ash content, and C/N ratios. Volcanic eruptions, ash content, and C/N were used as environmental explanatory variables for changes in TA communities. In order to convert volcanic eruptions as a specific event in time into a qualitative variable for assessment, a ‘dummy variable’ was created, where the value ‘1’ was assigned to the presence of an eruption and the value ‘0’ was assigned when there was no volcanic eruption present. Finally, the significance of the ordination axes and variance explained by each factor was assessed.

Chapter 5

5) Results

5.1. Chronostratigraphy

All sixteen ^{14}C (Table 5.1) estimates were accepted and allowed for the construction of an age-depth model (Figure 5.1). Ages older than 14,500 cal yr BP were modeled through extrapolation, but will not be discussed in this thesis as the hydrological record (obtained through testate amoeba modelling as a proxy) begins at approximately 9,600 cal yr BP. In the upper part of the sequence, in addition to the ^{14}C age estimates, the absolute age of the historical SH1964 (AD 1964) marker tephra (Table 5.2) was used. The age-depth model shows a relatively uniform accumulation rate between 9,500 cal. yr BP and present. During this time, almost 7 m of peat was deposited in the centre of the kettle basin. There was ~20 cm of clay-gyttja below the peat, likely deposited in a shallow pond environment. The clay-gyttja deposit in characterized by low accumulation rates, between 11,500 and 9,500 cal. yr BP.

Table 5.1: Radiocarbon age measurements for Krutoberegovo, Kamchatka Peninsula, Russia and their associated calendar age ranges (95% probability).

Sample name	BETA ID #	Depth (cm)	Sample Material	Radiocarbon age (yr BP)	2σ probability cal age (y BP)	
					1st	2nd
JB112-45	320725	44-45	*Myrica tomentosa* (twig)	310 ± 30	300-470	n/a
JB112-96.5	320726	94.5-96.5	*Myrica tomentosa* (twig)	1250 ± 30	1120-1270	1080-1110
JB112-145	305864	139.5-145	*Myrica tomentosa* (seeds)	1800 ± 30	1690-1820	1630-1660
JB112-208.5	320727	207.5-208.5	Cyperaceae leaf epidermis	2640 ± 30	2740-2780	n/a
JB112-260	320728	259-260	Cyperaceae leaf epidermis	3560 ± 30	3950-3960	3820-3920
JB112-304	320729	301.5-304	Cyperaceae leaf epidermis	4020 ± 30	4560-4570	4420-4530
JB112-334	305865	331.5-334	*Carex spp.* seeds	4140 ± 30	4560-4820	4540-4550
JB112-381	320730	380-381	Cyperaceae leaf epidermis	4710 ± 30	5530-5580	5440-5480
JB112-465	320731	464-465	Cyperaceae leaf epidermis	5590 ± 30	6430-6430	6300-6410
JB112-546	320732	545-546	*Betula ermanii* wood and bark	6210 ± 30	7220-7240	7140-7180
JB112-556.5	305866	555-556	*Alnus fructicosa* twig	6980 ± 40	7890-7930	7700-7880
JB112-616	320733	615-616	Cyperaceae leaf epidermis	8000 ± 40	8720-9010	n/a
JB112-660	294573	659-660	Cyperaceae leaf epidermis	8330 ± 50	9470-9250	9170-9140
JB112-670	305867	669-670	pollen aliquot	9040 ± 50	10170-10250	n/a
JB112-683	320735	682-683	gyttja	10080 ± 40	11400-11820	n/a
JB112-695	305868	694-695	gyttja	11860 ± 200	13310-14110	n/a

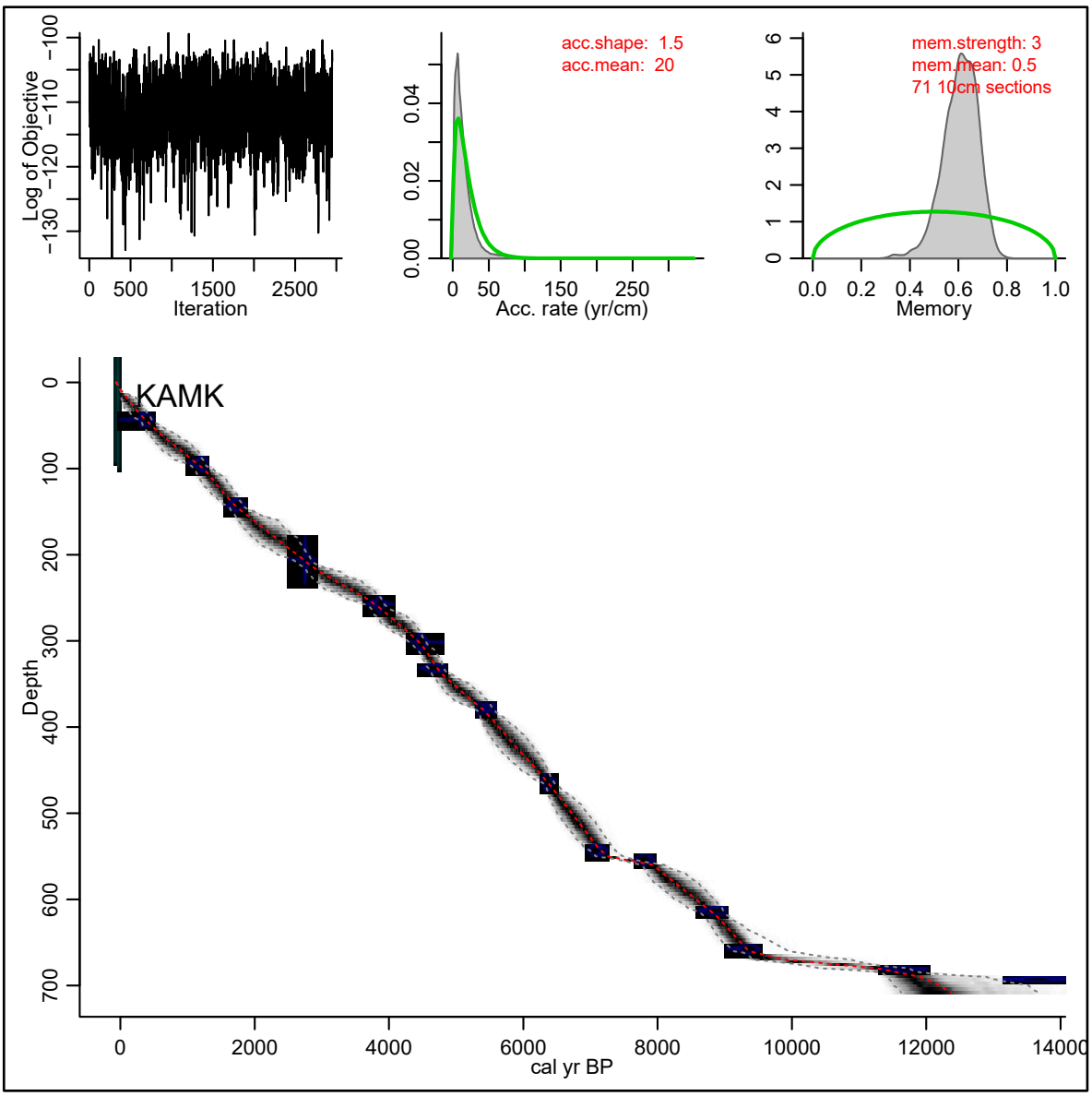

Figure 5.1: The age-depth model for Krutoberegovo, Kamchatka Peninsula, Russia, based on radiocarbon dates and the age of modern tephra (AD 1964) as constructed by the Bacon software (Blaauw & Christen, 2011). The shaded areas represent the 95% confidence interval of calendar ages. The model divides a dated sequence into many short sections for which accumulation rates (in yr cm-1) are modeled. The accumulation rate of any individual section "*i*" depends on the prior information, and to a certain degree, on the accumulation rate of previous sections (*i*-1). In this way, a "memory" of accumulation rate throughout time is obtained, aimed to reflect environmental conditions that might change gradually over time.

5.2 Regional tephra markers

Kamchatka Peninsula has experienced extensive heavy tephra falls throughout the Holocene. Thirty-four different tephra markers were identified over the past 11600 cal. yr BP. A tephrochronological summary of these layers for the Krutoberegovo region is presented in stratigraphic order in Table 5.2.

Based on stratigraphic records of visible tephra, the average frequency rate of heavy tephra fall events during the last 6800 years was approximately one event per 191 years (Pevzner et al., 1998). Heavy tephra fall frequency rate was variable over time, with the highest rates occurring between 2100 and 1400 cal. yr BP (one event per ~60 yr BP) and 4700 and 4000 cal. yr BP (one event per ~90 yr BP). Since these records are based solely on visible tephra layers, actual tephra fall occurrence was probably much higher for the time periods. For example, since the last major eruption of Shiveluch (SH_{1964}), only one visible layer of tephra has been deposited in the area (SH_{2010}) (Ovsyannikov & Manevich, 2010). However, the actual number of tephra falls that were reported since SH_{1964} has been much higher and include such ash falls from Bezymianny (e.g., 1993 and 1995), Kliuchevskoi (e.g., 1990 and 1994), and Shiveluch (e.g., 1990, and 1993) eruptions (Pevzner et al., 1998).

The unique stratigraphic order and colour characteristics of the tephra layers found within the peat profile made field identification of tephra a rather straightforward process (Pendea et al., 2016). The oldest tephra layers in this study PL_1 and PL_2 (~11600 and ~10200 cal. yr BP respectively) are uniquely distinguished by their black to dark-brown cinder, and coarse to very fine sand grain characteristics, belonging to the small late-Quaternary/early-Holocene basaltic shield volcano Plosky.

Two of the Holocene marker tephras, KS_1 and KS_2, are attributed to Ksudach volcano, located ~600 southwest of the study area (Southern Kamchatka). The most recent eruption KS_1 (~1750 cal. yr BP) was produced by the caldera-forming eruption of Ksudach and it is easily identifiable due to its colour (pale, light-yellowish with light-gray top) and grain size characteristics (fine silt to very fine sand/ash) (Braitseva et al., 1996). It is also the most widely dispersed, with a uniform thickness of 5-8cm, making it one of the most important markers in the study region (e.g., Bourgeois et al., 2006; Pinegina et al., 2013). The oldest Ksudach tephra layer in this study is KS_2 (~6000 cal. yr BP), has the same granulometric characteristics as KS_1, but appeared more greenish-gray in colour and only had a thickness of 1cm.

Nineteen of the tephra layers in the Krutoberegovo region are attributed to Shiveluch volcano, located ~80 km northwest of the study area. These tephra layers are identified as being medium to fine coarse grain sand, light or mixed colour (i.e., "salt-and-pepper"), with bulk andesitic and glass rhyolitic compositions (Kyle et al., 2011; Ponomareva et al., 2015). The most recent tephra layer SH_{1964} (AD 1964), SH_{1450} (~1350 cal. yr BP), and SH_{dv} (4700 cal. yr BP) are the most prominent of the andesitic tephra from Shiveluch.

The remaining four tephra markers identified in this study belong to source volcano Kliuchevskoi, situated ~125 km west from the study site. All of these tephra markers are distinctively associated with dark-gray cinder and very-fine to fine sand and moderately crystalized glass shards.

Table 5.2: Holocene tephra for Krutoberegovo, Kamchatka Peninsula, Russia. Tephra are listed by depth, source volcano, age (cal. yr BP) and includes their granulometric characteristics and colour appearance. Major marker tephras are highlighted in gray. They were determined based on unique geochemical features, thickness, and area of dispersal.

Tephra Depth	Tephra Code	Tephra Source	Age (cal. yr BP) based on earlier estimates	Age (cal yr BP) based on the Krutoberegovo age-depth model	Thickness (cm)	Description
6.5-9	SH1984	Shiveluch	-14 (AD1964)	-14 (AD1964)	2.5	Salt-and-pepper medium sand
30-31	KL	Kliuchevskoi	-	227	1	Dark-gray very fine to fine sand
69	SH#8	Shiveluch	1073	765	0.5	Salt-and-pepper fine sand
94-96.5	SH#12 (SH1450)	Shiveluch	1403	1175	1	Salt-and-pepper reverse graded very fine to medium sand
114-115	KL	Kliuchevskoi	-	1404	1	Dark-gray fine sand
139-144	KS_1	Ksudach	1686 1785* 1742**	1725	5	Light-yellow-tan silt to very fine sand
153	SH#19a	Shiveluch	1742	1895	0.1	Salt-and-pepper fine sand
172.5-174	SH#21 (SH_5)	Shiveluch	1852 1951”	2194	1.5	Pale-yellow to salt-and-pepper reverse graded silt to fine sand
197	KL	Kliuchevskoi	3038	2590	0.1	Dark-gray fine sand
208.5-209.5	SH unit b (SH2800)	Shiveluch	2906*** 3170”	2760	1	Beige-light gray to salt-and-pepper reverse graded silt to fine sand
242.5-243	KL	Kliuchevskoi	3547”	3498	0.5	Dark-gray fine sand
259-259.5	SH#28 (SH_{sp})	Shiveluch	3959 3956”	3845	0.5	Dark-gray fine sand
265-266.5	SH#30	Shiveluch	4059	3943	1.5	Salt-and-pepper medium to coarse sand
280.5-281	SH#31?	Shiveluch	4109	4168	0.5	Light-tan very fine to fine sand
289	SH	Shiveluch	-	4285	0.1	Salt-and-pepper medium to coarse sand
296-296.7	SH#32	Shiveluch	4158	4387	0.7	Salt-and-pepper coarse sand
301.5-303.5	SH#33	Shiveluch	4372	4495	2	Light-tan medium to very coarse sand
331.5-333.5	SH#34 (SHdv)	Shiveluch	4892	4680	2	Light-yellow-tan silt to very fine sand

348-349	SH	Shiveluch	-	4925	1	Salt-and-pepper very fine to fine sand
380-381	SH#37	Shiveluch	5634	5450	1	Salt-and-pepper medium sand
384	SH+KL	Shiveluch + Kliuchevskoi	-	5488	0.2-0.3	Light-gray very fine sand
394	KL	Kliuchevskoi	-	5597	0.2	Black very fine to fine sand
405	KL	Kliuchevskoi	-	5717	tiny lense	Dark-gray silt
525	KL	Kliuchevskoi	-	6933	tiny lense	Pale silt
539-541	KL	Kliuchevskoi	-	7083	2	Dark-gray fine sand
546	KS_2	Ksudach	6886 6847** 7287^	7204	0.3	Greenish-gray very fine to fine sand
555.5-556.5	SH#42	Shiveluch	7727	7780	1	Salt-and-pepper medium sand
610-611	SH#47	Shiveluch	8498	8756	0.1-0.2	Salt-and-pepper medium to coarse sand
654-655	SH#48	Shiveluch	8703	9300	1	Gray very fine to coarse sand
659-660	SH#54	Shiveluch	9685	9320	1	Gray very fine to coarse sand
660-664	SH#56	Shiveluch	9916	9700	4	Yellow medium sand
664-670	PL2	Plosky volcanic massif	10200****	10178	6	Dark-brownish-gray coarse sand
670-677	SH#59	Shiveluch	10741	10802	9	Beige - dull-yellow fine sand
682-683	PL1	Plosky volcanic massif	11650****	11556	1	Black very fine sand

Notes: Major marker tephras discussed in the paper are highlighted in gray. Identified tephra are labeled according to Braitseva et al. (1996) and Ponomareva et al. (2013, 2015). Shiveluch tephras are labeled SH followed with the number of the unit (Ponomareva et al., 2015); earlier published codes for several tephras are given in brackets. SH and KL are labels for non-identified Shiveluch and Kliuchevskoi tephras, respectively. Identification of tephra layers is based on microprobe analyses and age estimates (Ponomareva et al., in prep). Most of the ages in column 3 are from Ponomareva et al. (2015); ages marked with " are based on the dates from Izvilisty site (Pendea et al., 2015); other ages are median probabilities of calibrated radiocarbon dates from Pinegina et al. (2013) (*); Braitseva et al. (1996) (**), Pevzner et al. (1998) (***), Ponomareva et al. (2013) (****), and Plunkett et al. (2015) (^).

5.3 Testate amoeba analysis and the interpretation of peat surface wetness conditions

The majority of testate amoeba (TA) levels sampled met the minimum sum requirements of 150 specimens per sample, as recommended by Booth, Lamentowicz, & Charman (2011). Due to low-test concentration, some samples had lower counts (100-150 specimens) and these were found at 84, 94.5, 208.5, 356, 385, 395, 406, 415, 426, 444,

486, 496, 506, 516, 618, 624, 630, 640, 655, and 660cm depth. According to Payne & Mitchell (2008), while most studies have aimed for 150 individuals per sample, it can be difficult or sometimes impossible to reach this total, and as such, 100 individuals is a sufficient count per samples.

Testate amoebae were identified to the lowest taxonomic level possible, with 56 species found in the 72 samples analyzed. A photo plate of commonly observed TA species is presented in Figure 5.3. TA percentages were calculated using the sum of TA counts, and plotted against depth (cm) and age (cal. yr BP) using Psimpoll 4.27 program (Bennett, 2007) and are included in Figures 5.4a-d. The TA diagram was subdivided into ten local TA assemblage zones (K-1 to K-10) using constrained cluster analysis by sum-of-squares (CONISS). These zones represent significant clusters according to the broken-stick method. The identified TA assemblage zones are as follows:

Zone K-1: (9700-6900 cal yr BP): intermediate/variable to high water table

The TA assemblage characterizing the period between 9700 and 6900 cal yr BP is dominated by indicators of intermediate/variable water table (IWT) conditions, which make up 60 to 40% of the assemblage. The most important taxa are *Euglypha rotunda*, *Centropyxis sylvatica, Centropyxis aerophila, Heleopera sphagni*, and *Difflugia pulex* (<6%). *Euglypha rotunda* peaks at 18% at the beginning of the zone and then steadily deceases to 7% before increasing again to 12%. At ~7083 cal yr BP, this species disappears entirely, coinciding with the volcanic eruption of Kliuchevskoi (KL) at the time. *Centropyxis sylvatica* occurs at moderate frequencies (7%-12%). High water table (HWT) indicators, such as *Centropyxis aculeata* (<19%) and *Phyrangella acropodia* (<13%) are also important, particularly towards the end of this zone, when they reach

~45% of the assemblage. Other high water table indicators present are *Centropyxis platystoma* (6%), *Arcella discoides* (6%), and *Difflugia lucida* (≤5%). Low water table (LWT) indicators exhibit a relatively stable abundance throughout the zone ranging from 10 to 15 % of the total assemblage. The most important LWT taxa are *Euglypha tuberculata* (7%), *Nebela tincta* (6%), and *Nebela collaris- Nebela bohemica* (6%).

Zone K-2: (6900-6100 cal yr BP): intermediate/variable water table

The TA assemblage characterizing the period between 6900 and 6100 cal yr BP is dominated by IWT taxa, which collectively reach up to 90% of the abundance. The most important constituents are *Euglypha rotunda* (15-40%) and *Centropyxis aerophila* (13-35%). Other ITW taxa present are *Difflugia pulex* (<20%), *Centropyxis sylvatica (*<8%), and *Nebela collaris-bohemica (*<8%). HWT taxa abundances range from 5% to 45 % of the total assemblage, with the most important species being *Centropyxis aculeata*, *Difflugia lucida* and *Arcella discoides. Centropyxis aculeata* represents a significant portion of the assemblage at the beginning and middle of zone K-2, peaking at 37%, before decreasing significantly and eventually disappearing at the end of K-2. LWT taxa vary substantially throughout zone K-2, ranging from 10-15%, at the beginning of this zone, to 0% at the end. The most representative species are *Trigonopyxis arcula (8%), Nebela tincta* (6%), *Euglypha tuberculata* (5%), and *Heleopera sylvatica* (5%).

Zone K-3: (6100-5750 cal yr BP): intermediate/variable water table

The TA assemblages of zone K-3 is characterized by a marked decrease in HWT indicators and the dominance of IWT taxa, the latter reaching up to 90% abundance. The most important IWT taxa include *Centropyxis aerophila* and *Euglypha rotunda. Centropyxis aerophila* is the most important species of zone K-3. Although it starts at

very low values at the beginning of this zone, it peaks to 43% towards the end. *Euglypha rotunda* is characterized by low abundance values at the beginning and the end of zone K-3, but peaks to 25% in the middle of this zone. HWT taxa reach up to 20% abundance with the most important constituents being *Arcella catinus* (5%), *Arcella hemispherica* (6%), *Difflugia bacillifera* (5%), and *Centropyxis aculeata* (5%). LWT indicators exhibit low values during zone K-3 with only one notable taxon reaching 7% (*Trigonopyxis arcula).*

Zone K-4: (5750-4700 cal yr BP): intermediate/variable to high water table

The TA assemblage characterizing the period between 5750 and 4700 cal yr BP is dominated by HWT taxa, which collectively reach up to 55% of the total TA sum. The most important species is *Centropyxis aculeata*, which reestablishes as a dominant species in K-4, peaking at 33%. Other important HWT species include *Phryganella acropodia* (15%), which appears at the end of zone K-4, *Arcella catinus* (6%), and *Centropyxis platystoma,* which peaks at 14%. IWT taxa, which previously dominated K-3, decrease in abundance to only 35% of the total assemblage. The most important IWT is *Centropyxis aerophila* (35% at its peak), although this taxon decreases in abundance towards the end of K-4 (15%). Other important IWT taxa are *Heleopera petricola* (9%) and *Nebela collaris-bohemica* (6%). Notably, *Euglypha rotunda*, one of the most dominant taxon in zone K-3, decreases dramatically to >5% of the total assemblage in K-4. LWT indicators comprise approximately 10-15% of the total TA sum. The most important taxa include *Trigonopyxis arcula* (9%), *Centropyxis cassis* (7%), and *Heleopera rosea* (6%).

Zone K-5: (4700-4300 cal yr BP): intermediate/variable water table

The period between 4700 and 4300 cal yr BP is characterized by the dramatic decrease in HWT indicators and an increase in IWT indicators, the latter reaching up to 70% of the total assemblage. The dominant IWT species is *Euglypha rotunda,* which is reestablished in K-5 and peaks at 39%. Other important IWT species include *Centropyxis aerophila* (21%), *Difflugia pulex* (8%), *Centropyxis sylvatica* (7%), *Heleopera petricola* (7%), and *Nebela wailesi* (5%). HWT taxa average 15% of the TA sum, but towards the end of K-5 account for 35% of the total assemblage. The most important taxa include *Centropyxis aculeata* (7%), *Phryganella acropodia* (9%), and *Tracheleuglypha dentata* (5%). Notably, the decreases in abundance of HWT species (and increases in IWT species), coincide with two major volcanic eruptions, SH#34 (SHdv) at 4680 cal yr BP and SH#33 at 4495 cal yr BP. LWT species reach a maximum of 20% of the assemblage, following volcanic eruption SH#34 (SHdv), and 7% of the assemblage for the remainder of K-5. The most important species include *Trinema lineare* (11%), *Euglypha tuberculata* (6%), *Trigonopyxis arcula* (5%), and *Centropyxis cassis* (5%).

Zone K-6: (4300-3200 cal yr BP): intermediate/variable to high water table

Zone K-6 (4300 and 3200 cal yr BP) is characterized by the co-dominance of IWT and HWT indicators, which at their peaks reach 50% of the total sum. Important IWT constituents include *Euglypha rotunda* (<5%-20%), *Centropyxis aerophila* (15%), *Heleopera petricola* (15%), *Difflugia pulex* (5%), and *Nebela collaris-bohemica* (5%). HWT indicators reestablish themselves as the other co-dominate taxa group for K-6 (50%). The dominant HWT taxon is *Centropyxis aculeata* peaking at 38%. *Tracheleuglypha dentata* has two moderate peaks, one at the beginning of K-6 and one at

the end (20% and 17%, respectively), but remains <5% of the total assemblage for the remainder of K-6. Other important HWT constituents include *Arcella catinus* (12%), *Phryganella acropodial* (10%), *Centropyxis platystoma* (5%), and *Hyalosphenia nobilis* (5%). LWT indicators exhibit low values (<10%) during zone K-6, with only three notable taxa *Trinema lineare* (9%), *Trigonopyxis arcula* (5%), and *Assulina muscorum* (7%).

Zone K-7: (3200-2300 cal yr BP): intermediate/variable to high water table

Zone K-7 is characterized by unstable peat surface hydrology conditions reflecting repeated changes in the dominant TA assemblages. The zone begins with the dominance of IWT taxa, which attain 60% of the total TA assemblage, followed by a substantial decrease of IWT taxa and a corresponding increase in HWT indicators, the latter reaching 65% abundance at ca. 2900 cal yr BP. The dominance of HWT indicators is, however, short-lived as IWT taxa become dominant again between 2900 and 2600 cal yr BP. Finally, at the end of zone K-7, the abundance of IWT taxa decreases considerably to the benefit of HWT indicators, which reach 60% of the total TA assemblage. *Phryganella acropodia* and *Centropyxis aculeata* are the dominant HWT indicator species, (17% and 15%, respectively). There is, however, a notable decrease in *Centropyxis aculeata*'s abundance compared to zone K-6. *Hyalosphenia papillio* appears in high abundances at the beginning of K-7 (22%), disappears in the middle of the zone and then reestablishes itself at the end of K-7 (15%). Other HWT indicator species include *Centropyxis platystoma* (5%) and *Arcella hemispherica* (at peak 14%). Important IWT indicator species include *Heleopera petricola* (10-33%), *Euglypha rotunda (*5-15%), *Cyclopyxis arcelloides* (1-11%), *Centropyxis sylvatica* (1-8%), and *Centropyxis*

aerophila (5-11%). LWT indicators constitute 10-15% of the total assemblage and, compared to zone K-6, show an overall increase in abundance. Important LWT indicators include *Assulina muscorum* (7%), *Trigonopyxis arcula* (5%), and *Nebela tincta* (8%).

Zone K-8: (2300-2000 cal yr BP): high water table

Zone K-8 is characterized by the dominance of HWT indicators, which reach their highest abundance in the peatland's history, owing to the dramatic appearance of *Amphitrema flavum*. From being virtually absent prior to 2500 cal yr BP, *A. flavum* becomes the most important TA species of K-8 with values between 25% and 38%. Other important HWT taxa include *Hyalosphenia papillio* (11-20%) and *Centropyxis aculeata* (7-14%). Taxa associated with IWT decrease considerably in zone K-8 and, for the first time in the site's history, are no longer the dominant TA group. The only IWT taxa with values above 5% are *Heleopera petricola* and *Centropyxis aerophila.* LWT testate amoebae abundance is stable throughout zone K-8 ranging from 10 to 15% of the total assemblage. Representative LWT taxa for zone K-8 are *Assulina muscorum* (5%), *Trigonopyxis arcula* (6%), and *Nebela tincta* (4%).

Zone K-9: (2000-1350 cal yr BP): high to intermediate/variable water table

Zone K-9 features a substantial decrease in HWT indicators to the benefit of IWT taxa, the latter increasing from ~20% in zone K-8 to 55% in zone K-9. However, HWT indicator taxa remain important throughout zone K-9 ranging from 35 to 55% of the total TA assemblage. The most important HWT species are *Centropyxis aculeata* (10-25%), which increases slightly compared to zone K-8, and *Hyalosphenia papillio* (0-22%). An interesting aspect of zone K-9 is the dramatic decrease in the abundance of *Amphitrema flavum*. The most representative IWT indicators are *Euglypha rotunda* (4-20%),

Heleopera petricola (4-15%), and *Centropyxis aerophila* (5-8%). LWT taxa abundances remain relatively unchanged from zone K-8, with the most important species being *Assulina muscorum* (5%), *Trigonopyxis arcula* (6%), and *Nebela tincta* (4%).

Zone K-10: (1350-present): intermediate/variable water table

The testate amoebae data for the last 1350 years features the co-dominance of HWT and IWT indicators in almost equal proportions. HWT taxa group varies from 35 to 55% and comprises of *Centropyxis platystoma* (0-38%), *Phryganella acropodia* (0-14), *Hyalosphenia papillio* (0-22%), *Centropyxis aculeata* (0-12%), *Amphitrema flavum* (0-12%) and *Arcella hemispherica* (0-5%). IWT indicators vary from 25% to 55% and are represented by species such as *Euglypha rotunda* (0-20%), *Heleopera petricola* (0-15%), and *Centropyxis aerophila* (0-15%). LWT taxa abundances remain relatively unchanged from zone K-9, with the most important species being *Centropyxis cassis* (0-7), *Nebela tincta* (0-7%), *Trigonopyxis arcula* (0-7%), and *Assulina muscorum* (0-5%). A notable development for zone K-10 is the relatively high proportions of unknowns and taxa that are not associated with any particular peat-surface moisture conditions.

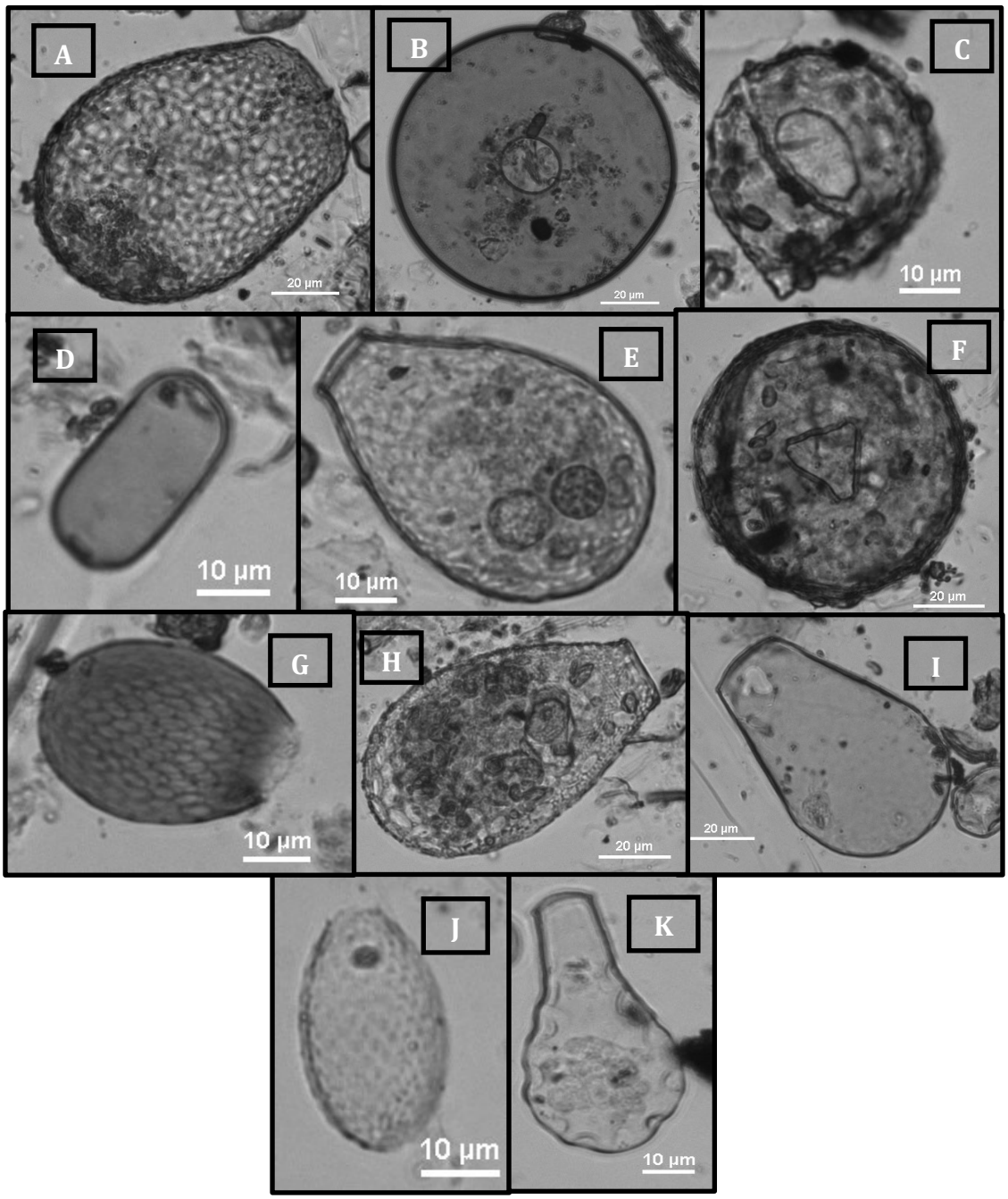

Figure 5.3. Testate amoeba photo plate of commonly identified TA species for Krutoberegovo, Kamchatka Peninsula, Russia. (A) *Heleopera petricola* (B) *Arcella catinus* (C) *Phryganella acropodia* (D) *Amphitrema flavum* (E) *Nebela collaris-bohemica* (F)*Trigonopyxis arcula* (G) *Assulina muscorum* (H) *Nebela tincta* (I) *Hyalosphenia papilio* (J) *Euglypha rotunda* and (K) *Hyalosphenia elegans.*

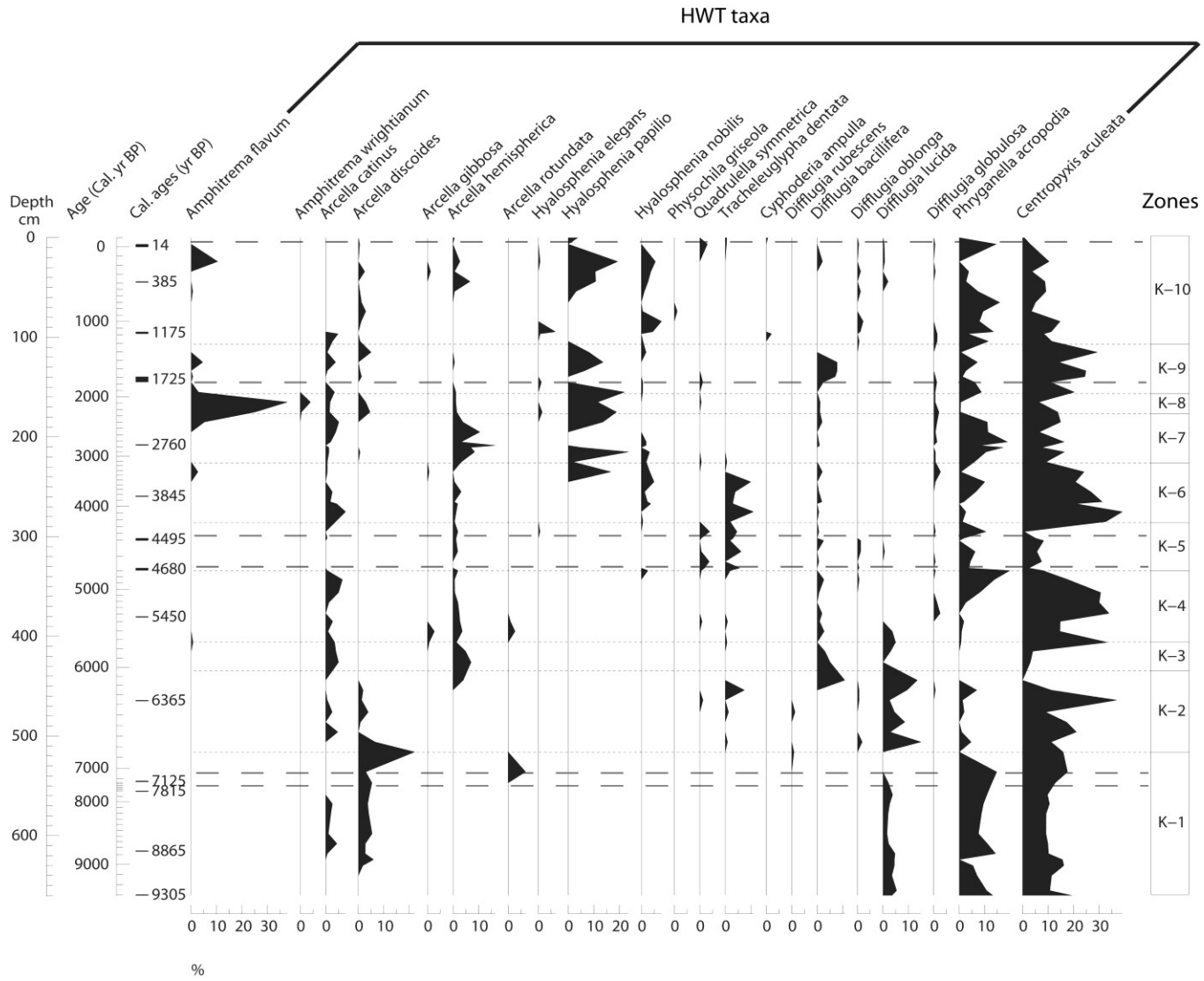

Figure 5.4.(a). Testate amoeba (TA) microfossil diagram for Krutoberegovo, Kamchatka Peninsula, Russia. TA percentages were calculated using the sum of TA counts, and plotted against depth (cm) and age (cal yr BP) using Psimpoll 4.27 (Bennett, 2007). TA taxa were divided into three groups: high water table taxa (HWT), Intermediate/variable water table taxa (IWT), and low water table taxa (LWT). The summary diagram for species groups is plotted at the end of the diagram (Fig. 5.3(d)). The diagram was subdivided into ten local TA assemblage zones using CONISS (Grimm, 1987); the boundaries of each zone are indicated by solid gray lines and located on the right side. Major volcanic eruptions (Table 5.2) are plotted using dashed gray lines.

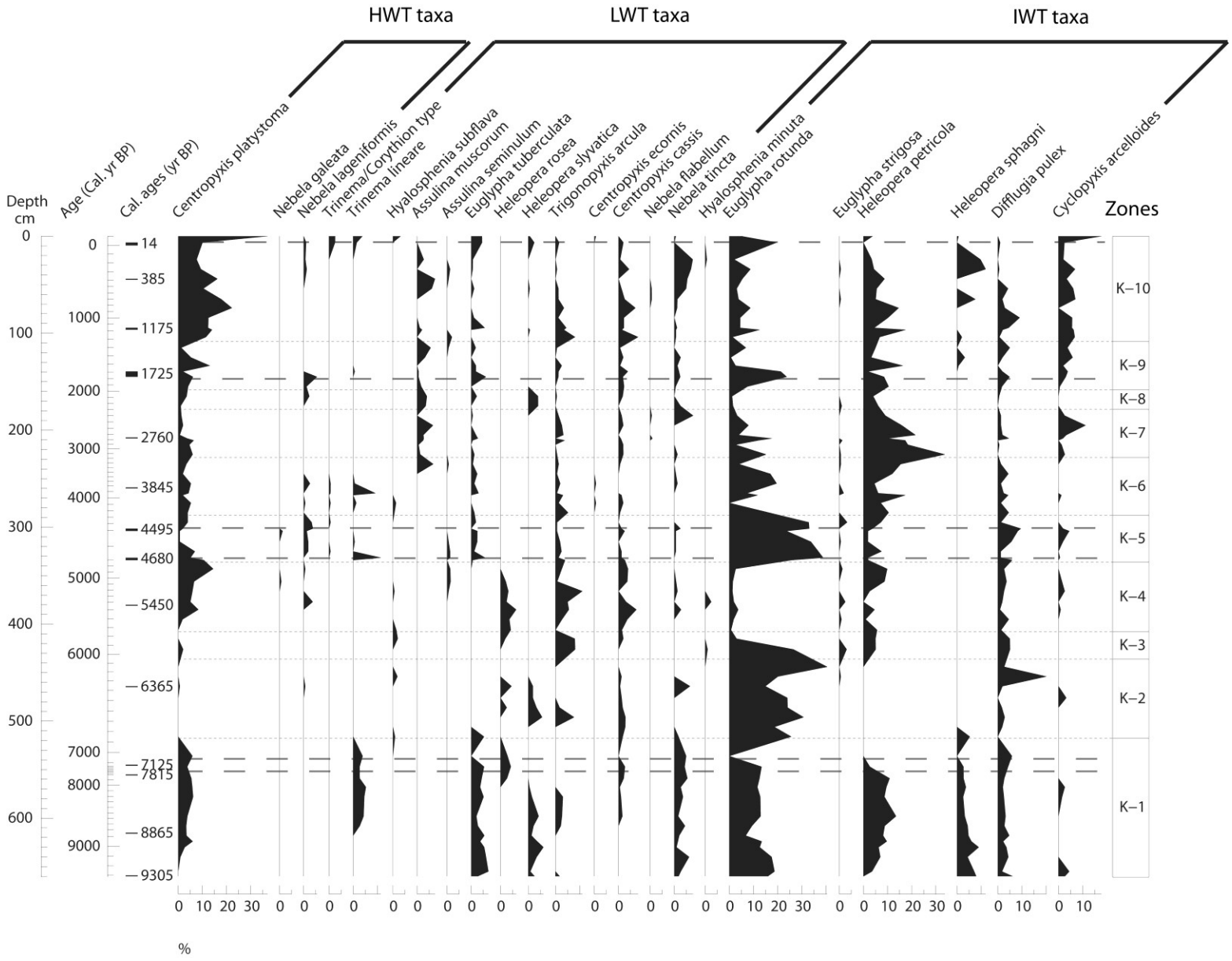

Figure 5.4.(b). Testate amoeba (TA) microfossil diagram for Krutoberegovo, Kamchatka Peninsula, Russia, continued, page 2/4

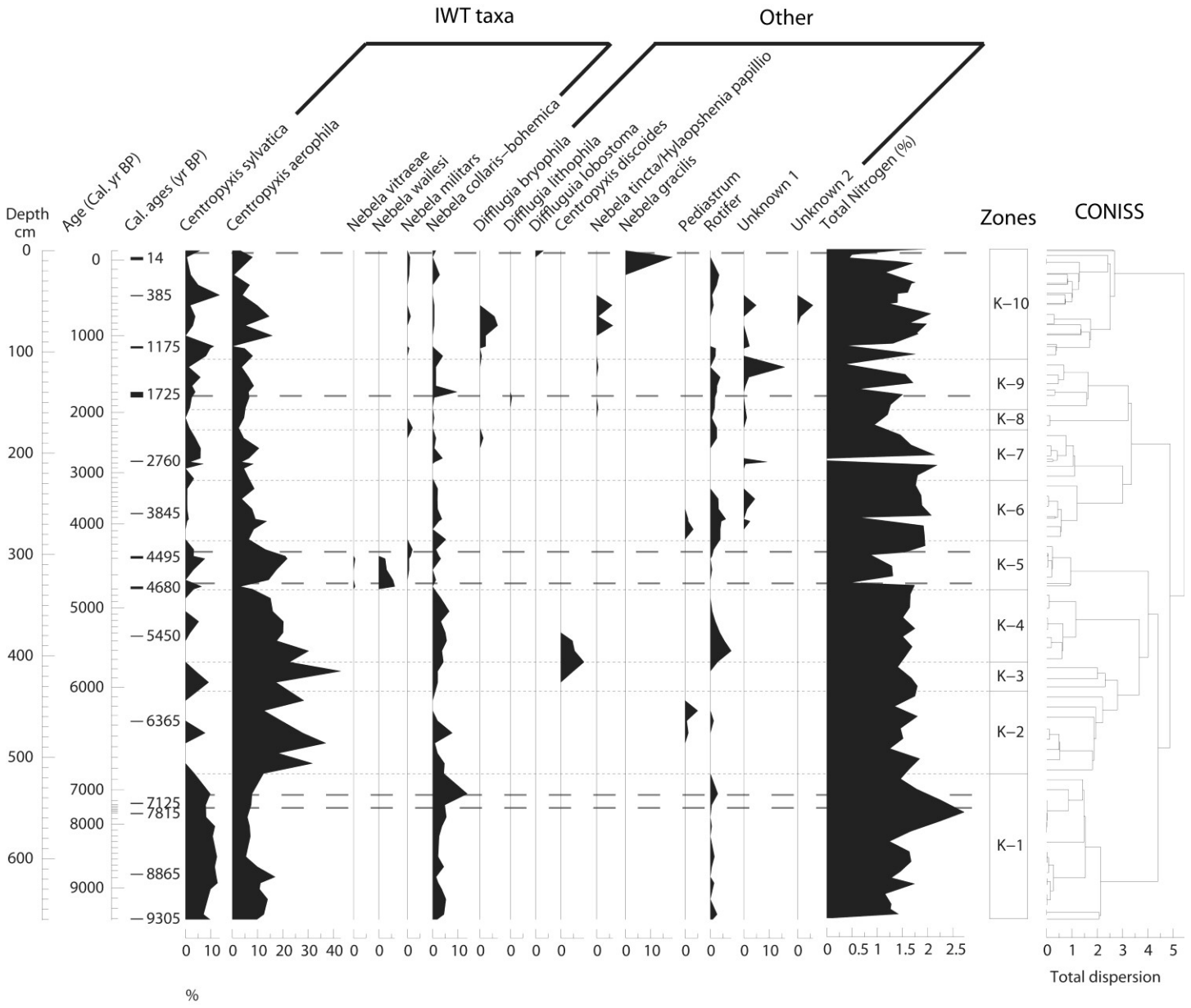

Figure 5.4.(c). Testate amoeba (TA) microfossil diagram for Krutoberegovo, Kamchatka Peninsula, Russia, continued, page 3/4

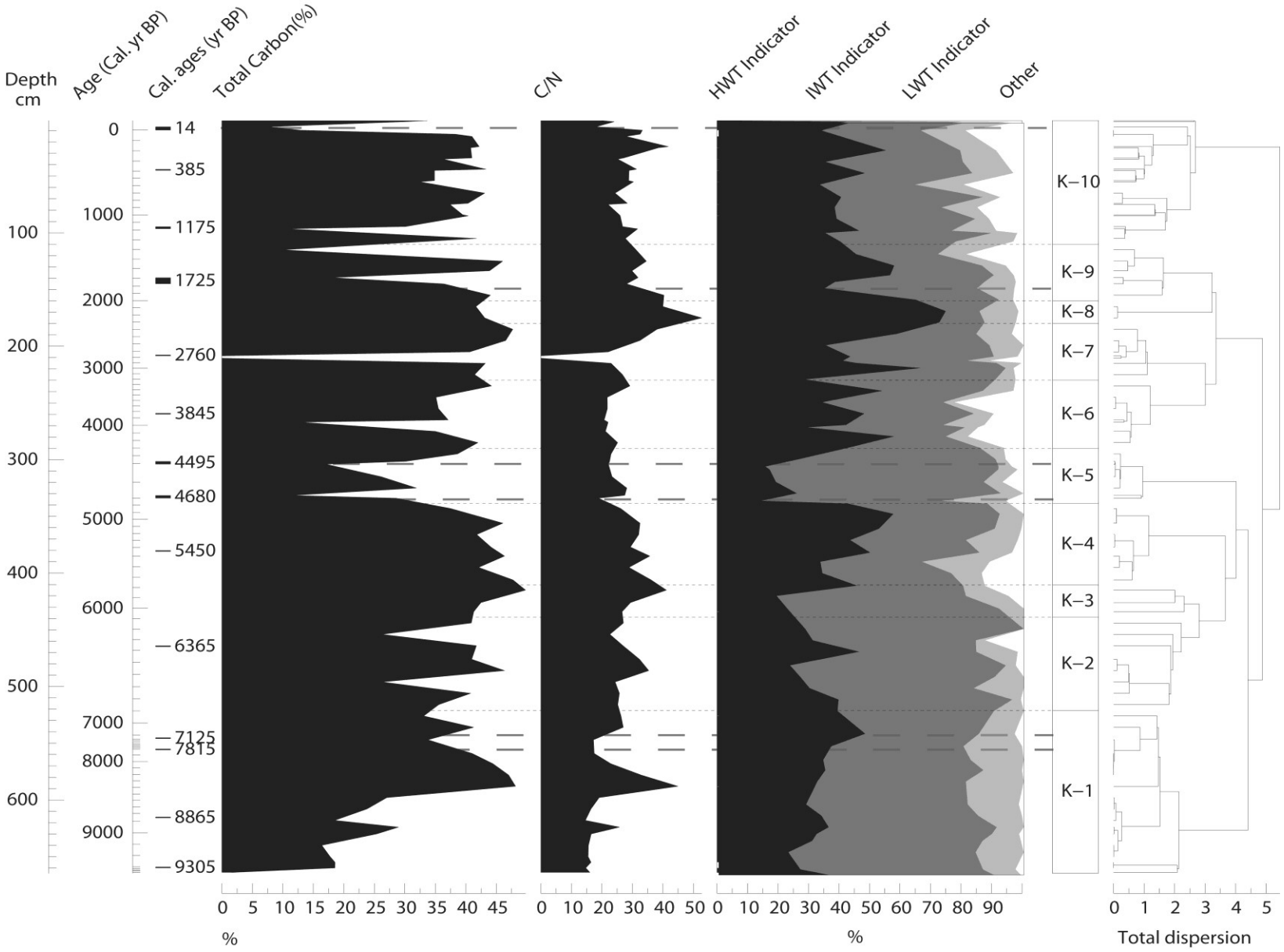

Figure 5.4.(d). Testate amoeba (TA) microfossil diagram for Krutoberegovo, Kamchatka Peninsula, Russia, continued- page 4/4

5.4 Geochemical Analysis

The geochemical analysis results for carbon content, nitrogen content, and C/N ratios are presented in Figure 5.5. The mean carbon content for the peatland profile is 31.69%, however, there is a large variability in the carbon content with values ranging from 0.311 to 49.802%. The carbon content during the inception of the peatland was low and stable, however, at 660cm, or ~9700 cal yr BP, the carbon content increases dramatically from 1.5% to 18.54%. It remains stable at ~16.5-18.5%, before increasing again to 25% at 630cm. Between 630cm and 598cm, carbon content percentages remain fairly stable before increasing significantly to 48% at 588cm. The values remain high between 588-559cm, before dropping slightly at 547cm (~7200 cal yr BP), and then increasing again at 536cm. Another significant increase occurs at 415cm to 49%. The carbon content remains in the 40% range up to 334cm-depth, where it drops dramatically to 28% and then to 11% at 331.5cm-depth (~4680 cal yr BP), coinciding with a major tephra deposition (SHdv). Another substantial increase is recorded at 325cm-depth (31.9%), after which it remains fairly stable up to 304 cm-depth (~4495 cal yr BP) where it decreases to 17%, coinciding with a tephra deposition (SH#33). Carbon content increases again between 301.5 and 275 cm-depth reaching ~39%, before it decreases substantially at 267cm-depth (~3943 cal yr BP), which coincides with a tephra deposition (SH#30). Carbon content percentages increases steadily between 255cm and 145cm-depth, before dropping again at 139.5cm (~1725 cal yr BP.), which coincides with the volcanic eruption KS_1 and the associated tephra deposition. Carbon content increases at 133.5cm and 125cm, before decreasing at 115cm (~1404 cal yr BP), coinciding with a tephra deposition (KL). It increases at 105cm to 41.7% but drops again at 96.6cm (~1175

cal yr BP), coinciding with the volcanic eruption of SH1450. Carbon content percentages increase and remain fairly stable (31-43%) between 94.5 and 13cm-depth, after which it decreases between 9.5 and 6.5cm (AD1964), coinciding with the volcanic eruption of SH1964. Since AD1964, carbon content has increased to an average of 32%.

The elemental analyzer results showed a mean nitrogen content for the entire sediment profile of 1.38%, with a variability range of 0.043-2.72% (Figure 5.5). Overall, the nitrogen content appears to have increased over time. Similar to the carbon content, nitrogen content remains fairly low and stable in the early peatland stages with less than 1%. Nitrogen content remains in the 1-1.7% range between 664-578cm, before increasing significantly at 559cm to 2.72%. The nitrogen content then decreases to 1.77% at 536cm and remains stable for an extended period. At 331.5cm (~ 4680 cal yr BP), the nitrogen content decrease to 0.4%. Between 301.5cm and 267cm (~ 3843 cal yr BP), an overall pattern of increasing and decreasing can be observed. Following a pattern similar to that of the carbon content, the nitrogen content increases to ~2%, before it decreases again at 139.5cm (~1725 cal yr BP) (KS_1 eruption) to 0.6%. Low nitrogen content values are recorded at 115cm (0.375%) (~ 1404 cal yr BP), coinciding with the KL eruption, and at 96.5cm (0.39%) (~ 1175 cal yr BP) coinciding with the SH1450 eruption. The nitrogen content increases and remains fairly stable between 94.5 and 13 cm, before dropping again between 9.5 and 6.5 cm-depth to 0.45% (AD1964) (SH1964 eruption). The period between AD1964 and present is characterized by increasing nitrogen content.

Overall, C/N ratios (Figure 5.5) show a variable but increasing trend from the peatland inception to present day. It is apparent, however, that peat deposited during periods of high tephra loading, such as between 5800 and 4000 cal yr BP, the C/N ratios

seem to decrease, while during periods of volcanic quiescence, such as between 8000 and 5800 cal yr BP, C/N ratios tend to increase.

Figure 5.5: Carbon and nitrogen chemistry and carbon accumulation rates (LORCA) for the Krutoberegovo peatland, Kamchatka Peninsula, Russia, by age (cal yr BP) and depth (cm). Gray dashed lines represent volcanic eruptions.

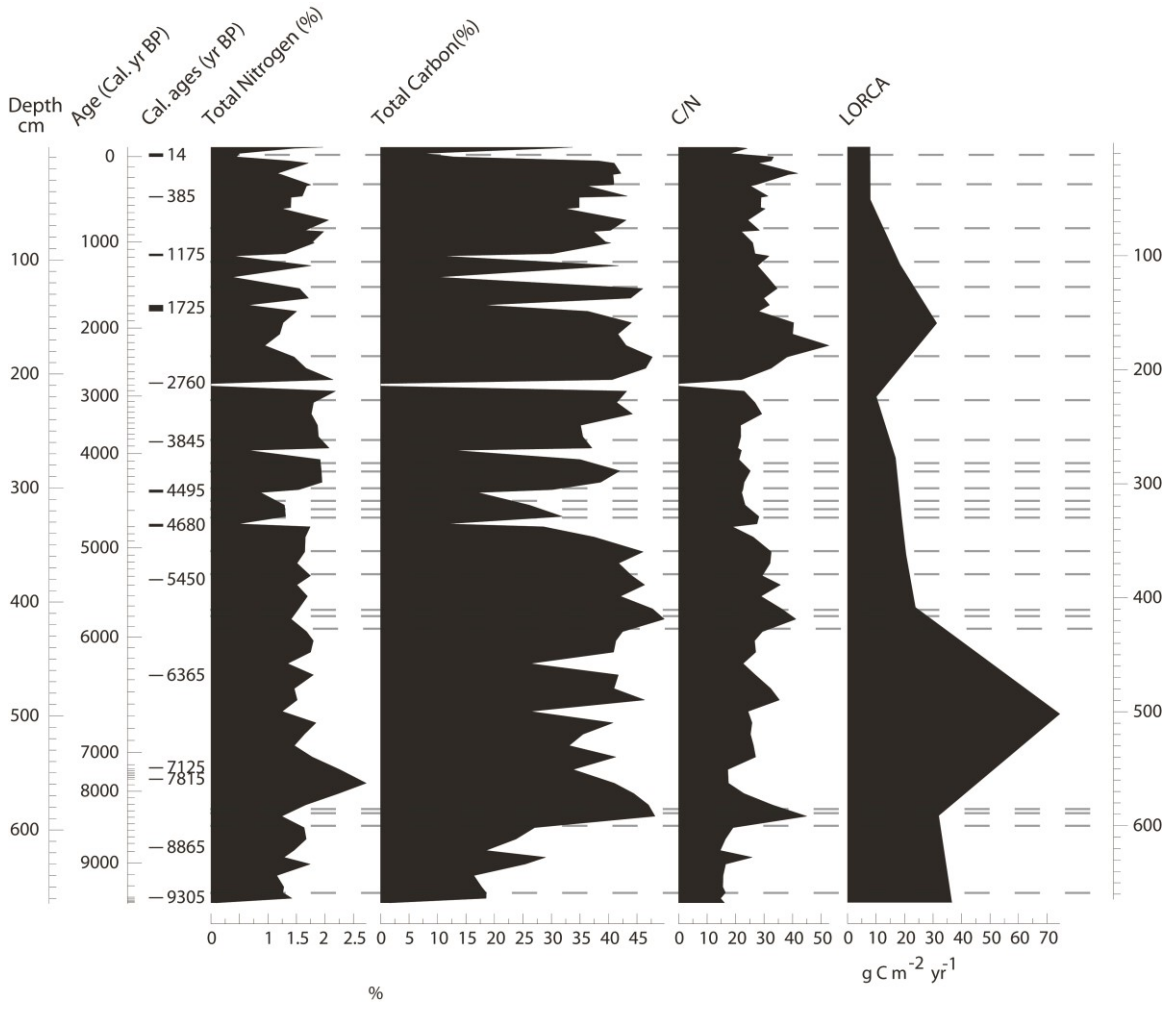

5.5 Carbon accumulation

Long-term apparent rates of carbon accumulation (LORCA) were calculated using the radiocarbon dates listed in table 5.1, the measured percentage of total organic carbon (TOC) for each sample, and rate of peat accumulation. LORCA are expressed in g C m^{-2} yr^{-1} and values are provided in Figure 5.6. Throughout the peat profile, average LORCA values showed considerable variation and an overall increase in LORCA was observed with increasing age. At ~9010 cal. yr. BP, carbon accumulation rates were estimated at 36 g C m^{-2} yr^{-1}. The rate at which carbon accumulated then decreased slightly from ~9010 to ~7240 cal. yr BP, to 32 g C m^{-2} yr^{-1}. Following this slight decrease, there was a dramatic increase in LORCA values to 74.5 g C m^{-2} yr^{-1} at ~6430 cal. yr BP. After ~6430 cal yr BP, LORCA dropped significantly to 23.8 g C m^{-2} yr^{-1}. This decreasing trend continued from ~5490 - ~2740 cal yr BP, with 20.5 g C m^{-2} yr^{-1} at 4690 cal yr BP, 19 g C m^{-2} yr^{-1} at ~4565 cal. yr. BP, 16.8 g C m^{-2} yr^{-1} at ~3900 cal yr. BP, and 10.1 g C m^{-2} yr^{-1} at ~2740 cal. yr. BP, respectively. At ~1755 cal. yr BP, LORCA values increased again to 31.3 g C m^{-2} yr^{-1}. After this increase, the LORCA dropped to 18.4 g C m^{-2} yr^{-1} at ~1180 cal. yr BP. Finally, the lowest LORCA values recorded for the entire profile were recorded at ~385 cal. yr BP and AD1964, with less than 10 g C m^{-2} yr^{-1} (7.96 and 7.91 g C m^{-2} yr^{-1}, respectively).

When comparing the LORCA values from this study to the mean LORCA values of various peatlands around the world, it can be seen that the LORCA values in this study are similar to those reported for northern peatlands. Northern peatland LORCA values range from 14.6 g C m^{-2} yr^{-1} to 22.5 g C m^{-2} yr^{-1} (Bunbury et al., 2012; Jones & Yu, 2010; Loisel & Garneau, 2010; Tolonen & Turunen, 1996; Bellen et al., 2011; Yu, 2011). In

contrast, the mean LORCA values for several temperate peatlands ranges from 22 g C m^{-2} yr^{-1} to 60 g C m^{-2} yr^{-1} (Cai & Yu, 2011; Poulter et al., 2006; Turunen et al., 2004). Finally, the mean LORCA of several tropical peatlands ranges from 28 g C m^{-2} yr^{-1} to 108 g C m^{-2} yr^{-1} (Lähteenoja et al., 2012; Page et al., 2003).

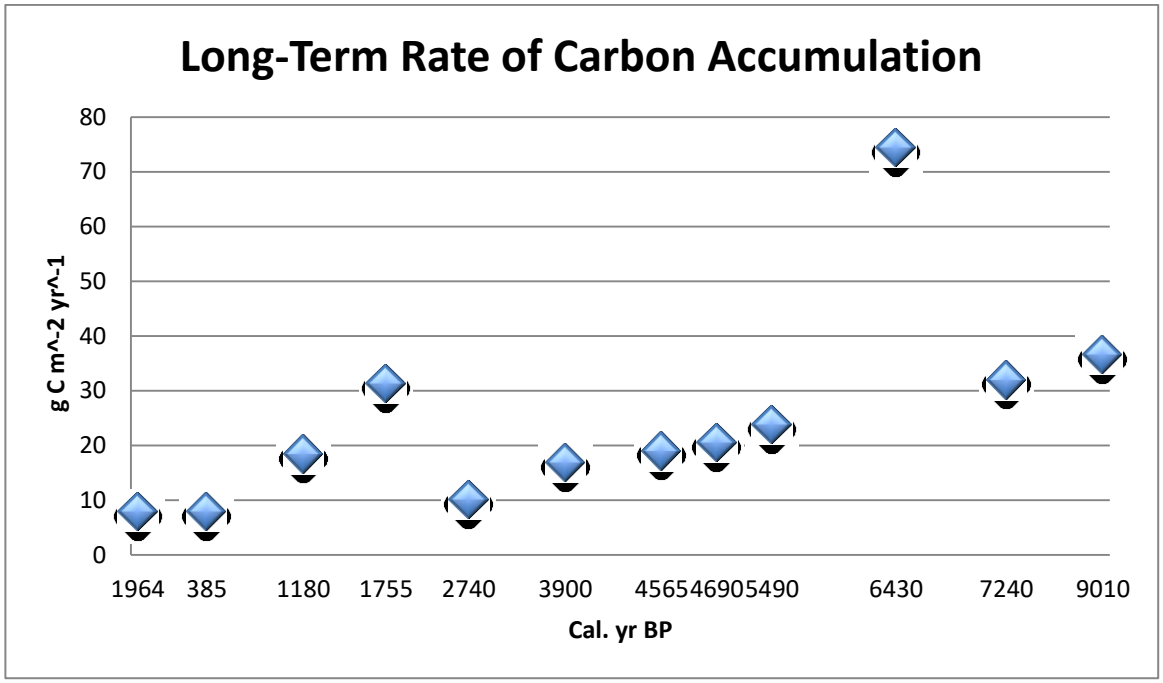

Figure 5.6: Long-term apparent rate of carbon accumulation (LORCA) results for Krutoberegovo peatland, Kamchatka Peninsula, Russia. Calculations based on 14C dating, measured TOC percentages, and rate of peat accumulation.

5.6. Statistical analysis: Redundancy Analysis (RDA)

The RDA results (Table 5.6) show the relationship between the environmental variables (total ash content, C/N, and volcanic eruptions) and the testate amoebae communities for the Krutoberegovo peatland, Kamchatka Peninsula, Russia. Total ash content accounted for 77.3% of the variation observed in the species dataset, the major volcanic eruptions as discrete events accounted for 6.3% of the variance, and C/N ratios accounted for 16.4% of the variance. The RDA ordination biplot (Figure 5.7) illustrates

the relationship between the selected TA taxa and the environmental variables. Some high water table indicators (HWT) (ex. *Amphitrema flavum, Amphitrema wrightianum, and Hylosphenia papillio)* are positively correlated with C/N and negatively correlated with major volcanic eruptions. Intermediate/variable water table (IWT) indicator species, such as *Euglypha rotunda, Difflugia pulex, Heleopera petricola, Cyclopyxis arcelloides*, *Centropyxis sylvatica,* and *Centropyxis aerophila,* appear all throughout the ordination plot, showing no strong correlation to any particular environmental variable. Some low water table taxa (LWT), such as *Trinema/Corythion*-type, and *Euglypha tuberculata* are positively correlated with major volcanic eruptions and negatively correlated with the C/N ratios.

Table 5.6 Results of redundancy analysis (RDA) of testate amoebae data for Krutoberegovo peatland, Kamchatka Peninsula, Russia. Data was log-transformed and shows percentage variance explained using three environmental variables: total ash content, C/N, and major volcanic eruptions as discrete events. Percentage variance and p-value determined by Monte-Carlo permutations tests (999 permutations).

Explanatory variable	% variance explained	*p-value*	F-ratio
Ash	77.3	0.3460	1.08
Carbon/Nitrogen Ratio	16.4	0.0020	5.01
Major Eruptions	6.3	0.9380	0.43

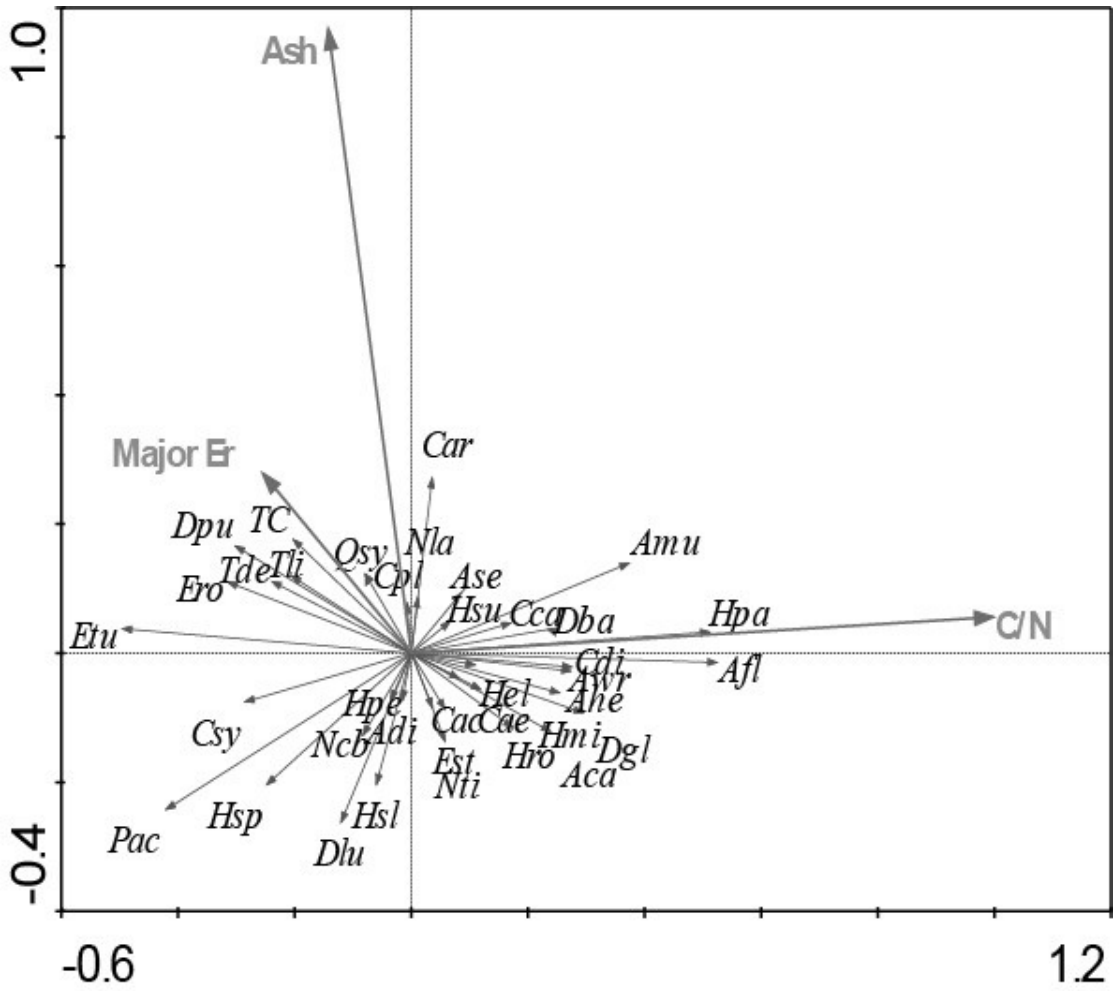

Figure 5.7: Redundancy Analysis (RDA) plot for Krutoberegovo peatland, Kamchatka Peninsula, Russia, of testate amoebae assemblages constrained by explanatory environmental variables: major volcanic eruptions, total ash content, and carbon/nitrogen (C/N) ratios.
Abbreviations for TA species are Afl=Amphitrema flavum, Aca=Arcella catinus, Adi=Arcella discoides, Ahe=Arcella hemispherica, TC=Trinema-Corythion Type, Tli=Trinema lineare, Hmi=Hyalosphenia minuta, Hel=Hyalosphenia elegans, Hpa=Hyalosphenia papillio, Tde=Tracheleuglypha dentate, Amu=Assulina muscorum, Ase=Assulina seminulum, Etu=Euglypha tuberculata, Ero=Euglypha rotunda, Hro=Heleopera rosea, Hsl=Heleopera sylvatica, Hpe=Heleopera petricola, Hsp=Heleopera sphagni, Dpu=Difflugia pulex, Dba=Difflugia bacillifera, Dlu=Difflugia lucida, Dgl=Difflugia, Car=Cyclopyxis arcelloides, Pac=Phryganella acropodia, Cac=Centropyxis aculeata, Cpl=Centropyxis platystoma, Cca=Centropyxis cassis, Csy=Centropyxis sylvatica, Cae=Centropyxis aerophila, Cdi=Centropyxis discoides, Nti=Nebela tincta, Ncb=Nebela collaris-bohemica, Nla=Nebela lageniformis.

Chapter 6

6) Discussion

6.1 Testate amoeba-inferred palaeohydrology in the context of local wetland vegetation development

Palaeoecological studies in peatlands have been widely used to reconstruct long-term changes in various environmental and climate parameters (e.g. Barber, 1981; Mauquoy et al., 2002a, b; Bellen et al., 2014). In peatland ecosystems, water table fluctuations are linked to changes in precipitation and temperature regime (e.g. Charman et al., 2004; Mauquoy & Yeloff, 2007). Testate amoebae (TA) are a group of protists that have been widely used in studies of palaeohydrological conditions in peatlands often combined with the analysis of other proxies, such as plant macrofossils, pollen, and stable isotopes (e.g. Charman et al., 1999; Loisel et al., 2009; Klimaschewski et al., 2015). In particular, the community composition of TA in peatlands is directly linked to peat surface wetness, measured as depth to water table (DWT) (e.g. Warner & Charman, 1994; Mitchell et al., 2013). Because of their decay resistant and morphologically distinct tests, identification of past assemblages is relatively straightforward. Studies of testate amoebae ecology and palaeoecology have been mostly restricted to North America and Europe. To assess the usefulness of TA communities around the world, modern and palaeoecological data on the structure of TA communities and the characterization of species-environment relationships are needed from a variety of regions and peatland types. In Kamchatka Peninsula, to our knowledge, only one study has used testate

amoebae from peatlands to reconstruct environmental changes (Klimaschewski et al., 2015).

In this thesis, a high-resolution testate amoebae record spanning the last 10,000 years was used to reconstruct relative moisture conditions of a small peatland basin near Krutoberegovo village, in eastern Kamchatka Peninsula, Russia. The TA derived moisture conditions were compared with pollen data from a parallel study (Pendea et al., 2016). Normally, peat surface wetness is derived quantitatively using transfer functions (e.g. Warner & Charman, 1994; Booth, 2008; Bellen et al., 2014) based on modern amoebae training sets sampled from surface peat with corresponding measurements of environmental variables, such as water table depth and pH. To date, there are no available modern TA training sets for Kamchatka. Although most testate amoebae species are cosmopolitan (i.e., not restricted to a specific region), there are regional variations in community composition and some taxa are limited to certain regions (e.g., Turner et al., 2013). It follows therefore, that quantitative data for peat surface conditions were unable to be derived at the study site. Instead, qualitative inferences of water table affinities of various testate amoebae species published in the literature (table 4.6.1) was used.

The testate amoebae-derived peat surface moisture conditions, together with pollen-derived wetland development at the Krutoberegovo site, reveal complex patterns of change over the last 10,000 years. To allow for comparison between this study and well-constrained chronologies for the Northern Hemisphere, the Holocene nomenclature suggested by Walker et al., (2012) was used as follows:

6.1.1. Early Holocene (9700-9000 cal yr BP)

While the pollen record (Figure 6.1. (a, b)) starts during the Late Glacial (ca.16000 cal yr BP), poor preservation of TA tests in the bottom sediments of the core does not allow a TA analysis before 9700 cal yr BP. The first TA community at the site indicates intermediate/variable water table (IWT) conditions, probably in response to an unstable supply of atmospheric moisture. A slight increase in high water-table (HWT) indicators towards the end of this period may indicate a transition towards higher water tables. This interpretation is supported by the pollen record, which shows a decrease in grasses (Poaceae) and an increase in ferns (Filicales) and horsetails (*Equisetum*) (Figure 6.1. (a, b)), suggesting an overall increase in atmospheric moisture during this period. In fact, the appearance of obligate aquatic pollen at the end of this period (*Potamogeton/Triglochin*) indicate that the peatland might have become a wet fen with pools of standing water.

6.1.2. Middle Holocene (9000-5000 cal yr BP)

The middle Holocene period is characterized by a high degree of variability in terms of both TA assemblages and pollen spectra. Between ca. 9000 and 7000 cal yr BP, a steady increase in HWT TA indicators, which reach a maximum ca. 7100 cal yr BP, suggests a rising water table throughout the peatland. This development is in agreement with the pollen-derived local vegetation development, which features the presence of a variety of aquatic and wetland taxa such as *Potamogeton/Triglochin,* sedges (Cyperaceae), horsetails (*Equisetum*), and brown mosses (Bryidae). This vegetation development together with TA data suggest that between 9000 and 7000 cal yr BP the Krutoberegovo peatland was characterized by a wet fen ecosystem dominated by brown

moss hummocks and pools of standing water. Between ca. 7000 and 5000 cal yr BP the peatland vegetation suffered a substantial transformation. Most of the aquatic, wetland, and wet soil indicators such as *Potamogeton/Triglochin,* Filicales, *Equisetum*, and brown mosses (Bryidae) all but disappear from the pollen spectra. The only notable exception is the sedges (Cyperaceae), which increase substantially during this time. The TA assemblages characterizing the peatland during this period is complex and reveals patterns that are only partly in agreement with the vegetation development. The period between 7000 and 5800 cal yr BP features a steady decrease in HWT TA taxa suggesting a progressing drying of the peat surface due to lower water tables, largely in agreement with the vegetation development. The period between 5800 and 5000 cal yr BP, however, is marked by a dissonance between the TA and pollen data. While the pollen-derived vegetation reconstruction indicates no increase in moisture availability during this period, the TA assemblages suggest a steady increase in water tables as HWT TA indicator communities increase considerably during this time to the detriment of IWT and LWT assemblages. The reason for the dissonance is unclear, however, on possible explanation for this discrepancy is that pollen is not only representative of the wetland itself, but also for surrounding and upland ecosystems as pollen has the ability to travel large distances from the place of origin and thus indicative of a much wider area. Testate amoebae however, is more representative of the immediate wetland and changes to the specific wetland under study.

6.1.3. Late Holocene (5000 cal yr BP-Present)

The late Holocene period debuts with a marked change in both wetland vegetation and testate amoebae communities. The wetland vegetation development is characterized

by a dramatic decrease in sedges (Cyperaceae), which corresponds with an increase in grasses (Poaceae). At the same time, brown mosses (Bryidae) reappear after being absent for almost two millennia, and probably represent the main peat forming vegetation type. While sedges, as a whole, have a fairly broad hydrological range, the increase in grasses and reappearance of brown mosses, with a simultaneously dramatic decrease in sedge appearance, would indicate that sedges in this scenario are indicative of more wet surface conditions. This vegetation development suggests a wetland succession from a sedge-dominated wet fen to a drier, moss-dominated ecosystem. The dramatic increase in grasses is certainly an indication of an overall drying of the landscape. This interpretation in strongly in agreement with changes in the peatland's protist community. Between 4800 and 4500 cal yr BP, there is a dramatic decrease in HWT TA indicator taxa, which indicates a substantial lowering of the water table at the site. It is unclear whether the peat surface moisture changes have a climatic significance or are the product of the deposition of two major tephra, which bracket this interval (see section 6.2 for further details).

The remainder of the late Holocene is characterized by changing wetland ecosystem conditions, paralleled by changes in peat surface moisture. Between 4500 and 3000 cal yr BP, the sedge (Cyperaceae) dominated wet fen, extant during the latter part of the middle Holocene, is reestablished as suggested by a dramatic increase in sedge pollen. However, the sedge-dominated fen is short lived as beginning ca. 3000 cal yr BP the composition of the wetland vegetation changes substantially and is marked by the appearance and the increase of low shrub bog species such as bayberry (*Myrica*) and heaths (Ericaceae). This vegetation development in conjunction with the notable appearance of *Sphagnum* mosses signals a profound shift in the wetland ecosystem,

namely the transition from rich sedge fen to *Sphagnum* and shrub poor fen. The TA inferred peat surface moisture conditions is characterized by an overall rise in water table, as indicated by increasing HWT TA indicator taxa and corresponding decrease in IWT TA indicators. The increase in HWT indicators culminates between ca. 2500 and 2000 cal yr BP, and represents the wettest period in the peatland's history.

The combined pollen and TA palaeoecological records (Fig. 6.1.a, b and Fig. 5.1. a-d), suggests that wetland development and peat surface moisture conditions may have been climatically driven. The appearance of cool oceanic climate indicators such as *Sphagnum* mosses, heaths (Ericaceae), and dwarf pine (*Pinus pumila)* suggest that the Late Holocene in eastern Kamchatka was cooler and wetter than the Middle Holocene. This interpretation is in agreement with existing paleoclimate reconstructions for Kamchatka (Self et al., 2015; Hammarlund et al., 2015; Pendea et al., under review) which indicate a Neoglacial cooling during the Late Holocene throughout Kamchatka. In particular, Hammarlund (2015), document the substantial expansion of dwarf pine (*Pinus pumila)* and interprets this as an indication of cool summers and cold winters with increased snow cover.

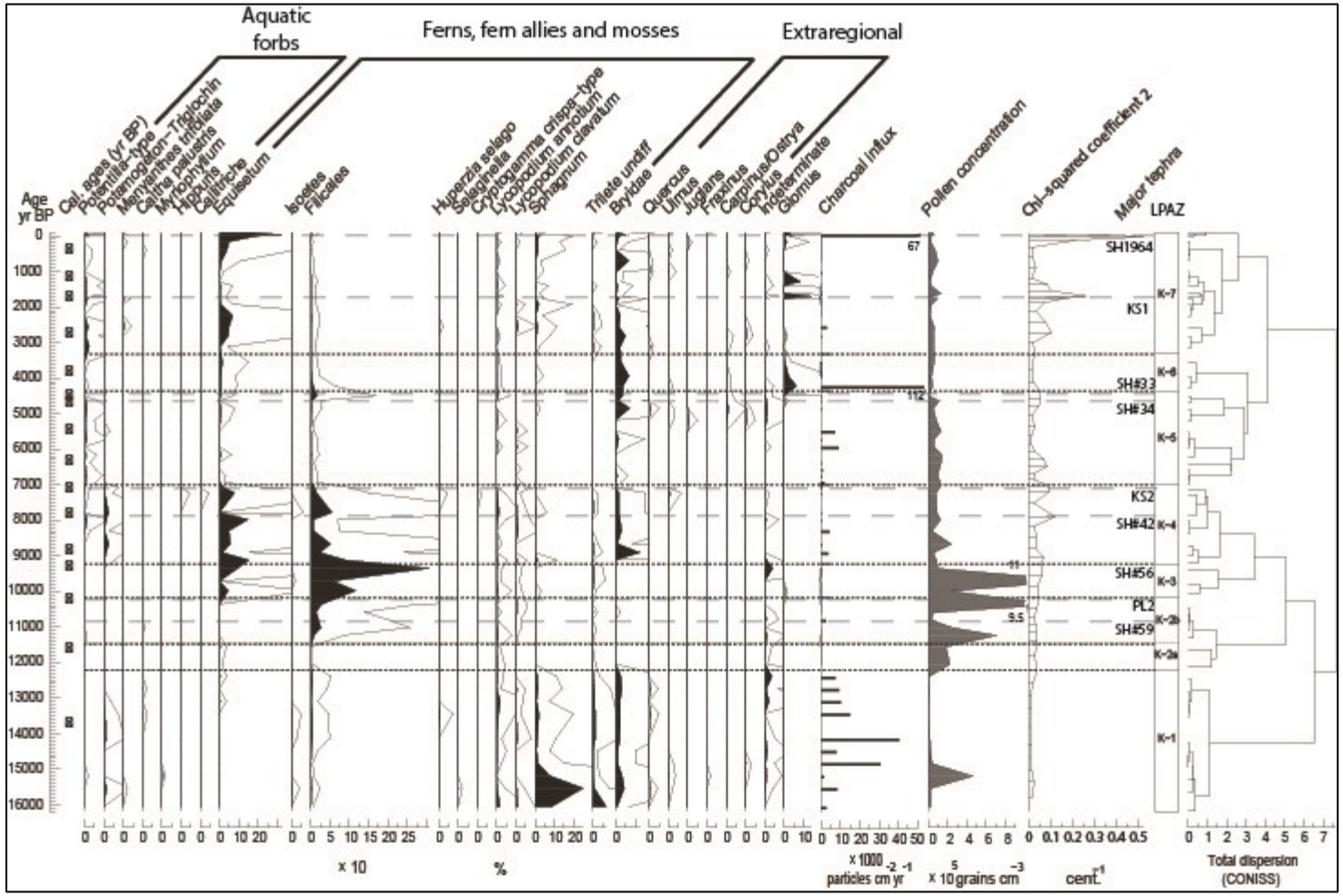

Figure 6.1.(a). Pollen diagram for Krutoberegovo, Kamchatka Peninsula, Russia (Pendea et al., under review). Pollen percentages were calculated using the sum of pollen counts, and plotted against depth (cm) and age (cal yr BP) using Psimpoll 4.27 (Bennett, 2007).

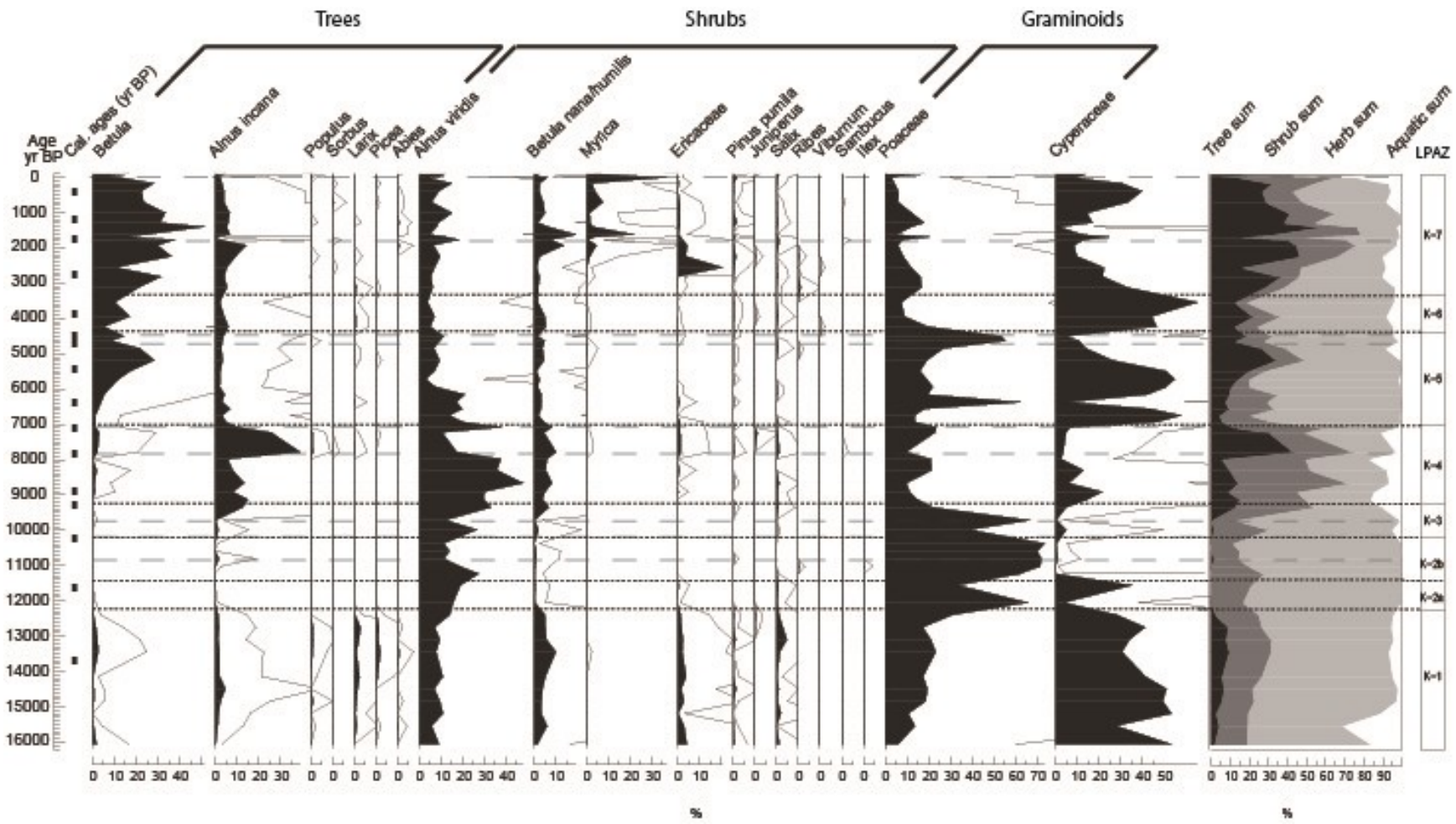

Figure 6.1.(b). Pollen diagram for Krutoberegovo, Kamchatka Peninsula, Russia (Pendea et al., under review). Pollen percentages were calculated using the sum of pollen counts, and plotted against depth (cm) and age (cal yr BP) using Psimpoll 4.27 (Bennett, 2007).

6.2. Tephra impact on testate amoebae communities as indicators of hydrological change

Volcanic eruptions can have significant impacts on global climate and catastrophic impacts on the areas in the immediate vicinity (Blackford et al., 2014). Many peatland areas lie within reach of volcanic activity and products of volcanic eruptions (tephras) have been found in peatlands around the world (e.g. Dugmore, 1989; Hang et al., 2006; Payne, 2012; Hughes et al., 2013). The impacts of these volcanic materials have been addressed by only a few studies, but there is reason to believe that the effect of tephra deposition on ecosystem might be relatively severe (e.g., Hotes et al., 2004; Payne & Blackford, 2005; Payne, 2012). Current understanding of tephra impacts on ecosystems is biased towards recent volcanic eruptions and while these studies provide valuable insights, most are of considerably smaller magnitude than many that have taken place during the course of the Holocene. Different proxy records, especially ice core data, show that large eruptions have caused global scale impacts on climate (e.g. LaMarche & Hirschboek, 1984; Baillie & Munro, 1988; Rampino & Self, 1992; Briffa et al., 1998; Zielinski, 2000). Research shows that the tephra impact on peatlands is primarily due to sulfate deposition (Payne et al., 2010). Peatlands that are exposed to sulfate deposition from both anthropogenic sources (fossil fuel burning) and natural sources (volcanoes) are affected by a reduction in methane production and emission (e.g. Payne et al., 2010), which is a highly important process in terms of global climate change. The mechanism through which sulfate deposition affects the methane flux in peatlands is believed to be related to microbial competitive shifts (Payne, 2012). Since testate amoebae are the dominant microbial group in peatlands, it can be hypothesized that shifts in testate

amoebae communities may be responsible for the reduction of methane production following tephra deposition.

In this thesis, changes in the TA microbial communities were documented in response to repeated tephra loading of peat surface. Previous studies have shown statistically significant changes in community composition with the reduced abundance of small bacterivorous taxa (Payne, 2010; Payne, 2012). The fact that the largest and most consistent changes are apparent in bacterivorous taxa appears to support the hypothesis of a sulfate-induced change in methane production via TA predation of methanogenic bacteria (Payne, 2012). However, studies documenting changes in microbial communities following volcanic eruptions are very few and therefore much more work needs to be done to test this hypothesis.

The deposition of more than thirty tephra layers over the last 10,000 years in the Krutoberegovo peatland, allows for an excellent opportunity to further document tephra impact on testate amoebae. The redundancy analysis (RDA) (Table 5.5), of the relationship between the testate amoebae community and tephra related environmental variables (total ash content and major eruptions) shows that tephra deposition explains to a large degree the shifts in TA communities. Total ash content explains 77.3% of the taxa variability, while major volcanic eruptions explains 6.3%. The taxa most affected by tephra deposition (Fig. 5.6) are *Euglypha rotunda, Euglypha tuberculata, Difflugia pulex, Trinema/Corythion type, Trinema lineare, Centropyxis platystoma, Tracheleuglypha dentata,* and *Quadrulella symmetrica*. While the changes in these taxa are statistically significant, the direction of change is not unequivocal. For instance, *Euglypha rotunda* disappears following the eruption of Ksudach (KS_2) volcano ca. 7200 cal yr BP (Figure

5.4a-d), but seems to increase considerably following three other later eruptions, namely Shiveluch (SHdv) at 4680 cal yr BP, Shiveluch #33 at 4495 cal yr BP, and Ksudach (KS_1) at 1725 cal yr BP. Similarly, *Centropyxis aculeata* decreases sharply in abundance across two Shiveluch tephras (SHdv and SH#33) but seems to increase following the eruptions of Shiveluch (SH#42) and Ksudach (KS_2) at 7780 and 7204 cal yr BP, respectively. This situation is not unique to the Krutoberegovo peatland. For example, Payne & Blackford (2008) found that *Amphitrema flavum* increases in abundance across three tephras and decreases in abundance across three others. Some taxa feature changes that are more consistent. For instance, *Heleopera petricola* disappears or decreases in abundance across all major eruptions (Figure 5.4). One possible explanation for the lack of consistency in tephra impact on TA taxa community change for some species is that these changes are not due to the direct toxicity of the volcanic products but rather to the volcanically forced microenvironmental changes, which vary substantially in space and time.

An important aspect of tephra impact on TA communities in the Krutoberegovo peatland is related to peat surface hydrology. The question is, are changes in TA communities across tephra deposition events indicative of hydrological change? The palaeoecological data in this thesis provides some evidence for hydrological changes following tephra deposition, but these changes are not straightforward and the mechanisms through which they occur is unclear. For instance, the RDA ordination analysis of TA taxa in relation to major volcanic eruptions (Fig. 5.6) shows that some taxa indicative of dry conditions, such as *Trinema/Corythion*-type and *Euglypha tuberculata* are positively correlated with major volcanic eruptions, while others

(*Heleopera rosea, Assulina muscorum,* and *Nebela tincta)* show no particular relationship with the deposition of major tephra. Similar results are illustrated in the TA diagram (Fig. 5.4.a-d), which shows an increase in the abundance of some LWT TA indicator taxa (e.g. *Trinema/Corythion type* and *Euglypha tuberculata*), following some of the major eruptions (e.g., SH1964). A possible drying of the peat surface is also suggested by the pollen data (Fig. 6.1.a, b), which shows a shift from sedges to grasses following some tephra deposition events. In fact, it is possible that tephra impact on peat surface hydrology is mediated by changes in wetland plant cover. For instance, Payne & Blackford (2008), suggest that tephra deposition might affect wetland plant functioning leading to a shift from bryophytes to monocotyledons.

Other mechanisms of tephra impact on TA assemblages suggested in the literature are the chemical impact of tephra and tephra-derived leachates as well as the impact of volcanic gases and volcanically derived acid rain (Payne & Blackford, 2008; Hughes et al., 2014). Among these chemical effects, the Krutoberegovo record may provide support for an increase in nutrient availability as indicated by decreases in carbon/nitrogen ratios (C/N) (Figure 5.5).

6.3 Tephra impact on peatland carbon and nitrogen chemistry

Although extensive tracks of boreal peatland occur throughout the Pacific Rim region, from Northern Japan and Eastern Russia, to the Pacific seaboard of North America, a region in close proximity with chains of active volcanos, there have been very few studies have addressed the role of tephra deposition in changes to peatland carbon chemistry (Hughes et al., 2013; Blackford et al., 2014; Watson et al., 2015). Even fewer studies have examined the impact of tephra on peatland nitrogen chemistry (Hughes et

al., 2013). Most of these studies document a significant influence of tephra deposition on peatland carbon stores, although they differentiate heavy tephra loading near volcanoes from more distal impacts. In terms of tephra impact on nitrogen chemistry – a major nutrient for plant development- the existing information (Hughes et al., 2013) is unclear. However, there is little doubt that tephra loading on peatlands is a complex, non-linear process, which, on one hand restricts plant growth (toxicity, physical damage) and on the other enhances it, through the delivery of nutrients to the ecosystem (Wolejko & Ito, 1986; Malmer et al., 2003; Hughes et al., 2013).

In the Krutoberegovo record, the long-term and repeated tephra-related disturbances, have left their mark on both carbon and nitrogen chemistry, as well as on nitrogen availability as expressed by C/N ratios (Figure 5.5) shows that most of the tephra deposition events resulted in a net loss of carbon and nitrogen during the period following the eruptions. The mechanism through which this loss occurs is unclear, but it is likely mediated by changes in the composition and/or structure of the wetland plant cover. Ratios of macronutrients provide a good diagnostic tool for ecosystem functioning (Koerselman & Meuleman, 1996). For instance, C/N ratios provide an excellent measure of nitrogen availability in nitrogen limited ecosystems, such as peatlands. In ecosystems with high C/N ratios, plant growth is often restricted because of the lack of available nitrogen. Conversely, low C/N ratios are indicative of nutrient-rich ecosystems, largely dominated by plants with high nitrogen requirements. In the Krutoberegovo record, C/N ratios exhibit a complex but overall increasing trend (Figure 5.5). The general increase in C/N ratios may be consistent with an autogenic wetland development characterized by a progressive shift from nutrient rich communities dominated by graminoids (sedges and

grasses) towards nutrient-poor communities dominated by shrubs and mosses (e.g., Ericaceae, *Sphagnum*). The appearance of *Sphagnum* mosses together with some low shrubs (*Myrica*, Ericaceae) during the late Holocene (Fig. 6.1.a,b) does seem to suggest that autogenic wetland development is certainly a possible cause for the general increase in C/N ratios over the last 10000 years. It is also apparent, however, that peat deposited during periods of high tephra loading, such as between 4700 and 4000 cal yr BP, the C/N ratios seem to decrease, while during periods of volcanic quiescence, such as between 8000 and 5800 cal yr BP, C/N ratios tend to increase. The decrease in C/N ratios following tephra deposition means an increase in nitrogen availability within the peatland ecosystem, which in turn would favour plant growth but also intensify decomposition by favouring microbial activity. The net effect of these processes would then be reflected in the peatland's long-term carbon accumulation rates.

6.4 Tephra impact on long-term peatland carbon sequestration rates

The rate of carbon accumulation in peatlands is dependent on the balance between primary production and peat decomposition (Charman, 2002). Most studies show that the mechanisms and controls that govern carbon accumulation are related to climate change (e.g. Yu et al., 2010; Charman et al., 2012). For instance, climate warming has the ability to enhance decomposition processes resulting in net loss of carbon through increased efflux of CO_2 and methane (e.g., Yu et al., 2010). Another way through which climate warming may affect peatland carbon balance is through an increase in evapotranspiration and lowering of the water table. Lower water tables drive the drying of the peat surface, which in turn favors humification processes that are also responsible for a net loss of peatland carbon. While the climatic factors that govern feedbacks between carbon

accumulation and climate are just beginning to be understand, there is still considerable uncertainty over key regional controls, such as the impact of volcanism on peatland ecology and carbon accumulation (Hughes et al., 2013). Some of the mechanisms by which volcanic eruptions may affect carbon accumulation in peatlands include hydrological and physical impacts of tephra, impacts of tephra leachates, and toxicity of aerosols and acids, as well as climatic change (Payne & Blackford, 2008; Payne et al., 2013). Recent research has suggested that the deposition of volcanogenic sulphate may be one of the lead causes of change to the carbon balance of peatland ecosystems (Stevenson et al., 2003; Gauci et al., 2008). These studies have shown that sulphate deposition may lead to a reduction in methane efflux as methanogenic bacteria are out-competed by sulphate-reducing bacteria. Other studies have shown that the addition of major nutrients, such as nitrogen and phosphorus, to peatland ecosystems through the deposition of volcanic tephra, produces shifts in plant communities from species producing decay-resistant litter, such as *Sphagnum,* to species that produce a more labile litter, such as vascular plants (Hughes et al., 2013). The net effect of such a process would be a reduction in carbon accumulation as enhanced litter decay increases the loss of peatland carbon through increased emission of carbon dioxide and methane (Malmer et al., 2003).

To my knowledge, only two studies have looked specifically at the effect of tephra deposition on carbon accumulation rates. The first study, by Hughes et al. (2013), examined the impact of high-tephra loading on Late-Holocene carbon accumulation in a peatland from Hokkaido, Japan. Their results show that a moderate to high tephra loading have shifted the peatland ecosystem from *Sphagnum* to monocotyledon-dominated plant communities. This vegetation change is associated with increased peat humification and

reduced carbon accumulation. The second study, by Blackford et al. (2014), examined the impact of the caldera-forming Aniakchak II eruption from western Alaska on peatland carbon sequestration. Their finds suggest that the eruption may have led to a widespread reduction in peatland carbon sequestration and that the impacts on ecosystem functioning were profound and long lasting. While the studies by Hughes et al. (2013) and Blackford et al. (2014) are critical for our understanding of the effects of tephra disturbance on carbon accumulation, their relevance to long-term trends in peatland accumulation are limited because of the low number of tephra they analyzed, only two in the study by Hughes et al. (2013) and only one in the study by Blackford et al. (2014). By contrast, the Krutoberegovo record offers the opportunity to look at changes in carbon accumulation rates following long-term and repeated disturbance by over 30 tephra deposition events during the last 10,000 years.

Figure 5.5 displays the relationship between tephra deposition and long-term apparent rates of carbon accumulation (LORCA) at the Krutoberegovo site over the last 10,000 years. The periods with a high number of tephra deposition events, such as the one between 6000 and 4000 cal yr BP, feature low LORCA values, while periods with rare or no deposition events, such as the one between 8300 and 6000 cal yr BP, are characterized by LORCA values that are almost an order of magnitude higher. The obvious question here is what are the possible mechanisms through which tephra deposition diminishes the long-term carbon accumulation rates in peatlands? Several possible mechanisms can be suggested based on studies of anthropogenic pollutants on peatlands and volcanic impacts on other ecosystems (Payne & Blackford, 2008); these are outlined below:

a) Indirect climatic impacts. Volcanic eruptions produce large quantities of sulphur gases, which combine with water to form acid aerosols. These aerosol particles induce scattering of solar radiation and atmospheric cooling (Payne & Blackford, 2008). Volcanic cooling may lead to diminished evapotranspiration and a wetter peatland surface, which in turn may decrease decomposition and increase carbon accumulation rates. However, climate cooling may also lead to changes in the peatland plant cover, favoring slow-growing taxa, such as *Sphagnum*, which in turn drives a decrease in the primary production of the peatland.

b) Physical impact of tephra. Tephra fallout is primarily composed of sharp, angular shards of volcanic glass and, therefore, the deposition of tephra may lead to abrasion of plant surfaces, inhibition of photosynthesis, blocking of stomata, and crushing of plant tissues (Cook et al., 1980; Bjarnason, 1991; Clarkson & Clarkson, 1994). These processes are particularly important in peatlands because peatland plants are low growing and include many bryophytes, lacking a protective leaf surface (Payne & Blackford, 2008). It follows, therefore, that tephra deposition on peatland plants leads to an overall reduction in primary productivity, which in turn would decrease carbon accumulation rates.

c) Chemical impacts of tephra. Although volcanic glass is generally well preserved in soils (Dugmore et al., 1992), chemical elements may be released through long-term leaching. Elements released by tephra most commonly include Cl, S, Na, Ca, and K (Smith et al., 1983). While it is possible that some of these tephra leachates will supply nutrients to the plants, others may be toxic to some organisms and,

therefore, reduce biomass growth and primary productivity (Payne & Blackford, 2008).

d) Volcanic gas and acids impact. Volcanic eruptions release large quantities of gases into the atmosphere, including carbon dioxide, sulfur dioxide, HCl, and HF (Symonds et al., 1988; Delmelle et al., 2002). These volcanic compounds may be deposited on the peat surface as gas, acidic precipitation, dry deposition, or acidic aerosols (Payne & Blackford, 2008). Plants exposed to these compounds show varying signs of lesions and burn spots and some lead to total defoliation and death (Clarkson & Clarkson, 1994; Delmelle et al., 2002). The sensitivity of peatland plants, in particular *Sphagnum,* to acid deposition has been demonstrated in contemporary studies (e.g., Ferguson & Lee, 1980). As volcanic acid deposition modifies the pH, the existing plant cover would be affected. A lower pH would shift plant communities towards slow-growing *Sphagnum* communities, which in turn would decrease primary productivity.

e) Impact on peatland hydrology. The deposition of a tephra layer across the peatland surface could affect the hydrology of the ecosystem. Some authors (e.g. Hotes et al., 2004) have suggested that tephra deposition could lead to peat surface drying due to enhanced aeration of the upper layers of peat. Drying of peat surface may lead to increased decomposition and an overall reduction in carbon accumulation rates.

In this study, I look specifically at the relationship between TA-inferred peatland hydrology and long-term carbon accumulation rates. The redundancy analysis (RDA) (Figure 5.7), of the relationship between the testate amoebae community and tephra

related environmental variables (total ash content and major eruptions) shows that tephra deposition explains to a large degree the shifts in TA communities. These shifts, however, are complex and do not seem to indicate that tephra deposition on peatland surface affects specifically a certain testate amoebae hydrological group. A possible drying effect following volcanic eruptions in the Krutoberegovo record, is indicated by the increase in the abundance of some LWT TA indicator taxa (e.g. *Trinema/Corythion type,* and *Euglypha tuberculata*), but there is no sufficient evidence to suggest a profound drying of the peat surface. It can be concluded, therefore, that changes in peatland hydrology are not a major cause of shifts in long-term carbon accumulation rates, but could be part of a combination of factors which together act to decrease LORCA following a tephra deposition event. Given the data obtained in this study, the most likely factors that could have affected carbon accumulation following tephra deposition events are ***changes in microbial activity*** and ***changes in vegetation cover***.

Changes in microbial activity.

The profound impact of tephra deposition on testate amoebae community implies that these volcanic materials may have widespread effect on microbial activity, in particular, bacterial and fungal activity that is responsible for decomposition of organic materials. Since testate amoebae are a group of predatory protists that feed on bacteria, fungi, nematods, and algae (e.g., Gilbert et al., 2000; Jassey et al. 2012) it can be hypothesized that changes in the testate amoebae community would affect the main peat decomposers such as bacteria and fungi. Unfortunately, no studies that look specifically at the relationship between testate amoebae predation, decomposers, and net peat

decomposition values have been found, but this hypothesis should be tested in future studies.

Changes in vegetation cover

The Krutoberegovo record gives some indication that changes in carbon sequestration following a tephra deposition event could be related to changes in wetland vegetation cover, specifically changes from sedge-dominated communities (Cyperaceae) to grasses (Poaceae) (Fig. 6.1.a,b). The mechanism through which the shift from sedges to grasses affect carbon accumulation rates is not clear but it could be related to two main processes:

First, the sedge to grass vegetation replacement is not immediate, but rather progressive and potentially involves a period with widespread damage to the vegetation cover and little or no biomass production. This process is quite plausible and has been documented before by Blackford et al. (2014), which found a period of no peat accumulation following tephra deposition of up to 200 years. This period seems rather short when considering carbon accumulation rates at millennial scale, however, given the high number of tephra deposition events in the Krutoberegovo record, which are closely spaced in time, their impact on long-term carbon accumulation rates could have been substantial. In fact, Figure 5.5 shows a clear-cut difference in carbon accumulation between periods with a high density of tephra deposition events and those with no tephra deposition events.

The second process that could be responsible for a reduction in carbon accumulation rates following tephra deposition in the Krutoberegovo peatland is related to the difference between sedge and grass ecosystems. As opposed to sedges, grass

communities live on drier substrates and thus the litter they produce decomposes more rapidly than that of sedges, which tend to form sedge peat in wetter environments. Enhanced decomposition of grass litter following a volcanic eruption could have contributed to lower carbon accumulation rates.

Chapter 7

7) Conclusions

Peatlands are abundant across the circum-boreal region and many peatland regions are within reach of volcanic products from sources in Iceland, eastern Russia, Japan and northwestern North America. Since many peatlands are naturally oligotrophic and receive their nutrients and moisture from the atmosphere, they are particularly sensitive to atmospheric inputs from volcanic ejecta or tephra (Payne & Blackford, 2008). The primary aim of this thesis was to decipher the impact of peat surface burial by volcanic ash on testate amoebae communities, water table regime, and carbon accumulation rates in a peat profile from Krutoberegovo, Kamchatka Peninsula, Russia.

The thesis debuts with an in-depth examination of the current available literature on peatland functions, carbon accumulation, peatland hydrology, and the impact of disturbance on the peatland ecosystem (**Chapter 2**). The available literature shows that northern peatlands are one of the most important global carbon reservoirs and significant progress has been made in understanding the carbon balance in peatlands and the importance of peatland hydrology in ecosystem functions and development. However, the mechanisms and processes through which peat surface disturbance affects peatland communities and carbon stocks are largely unclear. Moreover, very few studies have taken into account the possible synergies that exist between disturbance, hydrology, and carbon sequestration as a casual continuum. In terms of volcanic disturbance in peatland ecosystems, the available knowledge is biased towards studies on recent or historical eruptions while long-term (millennial scale) impacts are relatively unknown. Regardless

of the time frame of the investigation, these studies suggest that volcanic disturbance in the form of tephra deposition has the ability to alter peatland ecosystem functioning and development and may drive a widespread reduction in peatland carbon sequestration potential.

Chapter 3 presents details on the study site located near Krutoberegovo village in eastern Kamchatka Peninsula, Russia. The Krutoberegovo peatland has been subjected to over 30 tephra deposition events over a period of 10,000 years and thus provides a unique and rare opportunity to examine the interactions between carbon accumulation, hydrology, and landscape disturbance.

Chapter 4 outlines the methodological approaches used to achieve the goals of this study. First, I use the data obtained in a parallel study (Ponomareva et al., in preparation) to obtain a chronological record of the major tephra deposition events that has affected the Krutoberegovo peatland. Second, I reconstruct the long-term changes in the testate amoebae communities over the last 10,000 years, and used these to infer relative changes in peat surface wetness. Third, I use a high-resolution record of carbon (C) and nitrogen (N) chemistry to reconstruct C/N ratios as a measure of ecosystem nutrient availability. Finally, I use the peat carbon concentration record and radiocarbon dating of sixteen discrete levels along the peat profile to reconstruct the long-term apparent rates of carbon accumulation (LORCA).

Chapter 5 presents the main findings of this study and **chapter 6** discusses the main implications. I specifically look at testate amoebae-inferred palaeohydrology in the context of local wetland vegetation development, tephra impact on testate amoebae

communities, tephra impact on carbon and nitrogen chemistry and, finally, tephra impact on LORCA.

The main conclusions of this study are the following:

a) The Krutoberegovo peatland experienced thirty-four different tephra deposition events during the last 12,000 years, of which nine are considered major regional markers, based on their thickness, unique geochemical signatures and area of dispersal;

b) The high-resolution analysis of testate amoebae communities over the course of the Holocene shows a high degree of variability with frequent shifts in taxa dominance. The statistical analysis of testate amoebae taxa in relation to tephra-related environmental variables (total ash content and major eruptions) shows that tephra deposition explains to a large degree the shifts in TA communities. Total ash content explains 77.3% of the taxa variability, while major volcanic eruptions as discrete events explain 6.3%. The taxa most affected by tephra deposition are *Euglypha rotunda, Euglypha tuberculata, Difflugia pulex, Trinema/Corythion type, Trinema lineare, Centropyxis platystoma, Tracheleuglypha dentata,* and *Quadrulella symmetrica*. While the changes in these taxa are statistically significant, the direction of change is not unequivocal as some taxa increase across some tephra deposition events and decrease across others. This lack of consistency in the tephra impact on testate amoebae communities may be related to tephra-forced microenvironmental changes of the peat surface (e.g., microtopography, plant cover) which vary considerably in space and time, rather than direct toxicity of the volcanic products.

c) The testate amoebae-inferred peat surface wetness in the Krutoberegovo peatland over the last 10,000 years is characterized by variable water table regimes, which may suggest an inherently unstable peat surface wetness. While the early Holocene is dominated by intermediate/variable (IWT) water table regimes, the mid Holocene is characterized by shifting peat surface wetness with two phases of high water tables, at ca. 7100 cal yr BP and between 5800 and 5000 cal yr BP. The Late Holocene features the wettest peat surface in the site's history, being dominated by testate amoebae taxa indicating high water tables. The data presented in this thesis suggest that the main driver of peat surface wetness variability is the climate, although tephra deposition events may have contributed to a temporary drying of the peat surface.

d) The analysis of carbon and nitrogen chemistry of the Krutoberegovo peat profile suggest that tephra loading of the peat surface induced a net loss of both carbon and nitrogen. The C/N ratios – a measure of nutrient availability in peatland ecosystems – show a variable but overall increasing trend, which may be related to an autogenic replacement of nutrient rich with nutrient poor wetland plant communities. However, periods with lower or decreasing C/N ratios seem to be associated with high tephra loading (i.e., allogenic factor); suggesting that tephra deposition may have also played a role.

e) The carbon sequestration potential of the Krutoberegovo peatland measured as long-term apparent rates of carbon accumulation (LORCA) shows a wide variability over the course of the Holocene ranging from 74.5 g C m^{-2} yr^{-1} to 7.91 g C m^{-2} yr^{-1}. This variability seems to be largely related to tephra loading of the peat surface and

probably mediated by tephra-induced shifts in microbial activity and changes in wetland vegetation cover.

7.1 Limitations and recommendations for future studies

Although this thesis provides a valuable insight into the complex impacts of volcanic tephra deposition on peatland testate amoebae community change, carbon and nitrogen chemistry, and carbon accumulation rates in a northern peatland from Kamchatka Peninsula, Russia, two main limitations underline the need for further research.

The first limitation is related to the nature of the reconstruction of peat surface wetness. In this study, peat surface wetness is reconstructed based on shifts in testate amoebae communities without a quantification of the depth to water table (DWT). Normally, peat surface wetness is derived quantitatively using transfer functions (e.g. Warner & Charman, 1994; Booth, 2008; Bellen et al., 2014) based on modern amoebae training sets sampled from surface peat with corresponding measurements of environmental variables, such as water table depth and pH. These measurements are usually conducted over multiple field seasons, a situation that is not feasible in the case of a Master's degree. To date, there are no available modern TA training sets for Kamchatka. Although most testate amoebae species are cosmopolitan (i.e. not restricted to a specific region), there are regional variations in community composition and some taxa are limited to certain regions (e.g. Turner et al., 2013). Future research should undertake the development of a transfer function specific to Kamchatka by sampling various locations throughout the peninsula.

The second limitation is related to the identification of the mechanisms through which tephra loading of peat surface affects long-term carbon accumulation rates. The

data presented in this study shows that repeated peat surface burial by volcanic ash has affected long-term carbon accumulation rates (LORCA), but the mechanisms involved in this process remain unclear. It is hypothesized that volcanic ash loading on peat surface drives changes in the microbial activity and wetland plant cover, which in turn would affect the carbon sequestration potential of the peatland ecosystem. To test these hypothesis future studies would need to undertake the following:

- Multiannual monitoring of wetland plant succession following simulated tephra deposition, and
- Multiannual monitoring of microbial activity following simulated tephra deposition on peat surface including gas flux studies to identify the net balance between peat formation and peat decomposition.

Bibliography

Aaby, B. (1976). Cyclic climatic variations in climate over the past 5500 yr reflected in raised bogs. *Nature, 263,* 281-284.

Alexeyev, V.A. & Birdsey, R.A. (1998). Carbon storage in forests and peatlands of Russia. General Technical Report. NE-244. Radnor, PA: U.S. Department of Agriculture, Forest Service, Northeastern Research Station. 137.

Alm, J., Schulman, L., Silvola, J., Walden, J., Nykänen, H. & Martikainen, P.J. (1999). Carbon balance of a boreal bog during a year with an exceptionally dry summer. *Ecology* 80, 161-174.

Baillie, M., & Munro, M. (1988). Irish tree rings, Santorini and volcanic dust vents. *Nature,* 332, 344-346.

Barber, K.E. (1993). Peatlands as scientific archives of past biodiversity. *Biodiversity and Conservation, 2,* 474-489.

Barber, K.E. (1981). *Peat stratigraphy and climate change: A palaeoecological test of the theory and cyclic peat bog regeneration.* A.a. Balkema: Rotterdam. 219.

Bastien, D. F., & Garneau, M. (1997). Macroscopic identification key of 36 sphagnum species in Eastern Canada. Geological Survey of Canada, Miscellaneous Report 61. Ottawa: Natural Resources Canada.

Bellen, S., Garneau, M., & Booth, R. (2011). Holocene carbon accumulation rates from three ombrotrophic peatlands in boreal Quebec, Canada: Impact of climate-driven ecohydrological change. *The Holocene*, 21(8), 1217-1231.

Bellen, S., Mauquoy, D., Payne, R., Roland, T., Daley, T., Hughes, P.D.M., & Pancotto, V. (2014). Testate amoebae as a proxy for reconstructing Holocene water table dynamics in southern Patagonian peat bogs. *Journal of Quaternary Science,* 29(5), 463-474.

Bennett, K.D. (2007). Psimpoll and Pscomb programs for plotting and analysis. University of Cambridge, Cambridge, UK. From URL: http://www.chrono.qub.ac.uk/psimpoll/psimpoll.html

Belyea, L. & Malmer, N. (2004). Carbon sequestration in peatlands: patterns and mechanisms of response to climate change. *Global Change Biology,* 10*,* 1043-1052.

Beta Analytic Inc. (n.d.) Introduction to Radiocarbon Determination by the Accelerator Mass Spectrometry Method. Retrieved from http://www.radiocarbon.com/accelerator-mass-spectrometry.html

Bindeman, I. N., Leonov, V. L., Izbekov, P. E., Ponomareva, V. V., Watts, K. E., Sheipley, N. K.,... & Chen, C. H. (2010). Large-volume silicic volcanism in Kamchatka: Ar-Ar and U-Pb ages, isotopic, and geochemical characteristics of major-pre-Holocene caldera-forming eruptions. *Journal of Volcanology and Geothermal Research*, 189, 57-80.

Blaauw, M., & Christen, J.A. (2011). Flexible paleoclimate age-depth models using an autoregressive gamma process. *Bayesian Analysis*, 6(3), 457-474.

Blackford, J.J., Payne, R.J., Heggen, M.P., De la Riva Caballero, A., & van der Plicht, J. (2014). Age and impacts of the caldera-forming Aniakchak II eruption in western Alaska. *Quaternary Research,* 82, 85-95.

Blodau, C. (2002). Carbon cycling in peatlands- A review of processes and controls. *Environmental Review,* 10, 111-134.

Booth, R.K. (2001). Ecology of testate amoebae (protozoa) in two Lake Superior coastal wetlands: implications for paleoecology and environmental monitoring. *Wetlands,* 21(4), 564-576.

Booth, R.K. (2008). Testate amoebae as proxies for mean and annual water-table depth in *Sphagnum* dominated peatlands of North America. *Journal of Quaternary Science,* 23, 43-57.

Booth, R.K., Lamentowicz, M., & Charman, D.J. (2011). Preparation and analysis of testate amoebae in peatland palaeoenvironmental studies. *Mires and Peat,* 7, 1-7.

Booth, R.K., & Sullivan, M.E. (2007). Testate Amoebae as palaeohydrological proxies in peatlands: Key to testate amoebae inhabiting *Sphagnum*-dominated peatlands with an emphasis on taxa preserved in Holocene sediments. *Lehigh University,* 1-35.

Botch, M. S., Kobak, K.I., Vinson, T.S., & Kolchugina, T.P. (1995) Carbon pools and accumulation in peatlands of the Former Soviet Union. *Global Biogeochemical Cycles*, 9. 37-46.

Bourgeois, J., Pinegina, T.K., Ponomareva, V.V., & Zaretskaia, N.E. (2006). Holocene tsunamis in the southwestern Bering Sea, Russian Far East and their tectonic implications. *Geology Society American Bulletin*, 11, 449–463.

Braitseva,O.A., Melekestsev, I.V., Ponomareva, V.V., & Kirianov, V. (1996). The caldera-forming eruption of Ksudach volcano about cal. AD 240, the greatest explosive event of our era in Kamchatka. *Journal of Volcanology Geothermal research,* 70(1-2), 49-66.

Braitseva, O. A., Ponomareva, V.V., Sulerzhitsky, L.D., Melekestsev, I.V., & Bailey, J. (1997). Holocene key-marker tephra layers in Kamchatka, Russia, *Quaternary Res.,* 47(2), 125–139.

Bridgham, S., Updegraff, K., & Pastor, J. (1998). Carbon, nitrogen, and phosphorus mineralization in northern wetlands. *Ecology,* 79(5), 1545-1561.

Briffa, K., Jones, P., Schweingruber, R., & Osborn, T. (1998). Influence of volcanic eruptions on Northern Hemisphere temperature over the last 600 years. *Nature,* 393, 450-455.

Bunbury, J., Finkelstein, S.A., & Bollmann, J. (2012). Holocene hydro-climatic change and effects on carbon accumulation inferred from a peat bog in the Attawapiskat River watershed, Hudson Bay Lowlands, Canada. *Quaternary Research,* 78, 275-284.

Bunting, M.J., & Warner, B.G. (1998). Hydroseral development in Southern Ontario: Patterns and controls. *Journal of Biogeography,* 25(1). 3-18.

Bjarnason, A.H. (1991). Vegetation of lava fields in the Hekla area, Iceland. In:Acta Phytogeographica Suecica, 77. University of Uppsala, Sweden.

Dirksen, V., Dirksen, O., & Diekmann, B. (2013). Holocene vegetation dynamics and climate change in Kamchatka Peninsula, Russian Far East. *Review of Palaeobotany and Palynology,* 190, 48-65.

Cai, S.S., & Yu, Z. (2011). Response of a warm temperate peatland to Holocene climate change in northeastern Pennsylvania. *Quaternary Research,* 75, 531-540.

Chambers, F.M., Beilman, D.W., & Yu, Z. (2010). Methods for determining peat humification and for quantifying peat bulk density, organic matter and carbon content for palaeostudies of climate and peatland carbon dynamics. *Mires and Peat,* 7(7), 1-10.

Chambers, F.M. & Charman, D.J. (2004). Holocene environmental change: contributions from the peatland archive. *The Holocene*, 14(1), 1-6.

Charman, D.J., Beilman, D.J., Blaauw, D.W., Booth, M., Brewer, R.K., Chambers, S., & Vitt, D.H. (2012). Carbon-cycle implications of climate-driven changes in peat accumulation during the last millennium. *Biogeosciences Discussions,* 9, 14327-14364.

Charman, D.J., Brown, A.D., & Hendon, D., et al. (2004). Testing the relationship between Holocene peatland palaeoclimate reconstruction and instrumental data at two European sites. *Quaternary Science Reviews,* 23, 137-143.

Charman, D.J., Hendon, D., & Packman, S. (1999). Multiproxy surface wetness records between Holocene peatland palaeoclimate reconstructions and instrumental data at two European sits. *Quaternary Science.* 14, 451-143.

Charman, D.J., Hendon, D., & Woodland, W.A. (2000). *The Identification of Testate Amoebae (protozoa: Rhizopoda) in Peats.* Technical Guide No. 9, Quaternary Research Association, London, 147.

Charman, D.J. (2002). Peatlands and Environmental Change. John Wiley and Sons, England. 301.

Clarkson, B.D., & Clarkson, B.R. (1994). Vegetation decline following recent eruptions on White Island (Whakaari), Bay of Plenty, New Zealand. *Journal of Botany,* 32, 21-36.

Convention on Wetlands of International Importance especially as Waterfowl Habitat. Ramsar, Iran, 1971. URL: http://www.ramsar.org/sites/default/files/documents/library/current_convention_text_e.pdf

Cook, R., Barron, J., Papendick, R, & Williams, G. (1980). Impact on agriculture of the Mount St. Helens eruptions. *Science,* 211, 16-22.

Clymo, R.S. (1984). The limits to peat bog growth. *Philosophical Transactions of the Royal Society London B,* 303*,* 605-654.

Clymo, R.S., Turunen, J., & Tolonen, K. (1998). Carbon accumulation in peatland. *Oikos,* 81(2), 368-388.

Cowles, H.C. (1901). The physiographic ecology of Chicago and vicinity. *Botanical Gazette,* 31, 145-182.

Davis, R.B., & Anderson, D.S. (2001). Classification and Distribution of Freshwater Peatlands in Maine. *Northeastern Naturalist,* 8(1), 1-50.

Dellmelle, P., Stix, J., Baxter, P., Garcia-Alvarez, J., & Barguerro, J. (2002). Atmospheric dispersion and heavy acid loading in the vicinity of Masaya volcano, a major sulfur and chlorine source in Nicaragua. *Environmental Science and Technology,* 35, 1289-1293.

Dugmore, A. (1989). Icelandic volcanic ash in Scotland. *Scottish Geographical Magazine,* 105, 168-172.

Dugmore, A., Larsen G, Newton, A., & Sugden, G. (2002). Geochemical stability of fine-grained silicic Holocene tephra in Iceland and Scotland. *Journal of Quaternary Science,* 7, 173-183.

Efremov, S.P., Efremova, T.T. & Melentyeva, N.V. (1998). Chapter 10. Carbon Storage in Peatland Ecosystems. In: Alexeyev, V.A. & Birdsey, R.A. (Eds.) Carbon storage in forests and peatlands of Russia. USDA Forest Service, Radnor, pp. 69-76.

Elliott, Roe, & Patterson. (2012). Testate amoebae as indicators of hydroseral change: An 8500-year record from Mer Bleue Bog, Ontario, Canada. *Quaternary International* 268, 128-144.

Ferguson, P. & Lee, J.A. (1980). Some effects of sulphur pollutants on the growth of *Sphagnum* species. *Environmental Pollution,* 16, 151-162.

Ganong, W.F. (1903). The vegetation of the Bay of Fundy salt and diked marshes: an ecological study. *Botanical Gazette,* 36, 429-455.

Gauci, V., Dise, N., & Blake, S. (2005). Long-term suppression of wetland methane flux following a pulse of simulated acid rain. *Geophysical Research Letters,* 32, L12804.

Gauci, V., Blake, S., Stevenson, D.s., & Highwood, E.J. (2008). Halving of the northern wetland CH_4 source by a large Icelandic volcanic eruption. *Journal of Geophysical Research,* 113.

Gilbert, D., Amblard, C., Bourdier, G., André-Jean, F., & Mitchell, E. A. (2000). Le régime alimentaire des thécamoebiens (Protista, Sarcodina). *L'année Biologique*, 39(2), 57-68.

Glenn-Lewin, D.C., Peet, R.K., & Veblen, T.T. (Eds.). (1992). Plant Succession: Theory and Prediction. Chapman and Hall, London.

Glenn-Lewin, D.C., & van der Maarel, E. (1992). Patterns and processes of vegetation dy- namics. In: Glenn-Lewin, D.C., Peet, R.K., Veblen, T.T. (Eds.), Plant Succession: Theory and Prediction. Chapman and Hall, London, pp. 11–59.

Gorham, E. (1991). Northern peatlands: Role in the global carbon cycle and probable response to climate warming. *Ecology Applied*, 1, 182–193.

Gorham, E., Bayley, S. E., & Schindler, D. W. (1984). Ecological effects of acid deposition upon peatlands: a neglected field in" acid-rain" research. *Canadian Journal of Fisheries and Aquatic Sciences*, 41(8), 1256-1268.

Gorham, E., Lehman, C., Dyke, A., Janssens, J., & Dyke, L. (2007). Temporal and spatial aspects of peatland initiation following deglaciation in North America. *Quaternary Science Reviews,* 26(3-4), 300-311.

Griggs, R. (1919). The character of the eruption as indicated by its effects on nearby vegetation. *Ohio Journal of Science*, 19, 173-209.

Halsey, L.A., Vitt, D.H. & Bauer, I.E. (1998). Peatland initiation during the Holocene in continental western Canada. *Climatic Change,* 40, 315-342.

Hang, T., Wastegard, S., Veski, S., & Heinsalua, A. (2006) First discovery of crytotephra in Holocene peat deposits of Estonia, eastern Baltic. *Boreas,* 35, 644-649.

Hammarlund, D., Klimaschewski, A., St. Amour, N., Andren, E., Self, A., Solovieva, N., Andreev, A., Barnekow, L., & Edwards, T. (2015). Late Holocene expansion of Siberian dwarf pine (pinus pumila) in Kamchatka in response to increased snow cover as inferred from lacustrine oxygen-isotope records. *Global and Planetary Change,* 134, 91-100.

Hoblitt, R.P, Miller, C.D., & Scott, W.E. (1987). Volcanic hazards with regard to siting nuclear-power plants in the Pacific Northwest: *U.S. Geological Survey Open-File Report 87-297*, 196.

Holden, J. (2005). Peatland hydrology and carbon release: why small-scale process matters. *Philosophical Transactions: Mathematics, Physical and Engineering Science, 363*(1837), 2891-2913.

Hotes, S. (2004). Influence of tephra deposition on mire development in Hokkaido, Japan. *Journal of Ecology,* 92, 624-634.

Hotes, S., Poschold, P., Takahashi, H., Grootjans, A.P. & Adema, E. (2004). Effects of tephra deposition on mire vegetation: a field experiment in Hokkaido, Japan. *Journal of Ecology,* 92, 624-634.

Hotes, S., Poschlod, P., & Takahashi, H. (2006). Effects of volcanic activity on mire development: case studies from Hokkaido, northern Japan. *The Holocene,* 16, 561-573.

Hughes, P.D.M., & Dumayne-Peaty, L. (2002). Testing theories of mire development using multiple successions at Crymlyn Bog, West Glamorgan, South Wales, UK. *Journal of Ecology,* 90, 456-471.

Hughes, P.D.M., Mallon, G., Brown, A., Essex, H.J., Stanford, J.D., & Hotes, S. (2013). The impact of high tephra loading on Late-Holocene carbon accumulation and vegetation succession in peatland communities. *Quaternary Science Reviews,* 67, 160-175.

Hughes, P.D.M., Mauquoy, D., Barber, K.E., & Langdon, P.E. (2000). Mire-development pathways and palaeoclimatic records from a full Holocene peat archive at Walton Moss, Cumbria, England. *The Holocene,* 10, 465-479.

Ireland, A., & Booth, R. (2012). Upland deforestation triggered and ecosystem state-shift in a kettle peatland. *Journal of Ecology,* 100, 586-596.

Jassey, V. E., Shimano, S., Dupuy, C., Toussaint, M. L., & Gilbert, D. (2012). Characterizing the feeding habits of the testate amoebae Hyalosphenia papilio and

Nebela tincta along a narrow "fen-bog" gradient using digestive vacuole content and 13 C and 15 N isotopic analyses. *Protist*, 163(3), 451-464.

Jones, M. C., & Yu, Z. (2010). Rapid deglacial and early Holocene expansion of peatlands in Alaska. *Proceedings of the National Academy of Sciences of the United States of America,* 107, 7347-7352.

Joosten, H. (2004). The IMCG Global Peatland Database. [2002]. www.imcg.net/gpd/gpd.htm

Joosten, H., & Clarke, D. (2002). Wise use of mires and peatland- Background and principals including a framework for decision-making. International Mire Conservation Group and International Peat Society, 304 pp.

Klimaschewski, A., Barnekow, L., Bennett, K.D., Andreev, A.A., Andren, E., Bobrov, A.A., & Hammarlund, D. (2015). Holocene environmental changes in southern Kamchatka, Far Eastern Russia, inferred from a pollen and testate amoebae peat succession record. *Global Planetary Change,* doi:10.1016/j.gloplacha.2015.09.010.

Krestov, P., Omelko, A.M., Vladivostok, & Nakamura, Y. (2008) Vegetation and natural habitats of Kamchatka. *Berichte der Reinhold-Tuxen-Gesellschaft*, 20, 195-218. Hannover

Korhola, A., Tolonen, K., Turunen, J., and Jungner, H. (1996). Estimating long-term carbon accumulation rates in boreal peatlands by radiocarbon dating. *Radiocarbon,* 37, 575–584.

Kuhry, P. & Vitt, D. (1996). Fossil carbon/nitrogen ratios as a measure of peat decomposition. *Ecology,* 77(1), 271-275.

Kyle, P. R., Ponomareva, V. V., & Schluep, R. R. (2011). Geochemical characterization of marker tephra layers from major Holocene eruptions, Kamchatka Peninsula, Russia. *International Geology Review*, 53(9), 1059-1097.

Lähteenoja, O., Reátegui, Y.R., Räsänen, M., Torres, D.D.C., Oinonen, M. & Page, S. (2012). The large Amazonian peatland carbon sink in the subsiding Pastaza-Marañón foreland basin, Peru. *Global Change Biology,* 18(1), 164-178.

LaMarche, V. & Hirschboek, K. (1984). Frost rings in trees as records of major volcanic eruptions. *Nature,* 207, 121-126.

Lamarre, A., Magnan, G., Garneau, M., & Boucher, E. (2013) A testate amoebae-based transfer function for paleohydological reconstruction from boreal and subarctic peatlands in northeastern Canada. *Quaternary International,* 306, 88-96.

Lamarre, A., Garneau, M., & Asnong, H. (2012). Holocene paleohydrological reconstruction and carbon accumulation of a permafrost peatland using testate

amoeba and macrofossil analyses, Kuujjuarapik, subarctic Québec, Canada. *Review of Palaeobotany and Palynology,* 186, 131-141.

Lamentowicz, M, & Mitchell, E. (2005). The ecology of testate amoebae (protists) in *Sphagnum* in North-Western Poland in relation to peatland ecology. *Microbial Ecology,* 50, 1, 48-63.

Loisel, J., & Garneau, M. (2010). Late Holocene paleoecohydrology and carbon accumulation estimates from two boreal peat bogs in eastern Canada: potential and limits of multi-proxy archives. *Palaeogeography Palaeoclimatology Palaeoecology*, 291, 493–533.

Loisel, J., Garneau, M, & Helie, J-F. (2009). Sphagnum ^{13}C values as indicators of palaeohydrological changes in a peat bog. *Holocene,* 20. 285-291.

Magyari, E., Sumegi, P., Braun, M., Jakab, G., & Molnar, M. (2001). Retarded wetland succession: Anthropogenic and climatioc signals in a Holocene peaty bog profile from North-East Hungary. *Journal of Ecology,* 89(6), 1019-1032.

Malmer, N., Albinsson, C., Svensson, B.M., & Wallen, B. (2003). Inferences between *Sphagnum* and vascular plants: effects on plant community structure and peat formation. *Oikos,* 100, 469-482.

Malmer, N. & Wallen, B. (2004). Input rates, decay losses and accumulation rates of carbon bogs during the last millennium: internal processes and environmental changes. *Holocene,* 14, 111-117.

Maltby, E., & Immirzi, P. (1993). Carbon dynamics in peatlands and other wetland soils, regional and global perspectives. *Chemosphere,* 27. 999–1023.

Mauquoy, D., Engelkes, T., Groot, M.H.M, Markesteijn, F., Oudejans, M.G., van der Plicht, J., & van Geel, B. (2002a). High-resolution records of late Holocene climate change and carbon accumulation in two north-west European ombrotrophic peat bogs. *Paleogeography, Paleoclimatology, Paleoecology,* 186, 275-310.

Mauquoy, D., van Geel, B., Blaauw, M., & van der Plicht, J. (2002b). Evidence from northwest European bog shows 'Little Ice Age' climatic changes driven by variations in solar activity. *The Holocene,* 12(1), 1-6.

Mauquoy, D. & Yeloff D. (2007) Raised peat bog development and possible response to environment changes during the mid- to Late-Holocene. Can the palaeoecological record be used to predict the nature and response of raised peat bogs to future climate change? *Biodiversity and Conservation.* 17, 2139-2151.

Meisterfield, R. (2001a). Order Arcellinida, Kent 1880. In: Lee, J.J., Leedale, G.F., & Bradbury, P. (eds.). *The Illustrated Guide to the Protozoa.* Allen Press, Lawrence, Kansas, 827-860.

Meisterfield, R. (2001b). Testate Amoeba with filopoda. In: Lee, J.J., Leedale, G.F., & Bradbury, P. (eds.) *The Illustrated Guide to the Protozoa.* Allen Press, Lawrence, Kansas, 1054-1084.

Mitchell, E. (2004). Response of testate amoebae (protozoa) to N and P fertilization in an Arctic wet sedge tundra. *Arctic, Antarctic, and Alpine Research,* 36(1), 78-83.

Mitchell, E., & Gilbert, D. (2005). Vertical distribution and response to nitrogen deposition of testate amoebae in *sphagnum*. *Journal of Eukaryotic Microbiology.* 51(4), 480-490.

Mitchell, E.A.D., Payne, R.J. & van der Knapp, W.O. (2013). The performance of single- and multi-proxy transfer functions (testate amoebae, bryophytes, vascular plants) for reconstructing mire surface wetness and pH. *Quaternary Research,* 79, 6-13.

Mitsch, W.J., & Gosselink, J.G. (1986). Wetlands. Van Nostrand Reinhold, New York.

Mullen, S.F., Janssen, J.A., & Gorham, E. (2000). Acidity of and the concentration of major and minor metals in the surface waters of bryophyte assemblages from 20 North American bogs and fens. *Canadian Journal of Botanics*, 78, 718–727.

Ovsyannikov, A.A., & Manevich, A.G. (2010). The October 2010 eruption of Shiveluch Volcano. Bulletin of Kamchatka Regional Association "Educational-Scientific Center". *Earth Sciences,* 16(2), 7-9.

Page, S.E., Wust, R.A.J., Weiss, D., Rieley, J.O., Shotyk, W., & Limin, S.H. (2003). A record of Late Pleistocene and Holocene carbon accumulation and climate change from an equatorial peat bog (Kalimantan, Indonesia): implications for past, present and future carbon dynamics. *Journal of Quaternary Science*, 19(7), 625-635.

Parish, F., Sirin, A., Charman, D., Joosten, H., Minayeva, T., Silvius, M. & Stringer, L. (Eds.) (2008). Assessment on Peatlands, Biodiversity and Climate Change: Main Report. Global Environment Centre, Kuala Lumpur and Wetlands International, Wageningen.

Payette, S. (1988). Late-Holocene development of subarctic ombrotrophic peatlands: allogenic and autogenic succession. *Ecology,* 69, 516-531.

Payne, R. (2010). Testate amoebae response to acid deposition in a Scottish peatland. *Aquatic Ecology,* 44, 373-385.

Payne, R. (2012). Volcanic impacts on peatland microbial communities: A tephropalaeoecological hypothesis-test. *Quaternary International,* 268, 98-110.

Payne, R. & Blackford, J. (2005). Simulating the impacts of distal volcanic products upon peatlands in Northern Britain: An experimental study on the Moss of Achnacree, Scotland. *Ecotoxicology and Environmental Safety,* 69, 130-138.

Payne, R., & Blackford, J. (2008). Distal volcanic impacts on peatlands: Palaeoecological evidence from Alaska. *Quaternary Science Reviews,* 27, 2012-2030.

Payne, R., Edwards, K.J., & Blackford, J. (2013). Volcanic impacts on the Holocene vegetation history of Britain and Iceland? A review and meta-analysis of the pollen evidence. *Vegetation History and Archaeobotany,* 22, 153-164.

Payne, R., Gauci, V., & Charman, D. (2010). The impact of simulated sulfate deposition on peatland testate amoebae. *Environmental Microbiology*, 59, 76-83.

Payne, R., & Mitchell, E. (2009). How many is enough? Determining optimal count totals for ecological and palaeoecological studies of testate amoebae. *Journal of Paleolimnology,* 42, 483-495.

Pickett, S.T.A., & White, P.S. (1985). *The ecology of natural disturbance and patch dynamics*. Academic Press: Orlando, Fl.

Pinegina, T.K., Bourgeois, J., Kravchunovskaya, E.A., Lander, A.V., Arcos, M.E., Pedoja, K., & MacInnes, B.T., (2013). A nexus of plate interaction: Vertical deformation of Holocene wave-built terraces on the Kamchatka Peninsula, Russia. *Geological Society America Bulletin,* 125(9-10), 1554-1568.

Pendea, I.F., Ponomareva, V., Bourgeois, J., Zubrow, E., Portnyagin, M., Ponkratova, I., Harmsen, H., & Korosec, G. (under review). Late glacial to Holocene palaeoenvironmental change on the northwestern Pacific seaboard, Kamchatka Peninsula (Russia). *Quaternary Science Reviews*.

Pendea, I. F., Harmsen, H., Keeler, D., Zubrow, E. B., Korosec, G., Ruhl, E., & Hulse, E. (2016). Prehistoric human responses to volcanic tephra fall events in the Ust-Kamchatsk region, Kamchatka Peninsula (Kamchatsky Krai, Russian Federation) during the middle to late Holocene (6000–500 cal BP). *Quaternary International*, 394, 51-68.

Pevzner, M.M., Ponomareva, V.V., & Malakestsev, I.V. (1998). Chernyi Yar- reference section of the Holocene ash markers at the northeastern coast of Kamchatka. *Volcanology Seismology,* 19(4), 389-406.

Plunkett, G., Coulter, S.E., Ponomareva, V.V., Blaauw, M., Klimaschewski, A., & Hammarlund, D. (2015). Distal tephrochronology in volcanic regions: Challenges and insights from Kamchatkan lake sediments. *Global Planetary Change,* 134, 24-40.

Ponomareva, V. V., Melekestsev, I., & Braitseva, O. (2007). Late Pleistocene-Holocene

volcanism on the Kamchatka Peninsula, Northwest Pacific Region. *Institute of Volcanology and Seismology, Petropavlovsk-Kamchatsky, Russia.* 165-198.

Ponomareva,V.V., Portnyagin, M., Derkachev, A., Pendea, I.F., Bourheois, J., Reimer, P.J., Garbe-Schonberg, D., Krasheninnikov, S., & Nurnberg, D. (2013). Early Holocene M~6 explosive eruption from Plosky volcanic massif (Kamchatka) and its tephra as a link between terrestrial and marine paleoenvironmental records. *International Journal of Earth Sciences,* 102(6), 1673-1699.

Ponomareva,V.V., Portnyagin, M., Pevzner., M., Blaauw, M., Kyle, Ph., & Derkachev, A. (2015). Tephra from andesitic Shiveluch volcano, Kamchatka, NW Pacific: Chronology of explosive eruptions and geochemical fingerprinting of volcanic glass. *International Journal of Earth Sciences (Geology Rundschau),* 104, 1459-1482.

Poulter, B., Christensen, N.l., & Halpin, P.N. (2006). Carbon emissions from a temperate peat fire and its relevance to interannual variability of trace atmospheric greenhouse gases. *Journal of Geophysical Research,* 111.

Proctor, M. C. F., & Maltby, E. (1998). Relations between acid atmospheric deposition and the surface pH of some ombrotrophic bogs in Britain. *Journal of Ecology*, 86(2), 329-340.

Koerselman, W., & Meuleman, A.F.M. (1996). The vegetation N:P ratio: a new tool to detect the nature of nutrient limitation. *Journal of Applied Ecology,* 13, 1441-1450.

Qin, Y., Mitchell, E.A.D., Lamertowicz, M., Payne, R., Lara, E., Gu, Y., huang, X., & Wang, H. (2013). Ecology of testate amoebae in peatlands of central China and development of a transfer function for paleohydological reconstruction. *Journal of Paleolimnology,* 50, 319-330.

Rampino, M.R., & Self, S. (1992). Volcanic winter and accelerated glaciation following the Toba super-eruption. *Nature,* 359, 50-52.

Reimer, P.J. Bard, E., Bayliss, A., Beck, J.W., Blackwell, P.G., Bronk Ramsey, C., Buck, C.E., Cheng, H., Edwards, R.L., Friedrich, M., Grootes, P.M., Guilderson, T.P., Halfidason, H., Hajdas, I., Hatt_e,C., Heaton, T.J., Hoffmann, D.L., Hogg, A.G., Hughen, K.A., Kaiser, K.F., Kromer, B., Manning, S.W., Niu, M., Reimer, R.W., Richards, D.A., Scott, E.M., Southon, J.R., Staff, R.A., Turney, C.S.M., & van der Plicht, J. (2013). IntCall3 and Marine12 radiocarbon age calibration curves 0-50,000 years cal BP. *Radiocarbon*, 55(4), 1869-1887.

Roulet, N.T. (2000). Peatlands, carbon storage, greenhouse gases, and the Kyoto Protocol: Prospects, and significance for Canada. *Wetlands*, 20*,* 605-615.

Roulet, N., Lafleur, P., Richard, P.J.H., Moore, T., Humphrey, E. & Bubier, J. (2007). Contemporary carbon balance and late Holocene carbon accumulation in a northern peatland. *Global Change Biology,* 13, 397- 411.

Rydin, H., & Jeglum, J. K. (2006). *The biology of peatlands*. Oxford University Press, Oxford, 360.

Self, A.E., Klimaschewski, A., Solovieva, N., jones, V.J., Andren, E., Andreev, A.A., Hammarlund, D., & Brooks, S.J. (2015). The relative dynamics of climate and volcanic activity on Holocene lake development inferred from a mountain lake in central Kamchatka. *Global and Planetary Change,* 134, 67-81.

Sharik, T.L., Ford, R.H., & Davis, M.L. (1989). Repeatability of invasion of eastern White Pine on dry sites in northern Lower Michigan. *American Midland Naturalist Journal,* 122, 133-141.

Sheng, Y., Smith, L.C., MacDonald, G.M., Kremenetski, K.V., Frey, K.E., Velichko, A.A., Lee, M., Beilman,D.W. & Dubinin, P. (2004). A high-resolution GIS based inventory of the west Siberian peat carbon pool. *Global Biogeochemical Cycles*, 18, GB3004, doi:10.1029/2003GB002190.

Shimwell, D.W. (1971). The Description and Classification of Vegetation. University of Washington Press, Seattle.

Singer, D.K., Jackson, S.T., Madsen, B.J., & Wilcox, D.A. (1996). Differentiating climatic successional influences on long-term development of a marsh. *Ecology,* 77, 1765-1778.

Smith, D.B., Zielinski, R.A., Taylor, H.E., & Sawyer, M.B. (1983). Leaching characteristics of ash from the May 18, 1980 eruption of Mount St. Helens volcano, Washington. *Bulletin of Volcanology,* 46, 103-124.

Song, L., Li, H., Wang, K., Wu, D., & Wu, H. (2014). Ecology of testate amoebae and their potential use as palaeohydrologic indicators from peatland in Sanjiang Plain, Northeast China. *Frontiers of Earth Science,* 8(4), 564-572.

Stevenson, D.S., Johnson, C.E., Highwood, E.j., Gauci, V., Collins, W.J., & Derwent, R.G. (2003). Atmospheric impact of the 1783-1764 Laki eruption: part 1 chemistry modelling. *Atmospheric Chemistry and Physics Discussions,* 3, 551-596.

Swindles, G. T., Charman, D. J., Roe, H. M., & Sansum, P. A. (2009). Environmental controls on peatland testate amoebae (Protozoa: Rhizopoda) in the North of Ireland: implications for Holocene palaeoclimate studies. *Journal of Paleolimnology*, 42(1), 123-140.

Symonds, R., Rose, W., & Reed, M. (1988). Contributions of Cl^- and F^- bearing gases to the atmosphere by volcanoes. *Nature,* 334, 415-418.

Talma, A.S., & Vogel, J.C. (1993). A simplified approach to calibrating (super 14) C dates. *Radiocarbon*, 35(2), 317-322.

Tarnocai, C. 1998. The effect of climate change on carbon in Canadian peatlands. *Global and Planetary Change*, 53, 222-232.

ter Braak, C.J.F. & Smilauer, P. (2002). CANOCO Reference manual and CanoDraw for Window's User's guide: Software for canonical community ordination (version 4.5). Microcomputer power. Ithaca, NY, USA. 500 pp.

Tolonen, K., & Turunen, J., 1996. Carbon accumulation in mires in Finland. In: Laiho, R., Laine, J., Vasander, H. (Eds.), Northern Peatlands in Global Climate Change, Pro- ceedings of the International Workshop on Northern Peatlands in Global Climatic Change, Finland, 8–12 October 1995, 250–255.

Transeau, E.N. (1903). On the geographic distribution and ecological relationships of the bog societies of northern North America. *Botanical Gazette,* 36, 401-420.

Turner, T.E., Swindles, G.T., Charman, D.J., et al. (2013) Comparing regional and supra-regional transfer functions for palaeohydrological reconstruction from Holocene peatlands. *Palaeogeography, Palaeoclimatology, Palaeoecology.* 369, 395-408.

Turunen, J., Roulet, N.T., & Moore, T.R. (2004). Nitrogen deposition and increased carbon accumulation in ombrotrophic peatlands in eastern Canada. *Global Biogeochemical Cycles,* 18.

Turunen J., Tahvanainen, T., & Tolonen, K. (2001). Carbon accumulation in West Siberian mires, Russia. *Global Biogeochemical Cycles,* 15(2). 285-296.

Turunen, J., Tomppo, E., Tolonen, K. & Reinikainen, A. (2002). Estimating carbon accumulation rates of undrained mires in Finland - Application to boreal and subarctic regions. *The Holocene,* 12, 69-80.

Tuittila, E., Juutinen, S., Frolking, S., Valiranta, M., Laine, A., Miettinen, A., et al. (2012). Wetland chronosequence as a model of peatland development: vegetation succession, peat, and carbon accumulation. *The Holocene*, 23(1), 25-35.

Vompersky, S., Tsyganova, O., Valyaeva, N. & Glukhova, T. (1996). Peat-covered wetlands of Russia and carbon pool of their peat. In: Luttig, G. (Ed.). Proceedings 10th International Peat Congress Bremen Vol. 2. Schweizerbart, Stuttgart, pp. 381-390.

Walker, D. (1970). Direction and rate in some British post-glacial hydroseres. *Vegetation History of the British Isles.* Cambridge University Press, Cambridge. 117-139.

Walker, M.J.C., Berkerlhammer, M., Bjo-Rck, S., Cwynar, L.C., Fisher, D.A., Long, A.J., Lowe, J., Newnham, R.M., Rasmussen, S.O., & Weiss, H. (2012). Formal subdivision of the Holocene series/epoch: a discussion paper by a working group of intimate (integration of ice-core, marine and terrestrial records) and the subcommission on quaternary stratigraphy (International Commission on Stratigraphy). *Journal of Quaternary Science,* 27(7), 649-659.

Warner, B.G. & Charman, D. (1994). Holocene changes on a peatland in northwestern Ontario; interprested from testate amoebae (Protozoa) analysis. *Boreas,* 23, 270-279.

Wolejko, L., & Ito, K. (1986). Mires in Japan in relation to mire zones, volcanic activity and water chemistry. *Japanese Journal of Ecology,* 72, 463-473.

Woodland, W.A., Charman, D., & Sims, P. (1998). Quantitative estimates of water tables and soil moisture in Holocene peatlands from testate amoebae. *The Holocene,* 8(3), 261-273.

Yeloff , D., Mauquoy, D., Barber, K., Way, S., Geel, B., & Turney, C. (2007) Volcanic ash deposition and long-term vegetation change on Subantarctic Marion Island. *Arctic, Antarctic, and Alpine Research,* 39(3), 500-511.

Yu, Z. (2012). Northern peatland carbon stocks and dynamics: a review. *Biogeosciences,* 9*,* 4071-4085.

Yu, Z. Beilman, D.W., Frolking, S., MacDonald, G.M., Roulet, N.T., Camill, P., & Charman, D.J. (2011). Peatlands and their role in the global carbon cycle. *EOS,* 92*,* 97-98.

Yu, Z., Loisel, J., Brosseau, D.P., Beilman, D.P., & Hunt, S.J. (2010). Global peatland dynamics since the last Glacial Maximum. *Geophysical Research Letters,* 37, http://dx.doi.org/10.1029/2010GL043584.

Zeilinski, G.A. (2000). Use of paleo-records in determining variability within the volcanism-climate system. *Quaternary Science Reviews,* 19, 417-438.

Appendices

1. Raw data for quantifying peat bulk density, organic matter and carbon content- page 1/3

Code	Depth (cm)	Depth range (cm)	Volume LOI (cm3)	Wet Weight LOI (g)	Dry Weight (g)	Ash Weight (g)	Water Content (%)	Bulk Density (g cm-3)	Organic Matter Content	Ash-Free Bulk Density (OM density; g cm-3) (%)	Organic Carbon 0.52gC/gOM
JB 112- 2	2	0-2	21.46	15.07	5.194	1.11495	65.53417	0.24203	59.74692	0.14461	31.06840
JB 112- 6.5	6.5	5.5-6.5	11.34	13.164	4.307	0.6622	67.28198	0.37981	63.96387	24.29386	33.26121
JB 112- 13	13	12-13	28.158	25.434	4.848	0.49075	80.93890	0.17217	80.27651	13.82131	41.74379
JB 112- 24	24	23-24	12.474	13.136	4.119	0.2833	68.64342	0.33021	83.00744	27.40962	43.16387
JB 112- 34	34	33-34	20.52	17.786	4.764	0.4556	73.21489	0.23216	80.43292	18.67361	41.82512
JB 112- 44	44	43-44	12.096	8.424	3.282	0.1157	61.03989	0.27130	84.63887	22.96253	44.01221
JB 112- 54	54	53-54	16.224	15.08	4.586	0.79905	69.58886	0.28267	61.71574	17.44504	32.09218
JB 112- 65	65	64-65	8.74	10.558	3.791	0.2305	64.09358	0.43375	81.34661	35.28432	42.30023
JB 112- 74	74	73-74	14	14.79	4.633	0.47325	68.67478	0.33093	77.93758	25.79177	40.52754
JB 112- 84	84	83-84	8.84	11.193	3.763	0.2621	66.38077	0.42568	78.68066	33.49268	40.91394
JB 112- 97	97	96.5-97	6.048	7.298	3.405	0.2072	53.34338	0.56300	75.32746	42.40906	39.17028
JB 112- 104	104	103.5-104	5.742	8.463	3.337	0.105	60.56954	0.58116	86.57632	50.31438	45.01969
JB 112- 115	115	114-115	4.004	7.482	4.659	1.82135	37.73055	1.16359	12.76850	14.85726	6.63962
JB 112- 125	125	124-125	7.82	9.451	3.505	0.121	62.91398	0.44821	87.58592	39.25686	45.54468
JB 112- 133.5	133.5	132.5-133.5	9.75	11.055	3.706	0.12855	66.47671	0.38010	89.09068	33.86360	46.32715
JB 112- 139.5	139.5	138.5-139.5	4.8	5.507	3.258	0.2801	40.83893	0.67875	59.61649	40.46470	31.00058
JB 112- 145	145	144-145	4.56	6.271	3.309	0.1847	47.23330	0.72566	75.62038	54.87453	39.32260
JB 112- 155	155	154-155	4.84	6.486	3.156	0.1822	51.34135	0.65207	69.35755	45.22571	36.06593
JB 112- 165	165	164-165	5.52	7.214	3.09	0.05285	57.16662	0.55978	90.01417	50.38837	46.80737
JB 112- 175	175	174-175	4.6	6.563	3.071	0.107	53.20737	0.66761	76.10540	50.80863	39.57481
JB 112- 185	185	184-185	5.236	7.047	3.173	0.04775	54.97375	0.60600	92.47972	56.04243	48.08946
JB 112- 195	195	194-195	6.912	9.201	3.521	0.1046	61.73242	0.50940	89.36776	45.52429	46.47123
JB 112- 205	205	204-205	6.72	10.143	3.882	0.2925	61.72730	0.57768	78.08168	45.10611	40.60247
JB 112- 215	215	214-215	6.21	8.229	3.513	0.1431	57.30952	0.56570	85.33661	48.27496	44.37504

1. Raw data for quantifying peat bulk density, organic matter and carbon content- page 2/3

Code	Depth (cm)	Depth range (cm)	Volume LOI (cm3)	Wet Weight LOI (g)	Dry Weight (g)	Ash Weight (g)	Water Content (%)	Bulk Density (g cm^3)	Organic Matter Content	Ash-Free Bulk Density (OM density; g cm^3) (%)	Organic Carbon 0.52gC/gOM
JB 112- 225	225	224-225	5.76	7.712	3.401	0.16025	55.89990	0.59045	81.52205	48.13481	42.39147
JB 112- 235	235	234-235	3.864	6.863	3.232	0.1016	52.90689	0.83644	85.22397	71.28464	44.31646
JB 112- 245	245	244-245	3.91	6.558	3.288	0.20195	49.86276	0.84092	72.16211	60.68261	37.52430
JB 112- 255	255	254-255	5.184	6.714	3.332	0.2464	50.37236	0.64275	68.31276	43.90781	35.52263
JB 112- 265	265	264-265	4.698	6.818	3.317	0.1943	51.34937	0.70605	74.24443	52.41992	38.60710
JB 112- 267	267	266-267	4.788	8.755	4.5	1.3626	48.60080	0.93985	30.11949	28.30779	15.66214
JB 112- 275	275	274-275	3.484	7.811	3.465	0.27905	55.63948	0.99455	70.25212	69.86900	36.53110
JB 112- 285	285	284-285	4.5	6.996	3.208	0.1159	54.14523	0.71289	82.03936	58.48495	42.66047
JB 112- 295	295	294-295	5.98	8.097	3.466	0.26275	57.19402	0.57960	71.87584	41.65914	37.37543
JB 112- 301.5	301.5	300.5-301.5	3.6	7.133	3.626	0.5352	49.16585	1.00722	49.29898	49.65503	25.63547
JB 112- 304	304	303-304	5.04	9.849	6.383	3.3368	35.19139	1.26647	12.01350	15.21472	6.24702
JB 112- 315	315	314-315	5.445	8.792	3.946	0.6715	55.11829	0.72470	52.26077	37.87346	27.17560
JB 112- 325	325	324-325	6.3	8.626	3.754	0.45675	56.48041	0.59587	62.17861	37.05056	32.33288
JB 112- 331.5	331.5	331.5	2.43	5.778	3.86	1.0136	33.19488	1.58848	20.18269	32.05975	10.49500
JB 112- 334	334	333-334	2.431	5.445	3.205	0.27875	41.13866	1.31839	55.70123	73.43581	28.96464
JB 112- 343	343	342-343	3.024	5.943	3.233	0.186	45.59987	1.06911	70.46212	75.33203	36.64030
JB 112- 356	356	355-356	8.12	10.024	3.554	0.112	64.54509	0.43768	88.96878	38.94028	46.26376
JB 112- 366	366	365-366	4.368	7.297	3.302	0.1208	54.74853	0.75595	83.40887	63.05314	43.37261
JB 112- 377	377	376-377	5.684	7.694	3.354	0.12625	56.40759	0.59008	83.86272	49.48550	43.60862
JB 112- 385	385	384-385	6.552	9.497	3.572	0.1578	62.38812	0.54518	85.23163	46.46633	44.32045
JB 112- 395	395	394-395	7.917	10.25	3.676	0.16925	64.13659	0.46432	85.15676	39.53976	44.28152
JB 112- 406	406	405-406	7.02	10.357	3.62	0.1278	65.04779	0.51567	88.44798	45.60993	45.99295
JB 112- 415	415	414-415	5.67	8.541	3.411	0.0969	60.06322	0.60159	88.90924	53.48667	46.23280
JB 112- 426	426	425-426	1.968	4.284	2.902	0.0865	32.25957	1.47459	75.62007	111.50886	39.32244

1. Raw data for quantifying peat bulk density, organic matter and carbon content- page 3/3

Code	Depth (cm)	Depth range (cm)	Volume LOI (cm3)	Wet Weight LOI (g)	Dry Weight (g)	Ash Weight (g)	Water Content (%)	Bulk Density (g cm-3)	Organic Matter Content	Ash-Free Bulk Density (OM density; g cm-3) (%)	Organic Carbon 0.52gC/gOM
JB 112- 434	434	433-434	1.485	4.22	2.887	0.07595	31.58768	1.94411	78.22222	152.07243	40.67556
JB 112- 444	444	434-444	1.518	4.298	2.923	0.0816	31.99162	1.92556	78.57143	151.29400	40.85714
JB 112- 454	454	453-454	1.584	4.327	3.031	0.20685	29.95147	1.91351	55.46345	106.12987	28.84099
JB 112- 464	464	463-464	1.656	4.692	3.028	0.1085	35.46462	1.82850	76.42329	139.74018	39.74011
JB 112- 476	476	475-476	1.29	4.147	2.906	0.0794	29.92525	2.25271	74.98425	168.91800	38.99181
JB 112- 486	486	485-486	1.32	4	2.867	0.0463	28.32500	2.17197	85.11254	184.86186	44.25852
JB 112- 496	496	495-496	1.64	4.106	3.012	0.14925	26.64394	1.83659	66.07569	121.35365	34.35936
JB 112- 506	506	504-506	1.107	3.652	2.836	0.0603	22.34392	2.56188	79.02609	202.45527	41.09357
JB 112- 516	516	515-516	1.32	4.257	3.021	0.16605	29.03453	2.28864	66.39004	151.94266	34.52282
JB 112- 526	526	525-526	1.404	4.17	3.033	0.1631	27.26619	2.16026	65.08242	140.59472	33.84286
JB 112- 536	536	535-536	1.053	3.71	2.91	0.0973	21.56334	2.76353	70.45247	194.69772	36.63529
JB 112- 547	547	545-547	1.23	4.051	3.038	0.1767	25.00617	2.46992	62.07341	153.31627	32.27817
JB 112- 559	559	558-559	1.716	4.05	3.016	0.14365	25.53086	1.75758	67.15445	118.02904	34.92032
JB 112- 568	568	567-568	1.332	3.762	2.981	0.076	20.76023	2.23799	78.78872	176.32822	40.97014
JB 112- 578	578	577-578	0.9	3.7	3.061	0.32605	17.27027	3.40111	31.79584	108.14118	16.53384
JB 112- 588	588	587-588	1.7	3.111	2.666	0.004	14.30408	1.56824	94.85199	148.75025	49.32304
JB 112- 598	598	597-598	1.19	3.767	2.973	0.1818	21.07778	2.49832	53.39656	133.40167	27.76621
JB 112- 608	608	607-608	0.88	3.541	2.903	0.1666	18.01751	3.29886	49.68288	163.89703	25.83510
JB 112- 618	618	617-618	0.84	3.546	2.917	0.17035	17.73830	3.47262	47.67317	165.55075	24.79005

2. Raw data for Carbon and Nitrogen Analysis- pg. 1/3

Sample #	Sample code	%total N	%total C	%carbonate C	%organic C	N mol	C mol	C/N
1	JB112-1	1.963	33.692	0.008	33.684	0.140202	2.807032	20.021377
2	JB 112- 2	1.460	30.161	0.011	30.150	0.104318	2.512476	24.084681
3	JB 112- 6.5	0.497	7.729	0.003	7.726	0.035513	0.643842	18.129899
4	JB112-9.5	0.450	12.860	0.003	12.857	0.032164	1.071412	33.310928
5	JB 112- 13	1.369	38.241	0.001	38.240	0.097812	3.186687	32.579719
6	JB112-15	1.709	40.999	0.004	40.995	0.122043	3.416262	27.992358
7	JB 112- 24	1.167	42.190	0.353	41.837	0.083331	3.486439	41.838401
8	JB112-25	1.234	40.800	0.004	40.796	0.088129	3.39966	38.575788
9	JB 112- 34	1.754	40.985	0.178	40.807	0.125257	3.400612	27.149083
10	JB112-35	1.677	36.290	0.008	36.283	0.119761	3.023543	25.246372
11	JB 112- 44	1.602	43.305	0.189	43.116	0.114439	3.592981	31.396477
12	JB112-45	1.406	34.855	0.004	34.851	0.100395	2.904257	28.928193
13	JB 112- 54	1.399	34.855	0.279	34.576	0.099955	2.881362	28.826569
14	JB112-55	1.244	32.446	0.010	32.436	0.088875	2.703017	30.413805
15	JB 112- 65	2.064	43.098	0.009	43.089	0.147441	3.590727	24.353662
16	JB 112- 74	1.653	40.339	0.127	40.212	0.118089	3.350965	28.376706
17	JB112-75	1.979	37.402	0.004	37.398	0.141344	3.116502	22.049094
18	JB 112- 84	1.785	39.477	0.129	39.348	0.127503	3.279004	25.717141
19	JB112-85	1.812	40.416	0.008	40.408	0.129398	3.367341	26.023054
20	JB 112- 94.5	1.309	30.096	0.008	30.088	0.093477	2.507299	26.822505
21	JB 112- 96.5	0.394	10.721	0.004	10.718	0.028133	0.893131	31.746968
22	JB 112- 105	1.758	41.771	0.004	41.767	0.125591	3.480545	27.71341
23	JB 112- 115	0.375	10.044	0.003	10.041	0.026812	0.836779	31.209451
24	JB 112- 125	1.553	46.048	0.008	46.040	0.110899	3.836688	34.596117
25	JB 112- 133.5	1.712	43.868	0.009	43.858	0.122296	3.654868	29.885427
26	JB 112- 139.5	0.652	18.063	0.255	17.808	0.046547	1.483997	31.881448
27	JB 112- 145	1.505	36.366	0.120	36.246	0.107468	3.020482	28.105863
28	JB 112- 155	1.266	44.037	0.233	43.804	0.090434	3.650318	40.364336
29	JB 112- 165	1.207	41.646	0.233	41.413	0.086209	3.451065	40.031353
30	JB 112- 175	0.945	43.097	0.369	42.728	0.067501	3.560672	52.750258
31	JB 112- 185	1.457	47.692	0.105	47.587	0.104094	3.965561	38.096093
32	JB 112- 195	1.668	46.525	0.113	46.412	0.11914	3.867643	32.463086
33	JB 112- 205	2.144	40.633	0.147	40.486	0.153145	3.3738	22.030152
34	JB 112- 215	2.186	43.201	0.077	43.124	0.156178	3.593641	23.00989
35	JB 112- 225	1.800	41.444	0.150	41.294	0.128537	3.441206	26.772155
36	JB 112- 235	1.761	44.217	0.133	44.084	0.125783	3.67364	29.206173
37	JB 112- 245	1.869	35.106	0.217	34.890	0.133503	2.907459	21.778236
38	JB 112- 255	1.886	35.493	0.225	35.268	0.13473	2.938979	21.813774
39	JB 112- 265	2.073	37.105	0.159	36.946	0.148082	3.078863	20.791597
40	JB 112- 267	0.653	12.892	0.546	12.346	0.046665	1.028816	22.046744

2. Raw data for Carbon and Nitrogen Analysis- pg. 2/3

Sample #	Sample code	%total N	%total C	%carbonate C	%organic C	N mol	C mol	C/N
41	JB 112- 275	1.915	35.001	0.195	34.806	0.136819	2.900494	21.199457
42	JB 112- 285	1.936	41.994	0.209	41.785	0.138272	3.482085	25.182811
43	JB 112- 295	1.948	38.612	0.193	38.419	0.13917	3.201579	23.004864
44	JB 112- 301.5	1.539	30.107	0.360	29.747	0.109916	2.478903	22.552792
45	JB 112- 304	0.873	17.099	0.524	16.575	0.062328	1.381221	22.16035
46	JB 112- 315	1.290	26.101	0.288	25.813	0.092175	2.151113	23.337197
47	JB 112- 325	1.310	31.921	0.277	31.643	0.093577	2.636931	28.179332
48	JB 112- 331.5	0.479	11.581	0.287	11.294	0.034207	0.941136	27.512736
49	JB 112- 334	1.740	28.580	0.322	28.258	0.124311	2.354856	18.943294
50	JB 112- 343	1.656	37.474	0.338	37.136	0.118259	3.094665	26.168457
51	JB 112- 356	1.646	46.084	0.229	45.856	0.117537	3.821306	32.511563
52	JB 112- 366	1.510	41.786	0.249	41.537	0.107835	3.46139	32.09908
53	JB 112- 377	1.746	44.099	0.147	43.952	0.124724	3.662707	29.366461
54	JB 112- 385	1.508	46.347	0.140	46.207	0.107711	3.850582	35.749284
55	JB 112- 395	1.692	42.097	0.153	41.945	0.12089	3.495407	28.913954
56	JB 112- 406	1.538	47.728	0.107	47.621	0.109841	3.968416	36.128624
57	JB 112- 415	1.407	49.802	0.137	49.665	0.10049	4.138764	41.186029
58	JB 112- 426	1.677	42.475	0.214	42.261	0.119774	3.521791	29.403605
59	JB 112- 434	1.796	41.292	0.255	41.037	0.128265	3.419736	26.661535
60	JB 112- 444	1.747	40.890	0.337	40.553	0.124802	3.379416	27.078244
61	JB 112- 454	1.346	26.254	0.148	26.106	0.096136	2.175486	22.629252
62	JB 112- 464	1.797	41.722	0.244	41.478	0.128372	3.456505	26.925697
63	JB 112- 476	1.461	40.968	0.462	40.506	0.104389	3.375522	32.335965
64	JB 112- 486	1.513	46.352	0.480	45.872	0.108054	3.822666	35.377268
65	JB 112- 496	1.251	26.295	0.175	26.119	0.089356	2.176613	24.358976
66	JB 112- 506	1.842	40.807	0.127	40.679	0.131574	3.389946	25.764555
67	JB 112- 516	1.639	35.538	0.122	35.417	0.117069	2.951404	25.210735
68	JB 112- 526	1.463	33.094	0.152	32.942	0.10447	2.745179	26.277117
69	JB 112- 536	1.776	41.300	0.150	41.150	0.126827	3.429165	27.038094
70	JB 112- 547	2.256	33.802	0.430	33.372	0.161178	2.780981	17.254121
71	JB 112- 559	2.723	41.014	0.174	40.841	0.194503	3.403402	17.497965
72	JB 112- 568	2.239	44.422	0.484	43.938	0.159903	3.661499	22.898214
73	JB 112- 578	1.662	47.000	0.180	46.821	0.118703	3.90171	32.869457
74	JB 112- 588	1.242	48.153	0.278	47.875	0.088718	3.989554	44.968701
75	JB 112- 598	1.635	27.039	0.264	26.775	0.116776	2.231214	19.106844
76	JB 112- 608	1.671	23.791	0.266	23.525	0.119362	1.96041	16.42411
77	JB 112- 618	1.455	18.506	0.287	18.219	0.10391	1.518285	14.61154
78	JB 112- 624	1.282	28.978	0.606	28.372	0.091562	2.36431	25.821986

2. Raw data for Carbon and Nitrogen Analysis- pg. 3/3

Sample #	Sample code	%total N	%total C	%carbonate C	%organic C	N mol	C mol	C/N
79	JB 112- 630	1.741	25.375	0.743	24.632	0.12439	2.052671	16.501872
80	JB112- 640	1.155	16.387	0.923	15.464	0.082495	1.288639	15.62079
81	JB 112- 650	1.278	17.743	0.754	16.989	0.091276	1.415766	15.510839
82	JB 112- 655	1.262	18.548	0.755	17.793	0.090113	1.48271	16.453921
83	JB 112- 660	1.420	18.541	0.592	17.950	0.101459	1.495805	14.742954
84	JB 113- 664	0.086	1.594	0.408	1.187	0.006138	0.098876	16.107465
85	JB 112- 669	0.091	2.058	0.967	1.091	0.006517	0.090878	13.943688
86	JB 112- 674	0.106	1.812	0.598	1.214	0.007546	0.101207	13.411875
87	JB 112- 679	0.119	1.571	0.188	1.383	0.008474	0.115221	13.596967
88	JB 112- 681	0.187	2.324	0.227	2.096	0.013364	0.174693	13.072244
89	JB 112- 684	0.077	1.297	0.561	0.736	0.005504	0.061359	11.147541
90	JB 112- 691	0.061	0.794	0.270	0.524	0.004371	0.043671	9.9911881
91	JB 112- 697	0.064	0.651	0.140	0.512	0.004554	0.042632	9.3606727
92	JB 112- 705	0.043	0.311	0.078	0.233	0.003079	0.019431	6.3098705

Dr. Florin Pendea,
Lakehead University
Peat and Lacustrine samples
March 15/2013

3. Raw data testate amoebae counts continued- pg. 1/15

Depth (cm)	Amphitrema flavum	Amphitrema wrightianum	Arcella catinus	Arcella discoides	Arcella gibbosa	Arcella hemispherica	Arcella rotundata	Trinema/ Corythion type	Trinema lineare	Hyalosphenia minuta	Hyalosphenia elegans	Hyalosphenia papilio
2	0	0	0	0	0	1	0	4	6	0	0	6
6.5	0	0	0	1	0	0	0	5	3	0	0	0
24	15	0	0	0	0	4	0	0	0	1	1	28
34	0	0	0	4	2	1	0	0	0	0	0	17
44	0	0	0	0	0	10	0	0	0	0	0	16
54	1	0	0	1	0	1	0	0	0	0	0	5
65	0	0	0	2	0	0	0	0	0	0	0	0
74	0	0	0	5	0	0	0	0	0	0	0	0
84	0	0	0	1	0	0	0	0	0	0	0	0
94.5	0	0	0	0	0	0	0	0	0	0	6	0
96.5	0	0	7	0	0	0	0	0	0	0	1	0
104	0	0	4	1	0	0	0	0	0	0	0	0
115	0	0	1	8	0	0	0	0	0	0	0	13
125	7	0	6	0	0	1	0	0	0	0	0	21
133.5	0	0	1	1	0	0	0	0	0	0	0	10
139.5	1	0	0	2	0	0	0	0	1	0	0	0
145	0	0	0	0	0	0	0	0	0	0	2	0
155	5	0	6	0	0	2	0	0	0	0	0	38
165	65	7	3	5	0	2	0	0	0	0	0	20
175	49	1	3	9	0	3	0	0	0	0	3	37
185	8	0	8	0	0	6	0	0	0	0	0	21
195	0	0	6	0	0	16	0	0	0	0	0	0
205	0	0	3	0	0	5	0	0	0	0	0	0
208.5	0	0	0	0	0	18	0	0	0	0	0	0
210.5	0	0	2	0	0	11	0	0	0	0	0	8

3. Raw data testate amoebae counts continued - pg. 2/15

Depth (cm)	Amphitrema flavum	Amphitrema wrightianum	Arcella catinus	Arcella discoides	Arcella gibbosa	Arcella hemispherica	Arcella rotundata	Trinema/ Corythion type	Trinema lineare	Hyalosphenia minuta	Hyalosphenia elegans	Hyalosphenia papilio
215	0	0	2	1	0	13	0	0	0	0	0	36
225	0	0	1	0	0	5	0	0	0	0	0	3
235	4	0	1	0	1	0	0	0	0	0	0	25
245	0	0	0	0	0	1	0	0	0	0	0	0
255	0	0	4	0	0	5	0	1	1	0	0	0
265	0	0	3	0	0	1	0	1	15	0	0	0
267	0	0	7	0	0	3	0	0	0	0	0	0
275	0	0	12	0	0	2	0	1	2	0	0	0
285	0	0	6	0	0	1	0	0	0	0	0	0
295	0	0	0	0	0	3	0	1	0	0	1	0
301.5	0	0	1	0	0	2	0	0	0	0	0	0
304	0	0	0	0	0	2	0	0	0	0	0	0
315	0	0	0	0	0	3	0	0	1	0	0	0
325	0	0	0	0	0	0	0	1	0	0	0	0
331.5	0	0	0	0	0	0	0	0	18	0	0	0
334	0	0	1	0	0	3	0	0	0	0	0	0
343	0	0	10	0	0	1	0	0	0	0	0	0
356	0	0	7	0	0	1	0	0	0	0	0	0
366	0	0	2	0	0	3	0	0	0	0	0	0
377	0	0	0	0	0	4	0	0	0	4	0	0
385	0	0	3	0	0	3	1	0	0	0	0	0
395	0	0	1	0	3	4	3	0	0	0	0	0
406	1	0	5	0	1	2	0	0	0	0	0	0
415	0	0	4	0	0	5	0	0	0	0	0	0
426	0	0	5	0	0	7	0	0	0	1	0	0
444	0	0	0	0	0	3	0	0	0	0	0	0
454	0	0	0	3	0	0	0	0	0	0	0	0
464	0	0	1	2	0	0	0	0	0	0	0	0

3. Raw data testate amoebae counts continued - pg. 3/15

Depth (cm)	Amphitrema flavum	Amphitrema wrightianum	Arcella catinus	Arcella discoides	Arcella gibbosa	Arcella hemispherica	Arcella rotundata	Trinema/ Corythion type	Trinema lineare	Hyalosphenia minuta	Hyalosphenia elegans	Hyalosphenia papilio
476	0	0	4	6	0	0	0	0	0	0	0	0
486	0	0	0	1	0	0	0	0	0	0	0	0
496	0	0	5	0	0	0	0	0	0	0	0	0
506	0	0	0	7	0	0	0	0	0	0	0	0
516	0	0	0	25	0	0	0	0	0	0	0	0
536	0	0	0	3	0	0	7	0	4	0	0	0
547	0	0	0	10	0	0	0	0	5	0	0	0
559	0	0	0	8	0	0	0	0	5	0	0	0
568	0	0	5	7	0	0	0	0	10	0	0	0
578	0	0	4	8	0	0	0	0	9	0	0	0
598	0	0	2	10	0	0	0	0	8	0	0	0
608	0	0	8	5	0	0	0	0	5	0	0	0
618	0	0	1	4	0	0	0	0	0	0	0	0
624	0	0	0	8	0	0	0	0	0	0	0	0
630	0	0	0	2	0	0	0	0	0	0	0	0
640	0	0	0	0	0	0	0	0	0	0	0	0
655	0	0	0	0	0	0	0	0	0	0	0	0
660	0	0	0	0	0	0	0	0	0	0	0	0
Total	156	8	155	150	7	158	11	14	93	6	14	304

3. Raw data testate amoebae counts continued - pg. 4/15

Depth (cm)	Hyalosphenia subflava	Hyalosphenia nobilis	Physochila griseola	Quadrulella symmetrica	Tracheleuglypha dentata	Assulina muscorum	Assulina seminulum	Euglypha tuberculata	Euglypha rotunda	Euglypha strigosa	Heleopera rosea	Heleopera slyvatica
2	5	0	0	0	1	0	0	7	8	0	0	1
6.5	0	0	0	6	1	0	0	9	39	0	0	5
24	0	8	0	0	0	4	0	1	3	0	0	0
34	0	6	0	0	0	0	2	1	14	1	0	0
44	0	4	0	0	0	11	1	0	8	0	0	0
54	0	2	0	0	0	10	0	2	5	0	0	1
65	0	0	0	0	0	0	0	0	6	1	0	0
74	0	1	2	0	0	0	0	0	15	0	0	0
84	0	7	0	0	0	0	0	1	4	0	0	0
94.5	0	4	0	0	0	1	0	5	4	0	0	0
96.5	0	0	0	0	0	3	0	0	18	0	0	1
104	0	1	0	0	0	0	3	0	2	0	0	0
115	0	3	0	0	0	9	1	3	11	0	0	0
125	0	0	0	0	0	5	0	0	1	0	0	0
133.5	0	0	0	0	0	0	0	3	4	0	0	0
139.5	0	0	0	1	0	1	0	3	33	0	0	0
145	0	1	0	2	0	1	0	10	39	0	0	0
155	0	1	0	0	0	3	0	0	13	0	0	0
165	0	0	0	1	0	7	0	4	2	0	0	7
175	0	0	0	0	0	7	0	0	3	2	0	8
185	0	0	0	0	0	0	0	1	5	0	0	0
195	0	0	0	0	0	10	0	0	12	0	0	0
205	0	3	0	0	0	4	0	3	6	0	0	0
208.5	0	2	0	0	0	3	0	3	19	0	0	0
210.5	0	0	0	0	0	4	0	1	19	2	0	0

3. Raw data testate amoebae counts continued - pg. 5/15

Depth (cm)	Hyalosphenia subflava	Hyalosphenia nobilis	Physochila griseola	Quadrulella symmetrica	Tracheleuglypha dentata	Assulina muscorum	Assulina seminulum	Euglypha tuberculata	Euglypha rotunda	Euglypha strigosa	Heleopera rosea	Heleopera slyvatica
215	0	5	0	0	0	1	0	0	4	0	0	0
225	0	3	0	1	1	2	0	2	23	1	0	0
235	0	5	0	0	0	10	1	1	6	1	0	0
245	0	8	0	0	16	0	0	4	27	0	0	0
255	0	2	0	0	6	0	0	2	30	0	0	0
265	0	4	0	0	5	0	0	5	12	3	0	0
267	0	6	0	0	5	0	0	0	19	0	0	0
275	2	0	0	0	17	0	0	0	0	0	0	0
285	1	1	0	0	3	0	0	2	25	0	0	0
295	0	0	0	6	7	0	0	3	50	5	0	0
301.5	0	0	0	1	5	0	0	0	52	0	0	0
304	0	0	0	0	3	0	0	4	37	0	0	0
315	0	0	0	1	10	0	1	4	54	1	0	0
325	0	0	0	6	0	0	2	2	59	0	0	0
331.5	0	0	0	3	9	0	2	9	61	0	0	0
334	0	4	0	1	3	0	0	1	39	0	0	0
343	0	0	0	0	0	0	2	0	4	2	0	0
356	0	0	0	0	0	0	2	0	2	0	3	0
366	1	0	0	0	0	0	1	0	2	0	5	0
377	0	0	0	0	0	0	0	0	3	4	4	0
385	0	0	0	1	1	0	0	0	4	0	7	0
395	0	0	0	0	0	0	0	0	2	1	4	0
406	2	0	0	0	1	0	0	0	1	0	6	0
415	2	0	0	0	0	0	0	0	3	0	2	0
426	0	0	0	0	0	0	0	0	26	3	0	0
444	0	0	0	0	0	0	0	0	30	0	0	0
454	3	0	0	0	12	0	0	0	32	1	0	0
464	0	0	0	2	0	0	0	0	23	0	7	3

3. Raw data testate amoebae counts continued - pg. 6/15

Depth (cm)	Hyalosphenia subflava	Hyalosphenia nobilis	Physochila griseola	Quadrulella symmetrica	Tracheleuglypha dentata	Assulina muscorum	Assulina seminulum	Euglypha tuberculata	Euglypha rotunda	Euglypha strigosa	Heleopera rosea	Heleopera slyvatica
476	0	0	0	0	2	0	0	0	37	0	0	3
486	0	0	0	0	0	0	0	0	28	0	3	4
496	0	0	0	0	0	0	0	0	32	0	0	6
506	0	0	0	0	1	0	0	0	20	0	0	0
516	1	0	0	0	0	0	0	6	29	0	0	0
536	0	0	0	0	0	0	0	0	0	0	3	0
547	0	0	0	0	0	0	0	10	25	0	8	0
559	0	0	0	0	0	0	0	8	23	0	5	0
568	0	0	0	0	0	0	0	7	22	0	0	1
578	0	0	0	0	0	0	0	10	25	0	0	3
598	0	0	0	0	0	0	0	4	24	0	0	8
608	0	0	0	0	0	0	0	5	17	0	0	4
618	0	0	0	0	0	0	0	8	10	0	0	2
624	0	0	0	0	0	0	0	5	18	0	0	5
630	0	0	0	0	0	0	0	6	14	0	0	7
640	0	0	0	0	0	0	0	7	20	0	0	4
655	0	0	0	0	0	0	0	8	21	0	0	1
660	0	0	0	0	0	0	0	3	18	0	0	3
Total	17	81	2	32	109	96	18	183	1306	28	57	77

3. Raw data testate amoebae counts continued - pg. 7/15

Depth (cm)	Heleopera petricola	Heleopera sphagni	Cyphoderia ampulla	Difflugia rubescens	Difflugia pulex	Difflugia bacillifera	Difflugia oblonga	Difflugia lucida	Difflugia globulosa	Difflugia bryophila	Difflugia lithophila	Difflugia lobostoma	Trigonopyxis arcula
2	6	1	1	0	0	0	0	0	0	0	0	5	0
6.5	0	0	0	0	2	0	1	1	1	0	0	0	3
24	5	14	0	0	0	3	0	1	0	0	0	0	0
34	7	19	0	0	1	0	2	0	1	0	0	0	1
44	13	0	0	0	0	0	0	3	0	0	0	0	0
54	9	0	0	0	7	0	2	0	0	0	0	0	2
65	8	12	0	0	3	0	0	0	0	9	0	0	2
74	25	0	0	0	5	0	0	0	0	12	0	0	6
84	9	0	0	0	8	0	2	0	0	2	0	0	1
94.5	4	0	0	0	4	0	1	0	1	2	0	0	4
96.5	25	0	3	0	3	0	0	0	2	0	0	0	5
104	10	3	0	0	1	0	1	0	2	1	0	0	12
115	8	0	0	0	8	0	0	0	0	0	0	0	1
125	5	5	0	0	3	12	0	0	0	0	0	0	0
133.5	25	1	0	0	0	12	0	0	0	0	0	0	4
139.5	3	0	0	0	3	11	0	0	1	0	0	0	2
145	14	0	0	0	8	4	0	0	2	0	1	0	2
155	18	0	0	0	3	0	0	0	1	0	0	0	0
165	7	0	0	0	1	2	0	0	1	0	0	0	1
175	12	0	0	0	0	2	0	0	4	0	0	0	0
185	14	0	0	0	2	3	0	0	2	2	0	0	2
195	24	0	0	0	2	0	0	0	1	0	0	0	4
205	33	0	0	0	3	1	0	0	2	0	0	0	5
208.5	11	0	0	0	5	1	0	0	0	0	0	0	0
210.5	27	0	0	0	0	0	0	0	0	0	0	0	6

3. Raw data testate amoebae counts continued - pg. 8/15

Depth (cm)	Heleopera petricola	Heleopera sphagni	Cyphoderia ampulla	Difflugia rubescens	Difflugia pulex	Difflugia bacillifera	Difflugia oblonga	Difflugia lucida	Difflugia globulosa	Difflugia bryophila	Difflugia lithophila	Difflugia lobostoma	Trigonopyxis arcula
215	28	0	0	0	1	0	0	0	1	0	0	0	0
225	51	0	0	0	0	0	0	0	1	0	0	0	1
235	23	0	0	0	2	3	0	0	4	0	0	0	2
245	19	0	0	0	7	0	0	0	1	0	0	0	1
255	7	0	0	0	2	1	0	0	0	0	0	0	3
265	10	0	0	0	4	3	0	0	0	0	0	0	1
267	28	0	0	0	7	0	0	0	0	0	0	0	5
275	11	0	0	0	2	1	0	0	0	0	0	0	2
285	16	0	0	0	7	0	0	0	0	0	0	0	8
295	11	0	0	0	2	1	0	0	1	0	0	0	1
301.5	6	0	0	0	15	0	0	0	0	0	0	0	1
304	3	0	0	0	13	4	2	0	0	0	0	0	1
315	3	0	0	0	9	0	2	1	0	0	0	0	3
325	12	0	0	0	2	1	0	0	1	0	0	0	4
331.5	3	0	0	0	2	0	1	0	0	0	0	0	2
334	3	0	0	0	9	0	0	0	1	0	0	0	6
343	15	0	0	0	4	4	1	0	0	0	0	0	4
356	12	0	0	0	5	1	0	0	0	0	0	0	1
366	4	0	0	0	4	0	0	0	2	0	0	0	17
377	0	0	0	0	3	3	0	0	4	0	0	0	8
385	5	0	0	0	1	1	0	0	0	0	0	0	6
395	1	0	0	0	5	3	0	4	0	0	0	0	3
406	8	0	0	0	2	0	0	7	0	0	0	0	0
415	5	0	0	0	5	3	0	3	0	0	0	0	8
426	5	0	0	0	5	5	0	0	0	0	0	0	8
444	0	0	0	0	2	8	0	10	0	0	0	0	0
454	0	0	0	0	32	0	1	15	1	0	0	0	0
464	0	0	0	0	3	0	1	4	0	0	0	0	0

3. Raw data testate amoebae counts continued - pg. 9/15

Depth (cm)	Heleopera petricola	Heleopera sphagni	Cyphoderia ampulla	Difflugia rubescens	Difflugia pulex	Difflugia bacillifera	Difflugia oblonga	Difflugia lucida	Difflugia globulosa	Difflugia bryophila	Difflugia lithophila	Difflugia lobostoma	Trigonopyxis arcula
476	0	0	0	2	0	0	0	7	0	0	0	0	0
486	0	0	0	0	2	0	0	10	0	0	0	0	2
496	0	0	0	0	3	0	0	3	0	0	0	0	8
506	0	0	0	0	2	0	2	16	0	0	0	0	0
516	0	6	0	1	0	0	0	0	0	0	0	0	0
536	0	0	0	0	6	0	0	0	0	0	0	0	0
547	5	5	0	0	8	0	0	4	0	0	0	0	0
559	20	5	0	0	5	0	0	7	0	0	0	0	0
568	18	7	0	0	4	0	0	5	0	0	0	0	0
578	17	5	0	0	5	0	0	4	0	0	0	0	6
598	25	6	0	0	6	0	0	3	0	0	0	0	5
608	16	8	0	0	5	0	0	4	0	0	0	0	4
618	12	7	0	0	7	0	0	7	0	0	0	0	0
624	13	8	0	0	3	0	0	6	0	0	0	0	0
630	7	10	0	0	4	0	0	5	0	0	0	0	0
640	8	5	0	0	5	0	0	4	0	0	0	0	0
655	4	8	0	0	2	0	0	6	0	0	0	0	0
660	0	9	0	0	7	0	0	4	0	0	0	0	2
Total	756	144	4	3	301	93	19	144	38	28	1	5	186

3. Raw data testate amoebae counts continued - pg. 10/15

Depth (cm)	Cyclopyxis arcelloides	Phryganella acropodia	Centropyxis aculeata	Centropyxis platystoma	Centropyxis ecornis	Centropyxis cassis	Centropyxis sylvatica	Centropyxis aerophila	Centropyxis discoides	Nebela vitraeae	Nebela wailesi	Nebela flabellum
2	28	0	1	58	1	0	9	5	0	0	0	0
6.5	5	29	6	20	0	4	1	16	0	0	0	0
24	3	0	15	11	0	1	3	1	0	0	0	0
34	11	6	6	15	0	7	8	11	0	0	0	0
44	5	4	13	24	0	0	20	6	0	0	0	0
54	10	12	15	17	0	2	3	16	0	0	0	1
65	11	25	8	28	0	4	6	23	0	0	0	1
74	0	16	6	38	0	12	5	9	0	0	0	0
84	5	7	13	11	0	2	0	14	0	0	0	0
94.5	5	12	10	11	0	2	10	0	0	0	0	0
96.5	9	5	12	20	0	2	14	7	0	0	0	0
104	10	17	17	17	0	12	12	12	0	0	0	0
115	6	1	47	2	0	1	2	6	0	0	0	0
125	9	11	22	8	0	3	9	10	0	0	0	0
133.5	3	4	38	20	0	1	4	13	0	0	0	0
139.5	6	2	38	3	0	6	6	10	0	0	0	0
145	5	10	18	10	0	3	4	11	0	0	0	0
155	1	15	35	7	0	4	3	9	0	0	0	0
165	0	1	11	6	0	3	0	8	0	0	0	0
175	0	1	27	2	0	0	3	5	0	0	0	0
185	4	17	23	2	0	2	6	7	0	0	0	1
195	17	17	10	3	0	3	9	16	0	0	0	0
205	5	29	25	1	0	0	9	10	0	0	0	0
208.5	2	9	12	4	0	1	2	4	0	0	0	1
210.5	0	27	12	10	0	2	11	13	0	0	0	0

3. Raw data testate amoebae counts continued - pg. 11/15

Depth (cm)	Cyclopyxis arcelloides	Phryganella acropodia	Centropyxis aculeata	Centropyxis platystoma	Centropyxis ecornis	Centropyxis cassis	Centropyxis sylvatica	Centropyxis aerophila	Centropyxis discoides	Nebela vitraeae	Nebela wailesi	Nebela flabellum
215	2	16	25	7	0	3	0	7	0	0	0	0
225	4	9	14	9	0	3	5	10	0	0	0	0
235	0	1	36	5	0	1	1	13	0	0	0	0
245	0	16	33	3	0	0	1	6	0	0	0	0
255	0	10	41	8	1	0	1	12	0	0	0	0
265	0	3	51	7	0	0	2	15	0	0	0	0
267	2	0	34	3	0	2	1	22	0	0	0	0
275	0	4	60	8	1	3	0	13	0	0	0	0
285	0	2	50	6	0	1	0	10	0	0	0	0
295	0	16	1	6	0	0	5	20	0	0	0	0
301.5	3	3	8	3	0	2	5	33	0	0	0	0
304	7	0	13	1	0	4	12	34	0	1	4	0
315	3	10	9	1	0	0	5	28	0	0	5	0
325	0	7	12	11	0	2	0	23	0	0	9	0
331.5	1	6	4	8	0	2	10	5	0	1	10	0
334	0	30	12	16	0	4	5	12	0	0	0	0
343	0	21	27	22	0	6	0	23	0	0	0	0
356	2	11	42	9	0	5	0	22	0	0	0	0
366	4	4	46	9	0	0	8	31	0	0	0	0
377	0	0	54	8	0	5	3	32	0	0	0	0
385	1	2	16	9	0	8	0	19	5	0	0	0
395	0	1	16	2	0	4	0	33	6	0	0	0
406	0	1	47	0	0	2	0	32	13	0	0	0
415	0	0	4	0	0	2	4	43	5	0	0	0
426	0	0	3	2	0	0	9	17	0	0	0	0
444	0	0	0	0	0	0	0	21	0	0	0	0
454	0	11	18	0	0	2	0	20	0	0	0	0
464	0	2	57	1	0	1	0	30	0	0	0	0

3. Raw data testate amoebae counts continued - pg. 12/15

Depth (cm)	Cyclopyxis arcelloides	Phryganella acropodia	Centropyxis aculeata	Centropyxis platystoma	Centropyxis ecornis	Centropyxis cassis	Centropyxis sylvatica	Centropyxis aerophila	Centropyxis discoides	Nebela vitraeae	Nebela wailesi	Nebela flabellum
476	5	3	14	0	0	2	12	43	0	0	0	0
486	0	0	20	0	0	2	0	43	0	0	0	0
496	0	1	22	0	0	3	0	19	0	0	0	0
506	0	5	12	0	0	3	0	34	0	0	0	0
516	0	0	18	0	0	2	4	14	0	0	0	0
536	0	15	18	6	0	0	10	8	0	0	0	0
547	0	24	24	7	0	5	15	14	0	0	0	0
559	0	20	18	10	0	4	15	11	0	0	0	0
568	5	18	20	11	0	1	22	13	0	0	0	0
578	3	17	18	12	0	2	21	14	0	0	0	0
598	0	14	17	7	0	3	23	10	0	0	0	0
608	0	20	18	6	0	0	21	18	0	0	0	0
618	0	21	15	5	0	0	18	25	0	0	0	0
624	0	0	21	8	0	0	17	15	0	0	0	0
630	0	6	18	3	0	0	11	12	0	0	0	0
640	0	8	13	1	0	0	10	16	0	0	0	0
655	5	12	12	0	0	0	8	14	0	0	0	0
660	3	15	22	0	0	0	11	11	0	0	0	0
Total	210	662	1493	588	3	166	454	1162	29	2	28	4

3. Raw data testate amoebae counts continued - pg. 13/15

Depth (cm)	Nebela militars	Nebela tincta/ Hylaopshenia papillio Hybrid	Nebela tincta	Nebela collaris-bohemica	Nebela gracilis	Nebela galeata	Nebela lageniformis	Pediastrum	Rotifer	Unknown 1	Unknown 2	Total Counts/ Depth
2	0	0	1	2	0	0	0	0	0	0	0	157
6.5	2	0	0	0	37	0	2	0	0	0	0	199
24	1	0	11	4	0	0	1	0	5	0	0	150
34	0	0	11	0	0	0	2	0	4	0	0	160
44	0	0	8	0	0	0	1	0	1	0	0	150
54	0	10	8	1	0	0	0	0	2	8	10	163
65	2	1	2	1	0	0	0	0	0	0	2	157
74	0	11	2	1	0	0	0	0	0	0	0	171
84	0	0	0	0	0	0	0	0	0	1	0	100
94.5	0	0	1	0	0	0	0	0	0	2	0	100
96.5	1	0	1	1	0	0	0	0	3	0	0	150
104	0	0	1	6	0	0	0	0	3	0	0	150
115	0	1	0	2	0	0	0	0	0	26	0	160
125	0	0	4	2	0	0	0	0	6	3	0	153
133.5	0	0	2	2	0	0	0	0	4	1	0	153
139.5	0	0	3	15	0	0	0	0	4	0	0	155
145	0	0	4	1	0	0	9	0	3	0	0	164
155	0	1	1	0	0	0	2	0	3	1	0	172
165	0	0	0	1	0	0	4	0	1	2	0	172
175	4	0	5	0	0	0	0	0	5	0	0	195
185	0	0	12	2	0	0	0	0	4	0	0	154
195	0	0	0	1	0	0	0	0	0	0	0	151
205	0	0	0	6	0	0	0	0	0	0	0	153
208.5	0	0	0	1	0	0	0	0	0	10	0	108
210.5	0	0	0	0	0	0	0	0	0	1	0	156

3 Raw data testate amoebae counts continued - pg. 14/15

Depth (cm)	Nebela militars	Nebela tincta/ Hylaopshenia papillio Hybrid	Nebela tincta	Nebela collaris-bohemica	Nebela gracilis	Nebela galeata	Nebela lageniformis	Pediastrum	Rotifer	Unknown 1	Unknown 2	Total Counts/Depth
215	0	0	0	0	0	0	0	0	0	0	0	152
225	0	0	2	0	0	0	0	0	0	0	0	151
235	0	0	0	3	0	0	0	0	0	0	0	150
245	0	0	1	3	0	0	0	0	5	7	0	159
255	0	0	2	3	0	0	4	0	5	2	0	153
265	0	0	0	6	0	0	0	2	10	0	0	163
267	0	0	0	4	0	0	0	2	7	4	0	161
275	0	0	0	0	0	0	1	5	6	0	0	153
285	0	0	0	8	0	0	0	0	6	0	0	153
295	3	0	0	2	0	0	5	0	2	0	0	152
301.5	2	0	4	4	0	0	6	0	1	0	0	157
304	1	0	1	5	0	2	2	0	0	0	0	156
315	1	0	1	0	0	0	3	0	1	0	0	160
325	0	0	1	2	0	0	3	0	0	0	0	160
331.5	0	0	0	0	0	0	0	0	0	0	0	157
334	0	0	0	1	0	0	0	0	0	0	0	151
343	0	0	0	5	0	0	1	0	0	0	0	152
356	0	0	1	9	0	1	0	0	1	0	0	137
366	0	0	2	5	0	0	0	0	3	0	0	153
377	0	0	0	8	0	0	6	0	6	0	0	159
385	0	0	3	6	0	0	0	0	6	0	0	108
395	0	0	0	4	0	0	0	0	9	0	0	109
406	0	0	0	6	0	0	0	0	4	0	0	141
415	0	0	0	2	0	0	0	0	0	0	0	100
426	0	0	0	2	0	0	0	0	0	0	0	100
444	0	0	0	0	0	0	0	0	0	0	0	105
454	0	0	0	0	0	0	0	8	0	0	0	159

3. Raw data testate amoebae counts continued - pg. 15/15

Depth (cm)	Nebela militars	Nebela tincta/ Hylaopshenia papillio Hybrid	Nebela tincta	Nebela collaris-bohemica	Nebela gracilis	Nebela galeata	Nebela lageniformis	Pediastrum	Rotifer	Unknown 1	Unknown 2	Total Counts/Depth
464	0	0	10	3	0	0	1	1	2	0	0	154
476	0	0	0	12	0	0	0	2	0	0	0	154
486	0	0	0	1	0	0	0	0	0	0	0	104
496	0	0	0	2	0	0	0	0	0	0	0	107
506	0	0	0	5	0	0	0	0	0	0	0	113
516	0	0	2	5	0	0	0	0	0	0	0	102
536	0	0	5	14	0	0	0	0	3	0	0	187
547	0	0	8	9	0	0	0	0	1	0	0	184
559	0	0	10	10	0	0	0	0	0	0	0	189
568	0	0	5	7	0	0	0	0	1	0	0	195
578	0	0	7	5	0	0	0	0	0	0	0	185
598	0	0	3	4	0	0	0	0	3	0	0	181
608	0	0	8	8	0	0	0	0	1	0	0	150
618	0	0	3	2	0	0	0	0	0	0	0	134
624	0	0	2	3	0	0	0	0	2	0	0	111
630	0	0	1	4	0	0	0	0	1	0	0	114
640	0	0	7	6	0	0	0	0	0	0	0	112
655	0	0	3	5	0	0	0	0	3	0	0	113
660	0	0	2	2	0	0	0	0	1	0	0	113
Total	17	24	171	244	37	3	53	20	138	68	12	

4. Systematic taxonomy of all identified taxa page 1/3

Taxa Name	Species included in the complex
Arcella catinus Penard,1890	
Arcella discoides Ehrenberg, 1843	*Arcella megastoma* *Arcella polypora*
Arcella gibbosa Penard, 1890	Morpho-complex with *A. hemispherica* and *A. intermedia* - Subspecies *Arcella gibbosa* var. *levis* Deflandre, 1928 *Arcella gibbosa* var. *mitriformis* Deflandre, 1928 *Arcella gibbosa* var. *aplanata* Van Oye, 1956
Arcella hemisphaerica Perty, 1852	In a recent study by Lahr and Lopes (2009) show that *Arcella hemisphaerica* and *A. rotundata* are indistinguishable. They consider both species as a single entity with 9 non-distinguishable nominal taxa within: *Arcella hemisphaerica* Perty, 1852 *Arcella hemisphaerica* Perty, 1852 *Arcella hemisphaerica* fma *undulata* Deflandre, 1928 *Arcella hemisphaerica* var. *depressa* Playfair, 1918 *Arcella hemisphaerica* var. *tuberculata* Stepanek, 1963 *Arcella rotundata* Playfair, 1918 *Arcella rotundata* var. *stenostoma* Deflandre, 1928 *Arcella rotundata* var. *stenostoma* fma *undulata* Deflandre,1928 *Arcella rotundata* var. *aplanata* Deflandre, 1928 *Arcella rotundata* var. *alta* Playfair, 1918 *Arcella rotundata* var. *alta* fma *undulata* Stepanek,1963
Arcella rotundata Playfair, 1918	In a recent study Lahr and Lopes (2009) show that *Arcella hemisphaerica* and *A. rotundata* are indistinguishable. They consider both species as a single entity. See *Arcella hemisphaerica* Perty, 1852
Arcella vulgaris Ehrenberg, 1830	
Archerella flavum synonym: *Amphitrema flavum* Archer, 1877	This genus is together with genus Amphitrema closely related to the Labyrinthulidae.
Amphitrema wrightianum Archer, 1869	This genus is together with genus *Archerella* closely related to the Labyrinthulidae.
Assulina muscorum Greeff, 1888	
Assulina seminulum Ehrenberg, 1848	Lüftenegger et al. (2009): Separation between *A. seminulum* and *A. muscorum* only by their size, which is in *A. seminulum* about 1.5 X greater than in *A. muscorum*
Centropyxis aculeata Ehrenberg, 1838	
Centropyxis aerophila Deflandre, 1929	*C. aerophila*-complex includes *Centropyxis aerophila aerophila, C. aerophila sphagnicola* and *C. aerophila sylvatica* Deflandre, 1929
Centropyxis cassis Wallich, 1864	*Centropyxis cassis cassis*
Centropyxis discoides Penard, 1902	
Centropyxis ecornis Ehrenberg, 1841	*C. cordobensis*
Centropyxis platystoma Penard, 1890	
Centropyxis sylvatica Deflandre, 1929	See *Centropyxis aerophila* Deflandre, 1929

4. Systematic taxonomy of all identified taxa page 2/3

Taxa Name	Species included in the complex
Cyclopyxis arcelloides Penard, 1902	
Cyphoderia ampulla Ehrenberg, 1840	
Difflugia bacillifera Penard, 1890	*Difflugia oblonga* complex includes *D. oblonga D. lanceolata D. yorkui D. bacillifera D. bryophila D. lascustris*
Difflugia oblonga Ehrenberg, 1838	*Difflugia oblonga* complex includes *D. oblonga D. lanceolata D. yorkui D. bacillifera D. bryophila D. lascustris*
Difflugia lucida Penard, 1890	
Difflugia globulosa Dujardin, 1837; Penard, 1902	
Difflugia rubescens Penard, 1891	
Difflugia pulex Penard, 1890	
Difflugia bryophila Penard, 1902; Jung, 1942	*Difflugia oblonga* complex includes *D. oblonga D. lanceolata D. yorkui D. bacillifera D. bryophila D. lascustris*
Difflugia lithophila Penard, 1902	
Difflugia lobostoma Leidy, 1879	
Euglypha rotunda Ehrenberg, 1845	Species complex includes *E. rontunda,* and *E. laevis*
Euglypha strigosa Ehrenberg, 1848	
Euglypha tuberculata Dujardin, 1841	
Heleopera petricola Leidy, 1879	
Heleopera sphagni synonym*: Heleopera picta* Leidy, 1874	
Heleopera sylvatica Pernard, 1890	
Heleopera rosea Pernard, 1890	
Hyalosphenia elegans Leidy, 1874	
Hyalosphenia minuta Cash, 1892	
Hyalosphenia papilio Leidy,1874	
Hyalosphenia subflava Cash and Hopkinson, 1909	
Hyalosphenia nobilis Cash, 1909	
Nebela lageniformis synonym *Padaungiella lageniformis* Penard, 1890	
*Nebela galeata synonym Gibbocarina galeata (*Penard, 1890)	Deflandre (1936) described a new variety of this species, P. g. var. *orbicularis*
Nebela flabellulum Leidy, 1974	
Nebela tincta Leidy, 1874	*Nebela tincta* major-*bohemica-collaris* complex
Nebela collaris-N. bohemica synonym *N. collaris* Ehrenberg, 1848	*Nebela tincta* major-*bohemica-collaris* complex
Nebela gracilis synonym *Gibbocarina gracilis* Penard, 1910	
Nebela militaris Penard, 1890	
Nebela wailesi synonym *Padaungiella wailesi* Deflandre, 1936	

4. Systematic taxonomy of all identified taxa page 3/3

Taxa Name	Species included in the complex
Phryganella acropodia Hertwig & Lesser, 1874; Pernard 1902	
Physochila griseola Wailes & Penard, 1911	
Tracheleuglypha dentata Deflandre, 1928	
Trinema/Corythion type Hoogenraad & De Groot, 1940	Trinematidae: Trinema type including *T. complanatum, T. enchelys, T. grandis, T. lineare,* & *T. penardi.* Corythion type including *C. asperulum, C. constricta, C. dubium, C. dubium* var. *gigas, C. delamarei*
Trinema lineare Penard, 1890	Trinema type including *T. complanatum, T. enchelys, T. grandis, T. lineare,* & *T. penardi*
Trigonopyxis arcula Pernard, 1912	
Quadrulella symmetrica Wallich, 1863	